

TESE DE DOUTORADO Nº 375

**DYNAMIC EVENT-TRIGGERED CONTROL OF NONLINEAR SYSTEMS: A  
QUASI-LPV APPROACH**

**Pedro Henrique Silva Coutinho**

DATA DA DEFESA: 05/10/2021



UNIVERSIDADE FEDERAL DE MINAS GERAIS  
ESCOLA DE ENGENHARIA  
PROGRAMA DE PÓS-GRADUAÇÃO EM ENGENHARIA ELÉTRICA

PEDRO HENRIQUE SILVA COUTINHO

# **Dynamic Event-Triggered Control of Nonlinear Systems:** a quasi-LPV Approach

**Supervisor:** Prof. Dr. Reinaldo Martínez Palhares

Belo Horizonte, Minas Gerais

2021

PEDRO HENRIQUE SILVA COUTINHO

# Dynamic Event-Triggered Control of Nonlinear Systems: a quasi-LPV Approach

A thesis presented to the Graduate Program in Electrical Engineering (PPGEE) of the Federal University of Minas Gerais (UFMG) in partial fulfillment of the requirements to obtain the degree of Doctor in Electrical Engineering.

**Supervisor:** Prof. Dr. Reinaldo Martínez Palhares

Belo Horizonte, Minas Gerais

2021

C871d

Coutinho, Pedro Henrique Silva.

Dynamic event-triggered control of nonlinear systems [recurso eletrônico]: a quasi-LPV approach / Pedro Henrique Silva Coutinho. - 2021. 1 recurso online (92 f. : il., color.) : pdf.

Orientador: Reinaldo Martinez Palhares.

Tese (doutorado) - Universidade Federal de Minas Gerais, Escola de Engenharia.

Bibliografia: f. 78-92.

Exigências do sistema: Adobe Acrobat Reader.

1. Engenharia elétrica - Teses. 2. Desigualdades matriciais lineares- Teses. 3. Sistemas não lineares – Teses. I. Palhares, Reinaldo Martinez. II. Universidade Federal de Minas Gerais. Escola de Engenharia. III. Título.

CDU: 621.3(043)

# **"Dynamic Event-triggered Control of Nonlinear Systems: A Quasi-LPV Approach"**

**Pedro Henrique Silva Coutinho**

Tese de Doutorado submetida à Banca Examinadora designada pelo Colegiado do Programa de Pós-Graduação em Engenharia Elétrica da Escola de Engenharia da Universidade Federal de Minas Gerais, como requisito para obtenção do grau de Doutor em Engenharia Elétrica.

Aprovada em 05 de outubro de 2021.

Por:



---

**Prof. Dr. Reinaldo Martínez Palhares**  
**DELT – UFMG - Orientador**



---

**Prof. Dr. André Ricardo Fioravanti**  
**UNICAMP**



---

**Prof. Dr. João Manoel Gomes da Silva Jr.**  
**UFRGS**



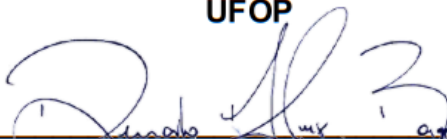
---

**Prof. Dr. Luciano Gonçalves Moreira**  
**IFSUL**



---

**Prof. Dr. Márcio Feliciano Braga**  
**UFOP**



---

**Prof. Dr. Renato Alves Borges**  
**UNB**

## AGRADECIMENTOS

Sou imensamente grato ao meu orientador, Professor Reinaldo Palhares, por ter me aceitado como orientando, desde o período do Mestrado, e por ter me dado tantas oportunidades de aprendizado e colaboração dentro e fora do laboratório D!FCOM. Gostaria também de agradecer pelo suporte oferecido e por todos os conselhos e ensinamentos que foram imprescindíveis para que eu pudesse concluir o doutorado, além dos ensinamentos valiosos para a carreira de um pesquisador.

Gostaria também de agradecer aos professores com quem tive a oportunidade de realizar colaborações nesse período. Em particular, sou muito grato ao Professor Miguel Bernal por todo o suporte que me foi dado durante todo o período que frequentei o Instituto Tecnológico de Sonora em Ciudad Obregón, México. Foi um período bastante enriquecedor e de muito aprendizado profissional e pessoal. Agradeço aos Professores Anh-Tu Nguyen e Márcio Júnior Lacerda pelas colaborações. Agradeço ao Professor Leonardo Torres pela colaboração e por todos ensinamentos e conselhos. Agradeço também ao Professor Thiago Chagas pela colaboração, pelo apoio e por ter sido sempre um grande incentivador desde o meu período de graduação.

Sou extremamente grato aos colegas do laboratório D!FCOM: Fúlvia, Gabriela, Iury, Luiz, Márcia, Matheus, Murilo, Rodrigo, Rosileide, Tiago e aos demais colegas e professores. Agradeço especialmente aos amigos Iury, Luiz e Murilo por terem me ajudado e colaborado em diversos momentos. Agradeço também aos amigos Luana e Rhonei, que seguiram comigo da UESC para a UFMG.

Agradeço aos membros do comitê de tese por terem aceitado julgar este trabalho e por todas as ideias e sugestões que foram dadas para sua melhoria.

Agradeço aos meus pais, meu irmão, minha noiva, Laís, e meu enteado, Raynã, por todo apoio, amor e compreensão ao longo desse período.

À Coordenação de Aperfeiçoamento de Pessoal de Nível Superior (CAPES) pelo apoio financeiro para desenvolver este trabalho.

## RESUMO

Esta tese trata do problema de projeto simultâneo de controladores e mecanismos dinâmicos de acionamento baseados em eventos para a classe de sistemas de controle não lineares via rede representados por modelos politópicos quasi-LPV. O principal objetivo desta proposta é obter condições de projeto simultâneo, via LMIs, tais que o número de eventos gerados seja reduzido tanto quanto possível. Em particular, são estudados dois tipos de mecanismos dinâmicos de acionamento baseados em eventos: o contínuo e o periódico. No caso de mecanismos dinâmicos de acionamento contínuos, considera-se um controlador com ganho escalonado e as condições de projeto simultâneo são construídas a partir da teoria de Lyapunov. Particularmente, a nova lei de acionamento proposta é tal que é possível cancelar completamente o efeito induzido pelo assincronismo dos parâmetros, já que os parâmetros do controlador são calculados em termos do estado disponibilizado pelo mecanismo de acionamento via rede de comunicação. Posto isto, a partir do tratamento adequado do efeito de assincronismo, consideram-se relaxações adicionais para reduzir o conservadorismo das condições LMI de projeto simultâneo. Finalmente, demonstra-se também que a estratégia proposta não produz comportamento de Zenão. No caso de mecanismos dinâmicos de acionamento periódicos, considerando a teoria de Lyapunov-Krasovskii, novas condições de projeto simultâneo são obtidas para garantir estabilidade do sistema em malha fechada com um controlador linear. Além disso, o efeito de retardo no tempo induzido pela rede é explicitamente levado em conta no projeto. Em ambos os casos, como os projetos se baseiam na representação local quasi-LPV da planta não linear, obtêm-se estimativas da região de atração dentro do domínio compacto onde a representação local é válida. Simulações numéricas são apresentadas para ilustrar a efetividade das condições de projeto simultâneo propostas em garantir a estabilidade do sistema em malha fechada requerendo um número reduzido de eventos quando comparados a mecanismos estáticos projetados via emulação e projeto simultâneo.

**Palavras-chave:** Sistemas de controle via rede. Sistemas não lineares. Controle baseado em eventos. Desigualdades matriciais lineares. Sistemas lineares com parâmetros variantes.

## ABSTRACT

This thesis concerns the co-design of controllers and dynamic event-triggering mechanisms for the class of nonlinear networked control systems represented by polytopic quasi-LPV models. The main objective of this proposal is to derive co-design conditions, via LMIs, such that the number of generated events is reduced as much as possible. In particular, two dynamic event-triggering mechanisms are studied: the continuous and the periodic. In the case of dynamic continuous event-triggering mechanisms, a gain-scheduling control law is considered and the co-design conditions are developed based on the Lyapunov theory. In particular, the new proposed triggering law is such that it is possible to completely cancel out the effect of the asynchronous parameters since the controller's parameters are computed in terms of the state available from the triggering mechanism via the communication network. Then, based on the adequate treatment of the asynchronism effect, extra relaxations are considered to reduce the conservativeness of the LMI-based co-design conditions. Finally, it is proved that the proposed strategy does not lead to Zeno behavior. In the case of dynamic periodic event-triggering mechanisms, a new co-design condition is developed considering the Lyapunov-Krasovskii theory to ensure the stability of the closed-loop system with a linear control law. The effect of network-induced time delays is explicitly taken into account in the design. In both cases, as the design conditions are based on the locally equivalent quasi-LPV representation of the nonlinear plant, estimates of the region of attraction are obtained inside the compact region where the local representation is valid. Numerical simulations are presented to illustrate the effectiveness of the proposed co-design conditions to ensure the stability of the closed-loop system requiring a reduced number of events when compared to static triggering mechanisms designed via emulation and co-design.

**Keywords:** Networked control systems. Nonlinear systems. Event-triggered control. Linear matrix inequalities. Linear parameter varying systems.

## LIST OF FIGURES

Figure 1.1 – Block diagram representations of (a) traditional control systems based on the point-to-point protocol and (b) networked control systems. . . .	15
Figure 1.2 – Representation of an ETC control setup, where $\mathcal{P}$ is the continuous-time plant, $\mathcal{C}$ is a static state feedback controller, $\mathcal{N}$ is the communication channel, $x(t)$ is the continuous state measurement, $x(jh)$ is the sampled state measurement, $x(t_k)$ is the most recently transmitted state measurement, $\hat{x}(t)$ is $x(t_k)$ possibly affected by network-induced effects, $u(t)$ is the control input. . . . .	17
Figure 1.3 – Representation of a CETC control setup, where $\mathcal{P}$ is the continuous-time plant, $\mathcal{C}$ is a static state feedback controller, $\mathcal{N}$ is the communication channel, $x(t)$ is the continuous state measurement, $x(t_k)$ is the most recently transmitted state measurement, $\hat{x}(t)$ is $x(t_k)$ possibly affected by network-induced delays, and $u(t)$ is the control input. . . . .	20
Figure 2.1 – Regions of state initial conditions $\mathcal{R}_{0,1}$ (in red), $\mathcal{R}_{0,2}$ (in black), and $\mathcal{R}_{0,3}$ (in magenta) obtained with [177, Corollary 5.2]. The initial conditions are denoted by ‘*’. . . . .	45
Figure 2.2 – Simulation of the closed-loop system (2.32) with the gain-scheduling control law (2.6) under the static ETM (2.12). . . . .	47
Figure 2.3 – Simulation of the closed-loop system (2.32) with the gain-scheduling control law (2.6) under the dynamic ETM (2.9)–(2.11). . . . .	48
Figure 2.4 – Region of state initial conditions $\mathcal{R}_0$ (in red) of the origin of the closed-loop system (2.7) with the dynamic ETM (2.9)–(2.11). The region $\mathcal{R}_0$ is contained in the polytopic region $\mathcal{D}$ (in black). The convergent (in blue) and divergent (in magenta) trajectories are also depicted considering initial conditions denoted by “×”. . . . .	49
Figure 2.5 – Simulation of the closed-loop system (2.36) with the gain-scheduling control law (2.6) equipped with the static ETC scheme (2.12). . . . .	50
Figure 2.6 – Simulation of the closed-loop system (2.36) with the gain-scheduling control law (2.6) equipped with the dynamic ETC scheme (2.9)–(2.11). . . . .	51
Figure 3.1 – Representation of the PETC control setup, where $\mathcal{P}$ is the continuous-time plant, $\mathcal{C}$ is a static state feedback controller, $\mathcal{N}$ is the communication channel, $x(t)$ is the continuous state measurement, $x(jh)$ is the sampled state measurement, $x(t_k h)$ is the most recently transmitted state measurement, $\hat{x}(t)$ is $x(t_k h)$ affected by network-induced delays, and $u(t)$ is the control input. . . . .	53

Figure 3.2 – Objective function $\beta\text{tr}(\tilde{\Xi} + \tilde{\Theta})$ of (3.67) with respect to $\rho$ for different values of $\epsilon$ . . . . .	69
Figure 3.3 – Sets $\mathcal{R}_0$ (in black) and $\mathcal{R}$ (in red) and convergent closed-loop trajectories (in blue) initiating in $\mathcal{R}_0$ . . . . .	71
Figure 3.4 – Sets $\mathcal{R}_0$ (in black) and $\mathcal{R}$ (in red) and convergent (starting at points “*”) and divergent (starting at points “o”) closed-loop trajectories (in blue). . . . .	72
Figure 3.5 – Simulation of the closed-loop system (2.36) with the control law (3.37) equipped with the dynamic PETC scheme (3.8), (3.10), (3.41). . . . .	72

## LIST OF TABLES

Table 2.1 – Mean of average inter-event times, in seconds, for the different approaches.	46
Table 3.1 – Minimum objective function $\beta \text{tr}(\tilde{\Xi} + \tilde{\Theta})$ and the related values of $\epsilon^*$ and $\rho^*$ for different values of $h$ in seconds.	70

## LIST OF ABBREVIATIONS

<b>ETC</b>	Event-triggered control
<b>ETM</b>	Event-triggering mechanism
<b>CETC</b>	Continuous event-triggered control
<b>ISS</b>	Input-to-state stability
<b>LKF</b>	Lyapunov-Krasovskii functional
<b>LMI</b>	Linear matrix inequality
<b>LPV</b>	Linear parameter-varying
<b>LTI</b>	Linear time-invariant
<b>MIET</b>	Minimum inter-event time
<b>NCS</b>	Networked control systems
<b>PETC</b>	Periodic event-triggered control
<b>TS</b>	Takagi-Sugeno
<b>ZOH</b>	Zero-order-hold

## LIST OF SYMBOLS

$\mathbb{B}$	The Boolean domain $\{0, 1\}$
$\mathbb{B}^p$	The $p$ -ary Cartesian power of the Boolean set $\mathbb{B}$
$\mathcal{P}(\mathbf{i})$	The set of permutations of a multi-index $\mathbf{i} = (i_1, \dots, i_p) \in \mathbb{B}^p$
$\mathbb{B}^{p+}$	The set $\{\mathbf{i} \in \mathbb{B}^p : i_j \leq i_{j+1}, j \in \mathbb{N}_{\leq p-1}\}$
$\mathbb{R}$	The set of real numbers
$\mathbb{R}_{\geq 0}$ ( $>0$ )	The set of non-negative (positive) real numbers
$\mathbb{R}^n$	The $n$ -dimensional Euclidean space
$\mathbb{R}^{m \times n}$	The set of real matrices of order $m$ by $n$
$\mathbb{N}$	The set of natural numbers, $\mathbb{N} = \{1, 2, \dots\}$
$\mathbb{N}_{\leq k}$	The set $\{1, 2, \dots, k\}$ for a given $k \in \mathbb{N}$
$\mathbb{N}_0$	The set $\{0\} \cup \mathbb{N}$
$\lambda_{\min(\max)}(A)$	The minimum (maximum) eigenvalue of a symmetric matrix $A$
$x^\top$ or $A^\top$	Transpose of a vector $x$ or a matrix $A$
$\ x\ $	Euclidean norm of a vector $x$
$ x $	Absolute value of a real number $x$
$\mathcal{C}_{[a,b]}^n$	Banach space of continuous functions $\phi : [a, b] \rightarrow \mathbb{R}^n$ with finite norm $\ \phi\ _{[a,b]} = \sup_{a \leq t \leq b} \ \phi(t)\ $
$\begin{bmatrix} A & B \\ \star & C \end{bmatrix}$ or $\begin{bmatrix} A & \star \\ B^\top & C \end{bmatrix}$	Shorthand notation for $\begin{bmatrix} A & B \\ B^\top & C \end{bmatrix}$
$\text{He}(A)$	Shorthand notation for $A + A^\top$ , where $A$ is any matrix expression
$P > 0$ ( $\geq 0$ )	$P$ is a symmetric positive (semi-)definite matrix
$\text{diag}(X_1, \dots, X_n)$	The diagonal matrix whose entries are $X_1, \dots, X_n$ , $n \in \mathbb{N}$
$\text{tr}(X)$	The trace of a square matrix $X$
$\mathcal{K}$	Set of continuous functions $\alpha : \mathbb{R}_{\geq 0} \rightarrow \mathbb{R}_{\geq 0}$ that are strictly increasing and satisfy to $\alpha(0) = 0$

$\mathcal{K}_\infty$	Set of continuous functions $\alpha \in \mathcal{K}$ that satisfy to $\alpha(s) \rightarrow +\infty$ as $s \rightarrow +\infty$
$\otimes$	Kronecker product
$I_n$	Identity matrix of order $n$ . If the order is clear in the context, it is omitted
$0_{n,m}$	Null matrix of order $n$ by $m$ . If the order is clear in the context, it is omitted

# CONTENTS

<b>1</b>	<b>INTRODUCTION</b>	<b>15</b>
1.1	Event-triggered control: literature review	18
1.1.1	Continuous and periodic ETC	20
1.1.2	Static, adaptive, and dynamic ETC	22
1.1.3	ETC design approaches	27
1.2	Motivation	29
1.3	Objectives	32
1.4	Thesis outline and contributions	32
<b>2</b>	<b>CANCELLATION-BASED DYNAMIC CETC</b>	<b>34</b>
2.1	Problem formulation	34
2.1.1	Perturbed model of the closed-loop system	36
2.2	Main results	37
2.2.1	Proposed dynamic CETC scheme	37
2.2.2	Co-design condition	40
2.2.3	Enlargement of inter-event times	42
2.2.4	Estimate of the region of attraction	43
2.3	Numerical examples	43
2.3.1	Example 1: van der Pol oscillator	43
2.3.2	Example 2: rotational motion of a cart with an inverted pendulum	47
2.4	Conclusion	51
<b>3</b>	<b>DYNAMIC PETC WITH NETWORK-INDUCED DELAYS</b>	<b>52</b>
3.1	Preliminary results	52
3.2	Problem formulation	53
3.2.1	Perturbed time-delay model of PETC systems	55
3.3	Main results	57
3.3.1	Local analysis of dynamic PETC systems	57
3.3.2	Delay-dependent co-design condition	60
3.3.3	Enlargement of inter-event times	68
3.4	Numerical examples	69
3.4.1	Example 1: van der Pol oscillator	69
3.4.2	Example 2: rotational motion of a cart with an inverted pendulum	70
3.5	Conclusion	73
<b>4</b>	<b>CONCLUDING REMARKS</b>	<b>74</b>
4.1	Future research	75

4.2 Publications . . . . .	76
<b>BIBLIOGRAPHY . . . . .</b>	<b>78</b>

## 1 INTRODUCTION

The point-to-point protocol is commonly assumed as communication architecture in traditional feedback control systems. In this case, the plant is connected to the controller via wires [1], and the design is often based on assumptions of perfect data transmissions [2], as illustrated in Figure 1.1(a). Nevertheless, with the growing use of embedded controllers, computer, and communication technology, which allows applications in smaller and less costly systems, the sensors and control data are often transmitted through digital communication channels [3].

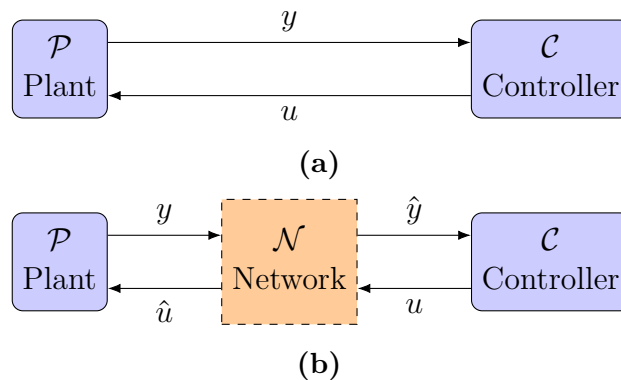


**Figure 1.1** – Block diagram representations of (a) traditional control systems based on the point-to-point protocol and (b) networked control systems.

This scenario motivated the development of networked control systems (NCS), in which systems that may be spatially distributed are interconnected with the presence of shared digital communication networks [4, 5], as illustrated in Figure 1.1(b). In this case, the measured signals  $y$  and  $u$  are sampled, converted to a digital format, and transmitted over the network as  $\hat{y}$  and  $\hat{u}$ , respectively. In contrast to traditional feedback control systems, in which the plant, sensors, controllers and actuators are connected regarding the point-to-point protocol, NCS offer the possibility of employing more flexible architectures, reduced installation costs and better maintainability [4, 6]. As a result, NCS have been considered in several engineering applications, such as car automation [7], microgrids [8], bilateral control of teleoperators [9], unmanned vehicles [10], among others [4, 11, 12].

In spite of several advantages of NCS over traditional control systems based on point-to-point architecture, the presence of shared communication networks often makes the stability analysis and controller synthesis for NCS more challenging since non-ideal network-induced phenomena should be properly taken into account [13]. The most common phenomena are listed as follows:

- a) Variable sampling/transmission intervals:

Due to the presence of the shared network, instead of continuous measurements of the output  $y$  and the control input  $u$ , as considered by traditional control systems, in NCS, these signals are sampled, encoded in a digital format, transmitted over the network, and then decoded for application. Data are transmitted at some specific instants  $t_k$ , named transmission times. Traditionally, especially for digital control systems, data are transmitted periodically with some pre-specified sampling period  $h \in \mathbb{R}_{>0}$ , *i.e.*,  $t_k = kh$ . However, the assumption of a fixed sampling period may be strong when NCS are concerned. As a result, efforts have been cast to compute the maximum allowable transmission interval for which the NCS stability is ensured [14, 15, 16] in a similar way as in sampled-data control systems [17, 18, 19, 20]. Although time-triggered communication schemes based on fixed sampling periods [21] or based on maximum allowable transmission intervals are of easy implementation, they often lead to redundant transmissions to ensure closed-loop stability or performance.

b) Network-induced delays:

The network-induced delays may be caused by the limited bandwidth, network traffic congestion, and the transmission protocol. Delays may appear in both sensor-controller and controller-actuator channels [5]. Even if network-induced delays may be time-varying and random, they are usually interval-bounded [22]. Therefore, alternatives to deal with their effects are mainly based on the characterization of the maximum allowable delay for which the stability of the NCS is ensured [1].

c) Packet dropouts:

Network-induced packet dropouts often result from transmission errors in physical network links, overloaded network traffic, and transmission time outs. Although the effect of packet dropouts can be modeled regarding stochastic theory methods, deterministic models are also available in the literature, which are especially useful in case of communication failures induced by malicious attacks [23]. Their effects can also be included together with those of network-induced delays and modeled as time-varying delays assuming a bounded number of successive packet losses [1, 22].

d) Quantization:

In control applications based on digital communication, data are usually quantized by elements called quantizers before transmitted. Quantizers are functions that map real-valued functions into piecewise constant ones over a finite set of values. They can be either uniform [24, 25] or logarithm [26] and there are appropriate methods to deal with the quantization effects depending on the considered quantizer mechanism [1, 22]. The data quantization generally

induces an error between the measured signal and its corresponding quantized representation.

The inherent network-induced effects have conducted to efforts to cast the analysis and synthesis problems for NCS taking them into account, but aiming to reduce the network resources consumption while still preserving desired control performance requirements. To avoid wasting of scarce communication resources frequently encountered in applications involving time-triggered control, instead of purely time specifications, resource-aware control techniques have been proposed to determine the instants when transmissions should occur to preserve stability or performance of the closed-loop system based on internal signals of the plant, such as state or output information [27].

The resource-aware control includes event-triggered control (ETC) [28, 29, 30] and self-triggered control [31, 32]. In self-triggered control, the mechanism computes the next sampling instant without requiring the constant monitoring of plant information, which allows self-triggering mechanisms to be used in an application without dedicated hardware. In ETC, the state information can be monitored (continuously or sampled), and a feedback mechanism is introduced into the sampling and communication process to determine the sampling instant when the state information deviates more than a certain threshold from the last sampled information or a desired value, offering the possibility of immediate compensation [27]. This work focuses on ETC.

The general ETC setup considered in this work is shown in Figure 1.2, where a static state feedback control law  $\mathcal{C}$  is employed to stabilize the continuous-time plant  $\mathcal{P}$ .

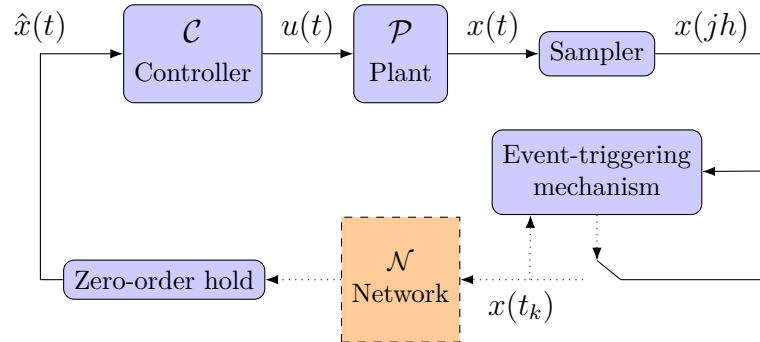


**Figure 1.2** – Representation of an ETC control setup, where  $\mathcal{P}$  is the continuous-time plant,  $\mathcal{C}$  is a static state feedback controller,  $\mathcal{N}$  is the communication channel,  $x(t)$  is the continuous state measurement,  $x(jh)$  is the sampled state measurement,  $x(t_k)$  is the most recently transmitted state measurement,  $\hat{x}(t)$  is  $x(t_k)$  possibly affected by network-induced effects,  $u(t)$  is the control input.

The sampler component is assumed to be periodically time-triggered with a fixed sampling time  $h \in \mathbb{R}_{>0}$ . Then, the sampled state measurement is sent to the event-generator, which is referred to in this work as event-triggering mechanism (ETM). The

ETM determines the appropriate instant to transmit the state, via a general purpose communication network  $\mathcal{N}$ , to the zero-order hold mechanism (ZOH), which converts the discrete signal into a piecewise continuous one to be available to the controller  $\mathcal{C}$ . In Figure 1.2, the dotted lines indicate that data flow occurs only at the event times  $t_k$ ,  $k \in \mathbb{N}_0$ , appropriately determined by the ETM. As the communication network may not be used exclusively for the control task, it may induce time-delays or even cause data loss [33].

### 1.1 Event-triggered control: literature review

The idea of event-based sampling behind ETC systems naturally arises in some engineering applications like: motion control, where signals of interest (as angles and positions) are measured via encoders that transmit a pulse when one of these signals change by a specific amount [34]; and systems with pulse frequency modulation [35, 36], where the control signal can only be either a positive or negative pulse with specific size, then the controller decides when these pulses should be applied with the correct sign. Moreover, it is interesting to mention that the human manual control is closer to the event-driven than time-driven control, since new human control actions are usually taken only when the measured signal deviates sufficiently from the reference.

The ETC system theory, as regarded in this work, has been mainly developed since the publication of the two seminal papers of Åström & Bernhardsson [34] and Åarzén [37]. Åström & Bernhardsson [34] developed an event-based sampling scheme for first-order stochastic systems, by comparing the proposed event-based strategy with traditional periodic sampling in terms of closed-loop variance and sampling rate, their findings showed up the better performance achieved with the event-based sampling. Åarzén [37] proposed an event-based PID controller aiming to ensure similar closed-loop performance as a conventional PID controller, but with reduced CPU utilization. The simulations and laboratory results indicated that it was possible reducing CPU usage with the event-based PID with minor performance degradation. Although these papers are acknowledged in the literature, the results are limited to the mentioned specific classes of dynamical systems and the authors highlight the interests in developing a system theory for ETC [37] and the need to extend the results for more general classes of dynamical systems [34].

The approaches to formulate ETC problems can be categorized into optimization-based and Lyapunov-based approaches. In optimization-based approaches, the ETC design is formulated as an optimization problem whose performance is expressed as an objective function, or cost, to be optimized [38, 39, 40, 41]. In Lyapunov-based approaches, with an appropriate model of the event-triggered NCS, the asymptotic stability, input-to-state (ISS) stability, or  $\mathcal{L}_p$ -stability of the closed-loop system can be studied regarding arguments of the Lyapunov stability theory [42].

Also, as discussed by Peng & Li [43], the main modeling tools for event-triggered NCS are: hybrid system models [44, 45, 46, 47, 6, 48, 49, 30], perturbed models [28, 29, 50, 51, 52, 53], and time-delay models [54, 55, 56, 1]. In the hybrid system model, the continuous and discrete behaviors of ETC systems are explicitly described in the model. The perturbed system model is obtained considering the transmission error as an internal perturbation. Although the perturbed model can be viewed as a less complex description, it provides less insights about the discontinuous nature of ETC systems. Finally, in the time-delay approach, a delayed control input is introduced to describe the aperiodic sampling. Also, it is an appropriate representation to be employed for systems with network-induced delays [1].

From the analytical point-of-view, the work of Tabuada [28] is well recognized in the ETC literature of Lyapunov-based approaches. Motivated by techniques employed to study problems related to control under communication constraints [24, 26, 57], the author proposed an ETM to determine the instants when control tasks should be executed whenever the norm of the error between the current and last transmitted state information becomes large when compared to the current state norm. The idea is developed for nonlinear systems and particularized for linear time-invariant (LTI) systems. The following class of nonlinear systems is considered:

$$\dot{x}(t) = f(x(t), u(t)), \quad (1.1)$$

where  $x(t) \in \mathbb{R}^n$  is the state,  $u(t) \in \mathbb{R}^m$  is the control input, and  $f : \mathbb{R}^n \times \mathbb{R}^m \rightarrow \mathbb{R}^n$  satisfies the assumptions for existence and uniqueness of solutions. Based on the assumption that there exists a state feedback control law

$$u(t) = k(\hat{x}(t)), \quad (1.2)$$

where  $\hat{x}(t)$  represents the last state available to the controller, that ensures the perturbed closed-loop system

$$\dot{x}(t) = f(x(t), k(x(t) + e(t))) \quad (1.3)$$

to be ISS stable with respect to the transmission error  $e(t) = \hat{x}(t) - x(t)$ , ETC design conditions are provided to ensure the closed-loop ETC system to be asymptotically stable. Another key contribution of this paper is the characterization and the formal proof of the existence of a positive minimum inter-event time (MIET) to avoid the existence of Zeno behavior<sup>1</sup> and ensures its applicability since communication networks do not have infinite bandwidth to support inter-event times arbitrarily close. As a result, a crucial property to guarantee the proper ETC implementation is the existence of a positive MIET in order to

<sup>1</sup> Zeno behavior is a concept related to the solution of hybrid dynamical systems [58]. In the context of ETC systems, it stands for the occurrence of an infinite number of events in a finite time, *i.e.*, the execution times become arbitrarily close resulting in an accumulation point [28, 6].

exclude Zeno behavior. Due to the above-mentioned aspects, the work of Tabuada [28] has motivated many subsequent works on ETC. In fact, according to the bibliometric analysis performed by Aranda-Escolástico *et al.* [59], Tabuada [28] is the most cited paper in the field<sup>2</sup>.

### 1.1.1 Continuous and periodic ETC

The ETC schemes can be distinguished in terms of how the state (or output) measurement is monitored by the ETM. The two main categories discussed here are continuous [28], and periodic [60, 47].

The continuous event-triggered control (CETC) setup is illustrated in Figure 1.3. In contrast to the setup shown in Figure 1.2, the state measurement  $x(t)$  is continuously monitored by the ETM, since there is no sampler mechanism in this case. It leads to the following continuous ETM [28]:

$$t_0 = 0, \quad t_{k+1} = \inf\{t > t_k : \Gamma(x(t), \hat{x}(t)) < 0\}, \quad \forall k \in \mathbb{N}, \quad (1.4)$$

where  $\Gamma(x, \hat{x})$  is an event-function which depends on the current state measurement  $x(t)$  and the last state information available to the controller by the ETM via communication network,  $\hat{x}(t)$ . By assuming that there is no delay induced by the network, one has  $\hat{x}(t) = x(t_k), \forall t \in [t_k, t_{k+1})$ , where  $t_k$  is the last time in which a state measurement has been transmitted. See [61, 62, 63, 27, 64, 29, 65, 50, 53] for applications of CETC schemes.

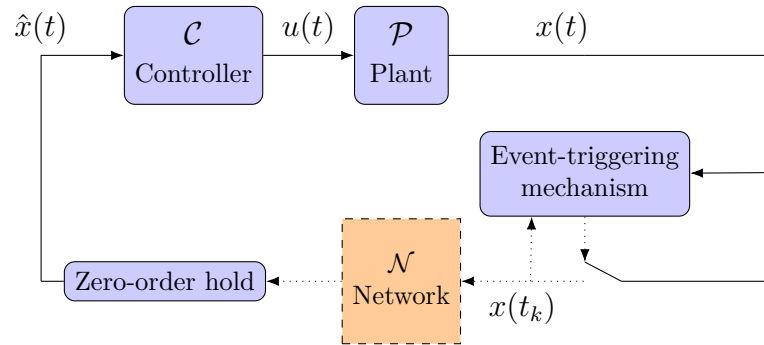


**Figure 1.3** – Representation of a CETC control setup, where  $\mathcal{P}$  is the continuous-time plant,  $\mathcal{C}$  is a static state feedback controller,  $\mathcal{N}$  is the communication channel,  $x(t)$  is the continuous state measurement,  $x(t_k)$  is the most recently transmitted state measurement,  $\hat{x}(t)$  is  $x(t_k)$  possibly affected by network-induced delays, and  $u(t)$  is the control input.

Although CETC strategies are easy to implement, they have some evident limitations. For instance, the event-function  $\Gamma(x, \hat{x})$  requires continuous state measurement instead of a sampled one as considered in Figure 1.2, which can be impractical for digital

<sup>2</sup> Tabuada [28] counts with 1484 citations reported by Aranda-Escolástico *et al.* [59] and more than 2800 citations reported by the Google Scholar database.

implementations, since continuous sensors have to be used. Also, to ensure the existence of a positive MIET may be not trivial, or even not possible, if the plant is subject to disturbances, or an output-based ETM is employed. For instance, Wang & Lemmon [66] studied ETC in distributed NCS accounting for the effects of packet loss and transmission delays regarding an input-to-output analysis, but a positive MIET is not provided in the case of disturbances. Yu & Antsaklis [67] studied the event-triggered output feedback control of NCS under communication delays and signal quantization and, from a passivity-based analysis, they showed that  $\mathcal{L}_2$ -stability can be achieved in the presence of these network imperfections. However, it is pointed out by Borgers & Heemels [44] that the CETC setup of Yu & Antsaklis [67] might not have a positive MIET in the presence of external disturbances and measurement noise.

The problems of output-based CETC with guaranteed  $\mathcal{L}_\infty$ -gain and decentralized triggering were studied by [63] and [68] focusing on LTI networked control systems. Based on an impulsive model of the event-triggered NCS, the authors provided conditions to guarantee  $\mathcal{L}_\infty$ -stability for the closed-loop system subject to disturbances and it is shown the existence of a positive MIET (for each node of the decentralized architecture). Nevertheless, with the proposed ETM, only practical stability is ensured in the absence of disturbance.

The effect of external disturbances and measurement noises over the MIETs of several CETC setups [28, 61, 27, 62] has been studied in detail by Borgers & Heemels [44]. The authors introduced different event-separation properties for ETC systems represented by hybrid models with state and output-based event-triggered closed-loop systems and continuous event-generators with relative, absolute, and mixed thresholds. It is shown that even if a positive MIET is found for the system in the absence of disturbance and measurement noise, it might not be possible to preserve it in the presence of arbitrarily small disturbances.

An effective alternative to improve robustness of CETC setups is to introduce a waiting time, or dwell-time [69], to enforce the existence of a positive MIET. This strategy is generally referred to as CETC with time-regularization. In this case, the continuous ETM in (1.4) is modified to:

$$t_0 = 0, \quad t_{k+1} = \inf\{t > t_k + T : \Gamma(x(t), \hat{x}(t)) < 0\}, \quad \forall k \in \mathbb{N}, \quad (1.5)$$

where  $T \in \mathbb{R}_{>0}$  represents the waiting time and clearly avoids accumulation points. The CETC with time-regularization has been effectively employed for both linear [70, 71, 72, 48, 73, 74, 51] and nonlinear [75, 45, 76, 6, 46, 77] ETC systems. Another approach employed to CETC with time-regularization is based on the formulation of the closed-loop system as a switched time-delay model [78, 79]. In spite of the advantages of CETC with time-regularization over standard CETC, such as the possibility to guarantee  $\mathcal{L}_p$ -stability in the presence of disturbances [45, 6] and to consider output-based ETMs [51, 52],

the disadvantage of requiring continuous state measurements also makes CETC with time-regularization hard to be implemented in digital platforms.

The periodic event-triggered control (PETC) has been proposed to avoid this limitation of CETC-based approaches [80]. It combines the simplicity of traditional periodic time-triggering with the effectiveness of ETC in reducing the number of transmissions. The PETC setup is illustrated in Figure 1.2 and a periodic ETM can be defined as follows:

$$t_0 = 0, \quad t_{k+1} = \min\{t > t_k : \Gamma(x(t), \hat{x}(t)) < 0, t \in \{jh\}, j \in \mathbb{N}\}, \quad (1.6)$$

where the trigger-function  $\Gamma(x, \hat{x})$  receives the state measurement only at the multiples of the sampling time  $h \in \mathbb{R}_{>0}$ , naturally excluding Zeno behavior. PETC strategies have been mainly developed for linear systems [60, 55, 81, 82, 47, 83, 84, 85, 86, 87], and linear switched systems [88], but also for nonlinear systems [89, 90, 91, 92, 93, 94, 95], polynomial systems [96], and Takagi-Sugeno (TS) fuzzy models [97, 98, 81, 99, 2, 100, 101, 56, 102, 103, 104, 105], which can provide exact or approximate local representations of nonlinear systems [106, 107]. Moreover, ETC strategies for discrete-time systems [108, 109, 110, 3, 111, 112, 113, 114, 115, 116] can also be viewed as PETC strategies, even though inter-event behavior is not explicitly taken into account in the analysis.

### 1.1.2 Static, adaptive, and dynamic ETC

ETC schemes can also be distinguished in terms of the trigger-function, which can be static, adaptive or dynamic. In static ETC, the transmission instants are determined based on the static trigger-function  $\Gamma(x, \hat{x})$  of the current state measurement and the last transmitted state. For instance, the three ETMs introduced before in (1.4), (1.5), and (1.6) are static.

To illustrate the static CETC operation, the strategy proposed by Tabuada [28] is briefly discussed in the sequel. The ISS property holds for the closed-loop nonlinear system (1.3), if there exists a continuously differentiable function  $V : \mathbb{R}^n \rightarrow \mathbb{R}_{\geq 0}$ , called ISS Lyapunov function, such that [28]:

$$\alpha_1(\|x\|) \leq V(x) \leq \alpha_2(\|x\|) \quad (1.7a)$$

$$\frac{\partial V}{\partial x} f(x, k(x+e)) \leq -\alpha(\|x\|) + \gamma(\|e\|), \quad (1.7b)$$

where  $\alpha_1, \alpha_2, \alpha, \gamma \in \mathcal{K}_\infty$ . Thus, if the event-function  $\Gamma(x, \hat{x})$  in (1.4) is selected as

$$\Gamma(x, e) = \sigma\alpha(\|x\|) - \gamma(\|e\|), \quad (1.8)$$

for some  $\sigma \in (0, 1)$ , while a new transmission does not occur, the inequality condition  $\gamma(\|e\|) \leq \sigma\alpha(\|x\|)$  is fulfilled until the error  $e(t)$  increases until (1.4) is satisfied again. In this case, from (1.7b), the ETM enforces the following inequality:

$$\frac{\partial V}{\partial x} f(x(t), k(x(t) + e(t))) \leq -(1 - \sigma)\alpha(\|x(t)\|) < 0, \quad \forall t \in [t_k, t_{k+1}), \quad k \in \mathbb{N},$$

thus ensuring that the zero equilibrium of the closed-loop system under the continuous ETM (1.4) is asymptotically stable.

Aiming to reduce the number of transmitted events without huge modifications on the ETC setup, new improved trigger-functions have been proposed based on the inclusion of dynamic variables. Notice that most of the references mentioned above concerns static ETC, with a few exceptions to be mentioned in the sequel.

One of the alternatives to introduce dynamics into the trigger-function is considering a time-varying weighting function instead of a constant weight  $\sigma$ . This class of ETC strategies will be referred to as adaptive ETC and it has been mainly developed in the context of PETC systems [117, 118, 119, 120, 121, 122, 123, 124, 114]. More recently, [125] studied  $\mathcal{L}_\infty$  adaptive CETC with a time-regularization for linear systems subject to stochastic deception attacks. A general form for the adaptive ETM is illustrated as follows:

$$t_0 = 0, \quad t_{k+1} = \inf\{t > t_k : \Gamma(x(t), e(t), \sigma(t)) < 0\}, \quad (1.9)$$

where

$$\Gamma(x, e, \sigma) = \sigma\alpha(\|x\|) - \gamma(\|e\|),$$

being  $\sigma \in (0, 1)$  a threshold which evolves according to some specified stable internal dynamics:

$$\dot{\sigma}(t) = \Omega(\sigma(t), e(t)) \quad (1.10)$$

with initial condition  $\sigma(0) \in (0, 1)$ . The function  $\Omega(\sigma, e)$  is generally defined as:

$$\Omega(\sigma, e) = \frac{1}{\sigma} \left( \frac{1}{\sigma} - \sigma_0 \right) \gamma(\|e\|),$$

where  $\sigma_0 > 1$  is a design parameter. In contrast to the static ETM in (1.4), the adaptive law given in (1.10) allows the threshold to be dynamically adjusted. When the error  $e(t)$  approaches to 0, then  $\dot{\sigma}(t) \rightarrow 0$ , enforcing  $\sigma(t)$  to converge to a constant value. If the initial condition is defined such that  $\sigma(0) = 1/\sigma_0$ , then  $\dot{\sigma}(t) = 0$ ,  $\forall t \in \mathbb{R}_{\geq 0}$ , and the adaptive ETM reduces to the static version.

To analyze the stability of the closed-loop system (1.3) under the adaptive ETM (1.9)–(1.10), consider the following Lyapunov function:

$$W(x, \sigma) = V(x) + \frac{1}{2}\sigma^2, \quad (1.11)$$

where  $V(x)$  is the ISS Lyapunov function defined in (1.7). The time-derivative of (1.11) along the trajectories of (1.1) is given by

$$\begin{aligned} \dot{W}(x(t), \sigma(t)) &= \frac{\partial V}{\partial x} f(x(t), k(x(t) + e(t))) + \sigma(t)\dot{\sigma}(t) \\ &\leq -\alpha(\|x(t)\|) + \gamma(\|e(t)\|) + \left( \frac{1}{\sigma(t)} - \sigma_0 \right) \gamma(\|e(t)\|), \end{aligned} \quad (1.12)$$

where the last inequality follows from property (1.7b). While a new event is not transmitted, the condition  $\gamma(\|\hat{x}(t) - x(t)\|) \leq \sigma(t)\alpha(\|x(t)\|)$  is fulfilled until the error  $\hat{x}(t) - x(t)$  increases up to condition (1.9) is satisfied again. In this case, it follows from (1.12) that

$$\dot{W}(x(t), \sigma(t)) \leq -\sigma(t)(\sigma_0 - 1)\alpha(\|x(t)\|) < 0, \quad \forall t \in [t_k, t_{k+1}), \quad k \in \mathbb{N}, \quad (1.13)$$

thus ensuring that the origin of the closed-loop system (1.3) equipped with the adaptive ETM in (1.9)–(1.10) is asymptotically stable.

Another approach to introducing dynamics into ETMs is the dynamic ETC [126, 29, 30]. Although dynamic ETC can also be referred to as adaptive ETC in the literature, such as in the work of Hu *et al.* [111] for discrete-time systems, the term dynamic ETC is more common in the literature and, for this reason, it is preferred in this work.

Girard [29] has considered the same class of nonlinear systems as [28], *i.e.*, the plant described in (1.1) with the state feedback control law (1.2) and the same assumptions about the ISS property or, equivalently, the existence of the function  $V(x)$  given in (1.7). The author has proposed a dynamic CETC strategy based on the following ETM:

$$t_0 = 0, \quad t_{k+1} = \inf\{t > t_k : \eta(t) + \theta\Gamma(x(t), e(t)) < 0\}, \quad \forall k \in \mathbb{N}, \quad (1.14)$$

where  $\Gamma(x, e)$  is defined as in (1.8),  $\theta \in \mathbb{R}_{\geq 0}$  is a design parameter and  $\eta(t) \in \mathbb{R}_{\geq 0}$  is a dynamic variable that evolves according to the following differential equation:

$$\dot{\eta}(t) = -\delta(\eta(t)) + \sigma\alpha(\|x(t)\|) - \gamma(\|e(t)\|), \quad (1.15)$$

where  $\eta(0) = \eta_0 \in \mathbb{R}_{\geq 0}$  is the initial condition,  $\delta \in \mathcal{K}_\infty$ ,  $\sigma \in (0, 1)$  and  $\alpha, \gamma$  are defined as in (1.7b). In this case, the solution  $\eta(t)$  can be viewed as a filtered version of the static trigger-function (1.8). The main advantage of dynamic ETC over static ETC relies on the possibility of ensuring the same closed-loop performance as its static counterpart but requiring a fewer number of transmitted events, which implies in less usage of communication resources in NCS. Indeed, an interesting result provided by [29, Proposition 2.3] is that, under the same initial conditions, the next transmission time given by the dynamic ETM is larger than or equal to that given by its static counterpart. As a consequence, the existence of a positive MIET follows directly if such a MIET exists for the static version of the dynamic ETM under study, as shown in [29, Theorem 1].

The stability of the closed-loop system (1.3) equipped with the dynamic ETM (1.14)–(1.15) is studied regarding the following Lyapunov function proposed by [29]:

$$W(x, \eta) = V(x) + \eta, \quad (1.16)$$

where  $V(x)$  is the ISS Lyapunov function defined in (1.7). The time-derivative of (1.16) along the trajectories of (1.1) is given by

$$\dot{W}(x(t), \eta(t)) = \frac{\partial V}{\partial x} f(x(t), k(x(t) + e(t))) + \dot{\eta}(t). \quad (1.17)$$

From inequality (1.7b) and the dynamics of  $\eta(t)$  given in (1.15), it follows that

$$\dot{W}(x(t), \eta(t)) \leq -(1 - \sigma)\alpha(\|x(t)\|) - \delta(\eta(t)) < 0, \quad \forall t \in [t_k, t_{k+1}). \quad (1.18)$$

Since  $\eta(t)$  is assumed to be positive, one can conclude that  $W(x, \eta)$  is a Lyapunov function that ensures that the zero equilibrium of the closed-loop system (1.3) under the dynamic ETM in (1.14)–(1.15) is asymptotically stable. Notice that as  $\theta \rightarrow \infty$  the dynamic ETM in (1.14) reduces to the static ETM in (1.4).

Given the advantages of dynamic ETMs, different ETC strategies have been proposed. For dynamic CETC [126, 30, 29, 127, 128, 129], beyond the previously discussed work in [29], Postoyan *et al.* [30] studied two different dynamic ETMs for nonlinear ETC systems based on the hybrid system theory analysis of the closed-loop system. The first dynamic ETM introduces a dynamic threshold variable to relax the static condition  $\Gamma(x, \hat{x}) < 0$ . The second approach is based on a state-dependent clock variable that is defined to adapt transmissions to the system state. This clock variable evolves according to a differential equation inspired by the time-triggering strategy proposed by [130].

Based on the proposal of [29], Wang, Zheng & Zhang [127] studied the dynamic ETC and dynamic self-triggered control of nonlinear stochastic systems to ensure the stochastic stability of the closed-loop system, by proving the existence of a positive MIET. Zuo *et al.* [128] developed dynamic ETC and self-triggered control schemes with anti-windup compensation for LTI systems subject to saturation. To exclude Zeno behavior, a decaying exponential variable is introduced into the trigger-function, preventing the existence of accumulation points. Yi *et al.* [129] proposed dynamic ETC and self-triggered control schemes for consensus of multi-agent systems modeled as single integrators. It is shown that the average consensus is achieved exponentially without Zeno behavior. Wu *et al.* [131] investigated the distributed event-triggered consensus problem for general linear multi-agent systems under a strongly connected communication graph, providing the conditions to ensure the absence of Zeno behavior. Finally, Wang *et al.* [132] tackled the problem of dynamic event-triggering fault estimation and accommodation for the class of LTI systems with external disturbance and subject to actuator fault. The avoidance of Zeno behavior is proved for the output-based dynamic ETM. In all the mentioned works, the efficiency of the dynamic schemes are put in evidence in contrast to their static versions. More recently, Huong, Huynh & Trinh [133] tackled the problem of dynamic continuous event-triggered state observer design for a class of nonlinear systems with Lipschitz nonlinearities subject to time delays and disturbances, Zhang *et al.* [134] developed a dynamic event-triggered resilient control for linear NCS subject to denial-of-service attacks, and the dynamic event-triggered  $\mathcal{L}_\infty$  control has been studied by Li, Ma & Zhao [135] for linear switched affine systems under limited communication resources.

The idea of dynamic ETMs was also exploited for dynamic CETC with time-regularization [45, 6, 136, 137, 138, 139, 140, 73, 74, 141]. Dolk, Borgers & Heemels [45]

proposed a dynamic event-triggered state feedback control strategy for nonlinear systems subject to disturbances and, based on the hybrid systems modeling, they derived conditions to ensure the  $\mathcal{L}_p$ -stability of the closed-loop system and evaluated the trade-off between transmission intervals and guaranteed performance, showing that, for a given  $\mathcal{L}_2$ -gain, the average inter-event times obtained with the dynamic ETM are larger than those achieved with static ETM. This strategy was employed for linear systems [136], extended for the case of output-based and decentralized dynamic ETC of nonlinear NCS [6], for ETC of nonlinear NCS considering the effect of packet losses [137], denial-of-service attacks [138], event-triggered quantized control of linear NCS with distributed output sensors [141], and applied to ETC of string-stable vehicle platooning [139] and consensus seeking of linear multi-agent systems subject to time-varying delays [140].

Also based on the hybrid systems modeling analysis, [Borgers, Dolk & Heemels](#) [73] have employed matrix Riccati differential equations to derive linear matrix inequality (LMI) conditions for  $\mathcal{L}_2$ -stability analysis of linear systems subject to communication delays. In this work, less conservative results were obtained with a piecewise quadratic Lyapunov functional. Finally, based on a perturbed system model, LMI-based conditions for observer-based feedback control design under a dynamic ETM with time-regularization are provided in [74].

The use of dynamic ETMs in the context of PETC was considered by [Borgers, Dolk & Heemels](#) [47], where new dynamic event-generators were proposed for the class of linear systems subject to disturbances. Based on the hybrid systems formalism, a Lyapunov-based condition is derived to ensure the  $\mathcal{L}_2$ -stability of the closed-loop system with guaranteed  $\mathcal{L}_2$ -gain. For the plant in the absence of disturbances, exponential stability with decay rate is ensured. [Liu & Yang](#) [86] studied dynamic ETC for LTI systems subject to disturbances. Regarding a time-delay model of the closed-loop system and an appropriate Lyapunov-Krasovskii functional (LKF), LMI-based conditions are derived to ensure  $\mathcal{L}_2$ -stability of the closed-loop system with guaranteed  $\mathcal{L}_2$ -gain. Also, [Luo, Deng & Chen](#) [87] proposed a dynamic PETC for linear stochastic systems subject to communication delays ensuring the mean-square exponential stability. For that, two approaches are concerned in this work: the first considers an impulsive switched system approach and the stochastic stability of the impulsive switched system is studied considering a time-dependent discretized Lyapunov function, the second is based on a switched time-delay model of the closed-loop ETC system whose stochastic stability is studied by means of a time-dependent LKF. The reduction on the number of transmitted events and the consequent enlargement of inter-event times is demonstrated in all the above mentioned works when dynamic ETMs are compared with static ones.

### 1.1.3 ETC design approaches

The efficacy of ETC systems depends on the appropriate design of the ETM and the controller  $\mathcal{C}$ , as illustrated in Figure 1.2. As extensively discussed in this section, the main objective of ETC systems is to ensure the closed-loop system performance while reducing the number of transmitted events aiming to increase the efficiency of the usage of network communication resources often scarce in NCS. There are essentially two approaches to ETC design: emulation and co-design.

Emulation-based design approaches are performed in two steps. Firstly, a controller is designed to ensure the stability or specified performance for the closed-loop system in the absence of the ETM and communication network, *i.e.*, by assuming point-to-point links as illustrated in Figure 1.1(a). Then, the second step is to take into account the presence of the ETM and the effects induced by the presence of a communication network to design the ETM in order to preserve the properties ensured by the previously designed controller [130, 27, 43]. As the ETM design is separated from the control design, the main advantage of this approach is that the ETM can be designed for a wide variety of control design methods, making the ETM design flexible. Nevertheless, this independence may limit the closed-loop performance of the ETC system and demands more transmissions than necessary.

The co-design approach is an alternative to overcome the limitations of emulation-based approaches by performing simultaneous design of the ETM and the control law. However, co-design is often recognized as a challenging problem since it may involve non-convex optimization or multi-objective optimization problems [142] due to the possible conflicting constraints related to the closed-loop performance and the enlargement of inter-event times [48, 143]. Another drawback of co-design is that the analysis is often limited to specific classes of controllers and ETMs.

The ETC co-design approach has been developed for the different ETC strategies. For static CETC, it has been proposed a co-design condition to design a linear state feedback control law for local stabilization of LTI systems subject to input saturation based on a perturbed model of the closed-loop system [50]. Also, [144] investigated the co-design for absolute stabilization of Lur'e systems using state feedback controllers.

For static CETC with time-regularization, [145] studied the co-design of output feedback controllers for stabilization of linear systems. This study was extended later to  $\mathcal{L}_2$ -stabilization of linear systems subject to disturbances [48]. The conditions of [48] has been improved by [143], which proposed relaxed co-design conditions providing larger inter-event times. Also based on the hybrid system formalism, a co-design condition was proposed by [49] for the same class of systems and controllers studied by [50]. [49] derived a co-design condition to ensure local exponential stability and LQ performance. The

co-design of an observer-based feedback control law and an output-based ETM for linear systems was studied by [72]. In the case of nonlinear systems, [52] focused on the co-design of observer-based event-triggered control for the class of linear systems with cone-bounded nonlinear inputs, illustrating the effectiveness of the proposal for logarithmic quantization and saturation functions. In the case of dynamic CETC with time-regularization, one can mention the work of [74] concerning the co-design of observer-based controllers and output-based dynamic ETMs for stabilization of linear systems. Also, a particular result is provided for the case when full state is available for measurement. All these works are based on the hybrid system formalism.

Some of the early efforts to obtain ETC co-design conditions were made in the context of static PETC. [55, 54, 81] have proposed conditions to perform the simultaneous design of state feedback controllers and periodic ETMs for LTI systems aiming to ensure the  $\mathcal{L}_2$ -stability of the closed-loop system represented as a time-delay model. In this case, the co-design conditions are derived based on appropriate LKFs together with the Jensen's integral inequality. The reciprocally convex combination lemma [146] is employed by [54] to provide a less conservative result. An outstanding feature of this methodology is the possibility to easily take network-induced delays into account. The co-design of output feedback controllers and adaptive periodic ETMs was investigated by [124] for stabilization of linear systems. In this work, an improved condition is obtained using an augmented LKF and the Wirtinger-based integral inequality [147].

The idea of introducing waiting time to a static PETC scheme was recently exploited by [88] for linear switched NCS with input saturation. The closed-loop system is formulated as a time-delay switched system and the co-design condition was derived regarding multiple LKF method and dwell-time technique [69].

For the class of TS fuzzy models, co-design conditions have been proposed to both static PETC [97, 98, 99, 100, 56, 148, 103, 102, 149, 105] and adaptive PETC [117, 118, 119, 120, 121, 122, 123, 124, 150, 151, 114].

In the context of dynamic PETC, [86] derived a co-design condition for state feedback controllers and dynamic ETMs for LTI systems subject to disturbances aiming to ensure the  $\mathcal{L}_2$ -stability of the closed-loop time-delay model.

By exploiting the linearity of LTI systems, partial linearity of Lur'e systems or linear systems with cone-bounded nonlinear inputs, or local linearity of TS fuzzy models, all the aforementioned works on ETC co-design have derived numerically implementable co-design conditions expressed in terms of LMIs, which can be efficiently solved by convex optimization methods [152, 153].

## 1.2 Motivation

Gain-scheduling control techniques are recognized as effective tools to solve analysis and synthesis problems related to nonlinear systems [154, 107, 155, 156]. In the particular case of quasi-linear parameter varying (LPV) scheduling, a local polytopic differential inclusion is obtained by subsuming the bounded nonlinear expressions of the plant into parameters that compose the polytopic model. These state-dependent parameters are thus considered to parameterize gain-scheduled control laws to stabilize the nonlinear plant. The two main modeling approaches employed to that purpose are the quasi-LPV and TS models. The quasi-LPV model is a particular class of LPV systems [19, 157, 158] whose parameters depend only on endogenous signals, such as the state. References [107, 156] have discussed about the use of the sector nonlinearity approach [159, 106, 107], a common method to obtain TS fuzzy models, to obtain polytopic quasi-LPV models of nonlinear systems. In this sense, [107] discuss the close relation between polytopic quasi-LPV models [160, 161, 18, 162, 163] and TS fuzzy models [164]. However, based on optimization techniques, one can obtain TS fuzzy models that provide only approximate representations for nonlinear systems, but in this case the designed gain-scheduled controller may not provide the expected performance requirements from the design when applied to the nonlinear plant. For this reason, the class of polytopic quasi-LPV models of nonlinear systems is preferred in this work.

Based on the discussion in Section 1.1, it is evident the interests in considering ETC to improve the efficiency of NCS due to its efficacy in reducing the required number of transmitted data to ensure the closed-loop stability or performance, thus saving scarce communication resources. Nevertheless, the literature review has revealed a lack on ETC of nonlinear systems, especially considering dynamic ETC co-design approaches.

Moreover, proposers of control methodologies have become increasingly aware of the need for providing numerically implementable design conditions, among which those of convex optimization framework are preferred, both in linear and nonlinear contexts, in the latter, generally based on gain-scheduling control techniques. Although there are ETC design methodologies expressed in terms of LMIs, most part of the ETC design conditions are not based on constructive nor numerically implementable methods, mainly when dealing with nonlinear systems. Thus, the first motivation of this thesis is:

- (i) to propose novel constructive co-design conditions, via LMIs, for nonlinear systems represented by polytopic quasi-LPV models equipped with dynamic triggering mechanisms.

In particular, LMI formulations of PETC co-design conditions are based on the time-delay model of the closed-loop ETC system [55, 1]. In this case, sufficient co-design conditions are obtained by employing appropriate manipulations to rewrite the

infinite-dimensional condition into a finite set of LMIs to be numerically solved. However, depending on the employed manipulation, co-design conditions may present different degrees of conservativeness. One of the sources of conservativeness is the manipulation to obtain quadratic upper-bounds to get the LMIs. To reduce such conservativeness, it can be considered improved LKFs, Bessel-Legendre integral inequalities, and the delay-dependent reciprocally convex lemma [165].

Nevertheless, most conditions for PETC co-design are still based on the Jensen's inequality together with the standard reciprocally convex lemma [146], which often lead to more conservative conditions than results based on the Wirtinger-based integral inequality or high-order Bessel-Legendre inequalities. However, their applications in the context of ETC design are still limited. A few exceptions are [99, 117, 103, 121, 123], which consider the Wirtinger-based integral inequality, but also with the standard reciprocally convex lemma. Also, Oliveira *et al.* [56] proposed a co-design condition for output-based static PETC of TS fuzzy models using the auxiliary function-based integral inequality and the standard reciprocally convex lemma; Wang *et al.* [166] employed the second-order Bessel-Legendre inequality and the delay-dependent reciprocally convex lemma [165, 167] for static PETC co-design for stabilization of linear active vehicle suspension systems; and Yan *et al.* [104] proposed integral-based static PETC co-design condition for TS fuzzy models considering the Bessel-Legendre inequality. However, the conditions in [104] were derived regarding the Bessel-Legendre inequality proposed by [168] for linear time-delay systems with constant delays. The extension for systems with time-varying delays was given later in [165]. Also, even though the conditions are given for arbitrary order Bessel-Legendre inequality, the only numerical example is provided for the first-order case, which reduces the application to a Jensen's integral inequality-based condition. The second motivation of this work is:

- (ii) to employ an improved LKF together with the delay-dependent reciprocally convex lemma and the Wirtinger-based integral inequality to derive PETC co-design conditions for stabilization of nonlinear systems represented by quasi-LPV models.

Moreover, if a gain-scheduled controller is considered in the ETC setups shown in Figures 1.2 or 1.3, as the state measurement  $\hat{x}(t)$  is updated to the controller only at specific event times  $t_k$  determined by the ETM possibly affected by the communication network imperfections (induced delays, quantization, packet loss), the scheduling functions to compute parameters of the gain-scheduled controller may differ from that of the polytopic quasi-LPV model, leading to the so-called asynchronous scheduling functions or asynchronous parameters. This is another source of conservativeness in LMI-based ETC design conditions to the class of quasi-LPV models with gain-scheduled controllers, since in this case it is not possible to directly employ LMI relaxations often considered in the

non-networked case, as in [169, 170]. If this asynchronous phenomenon is not properly accounted, the gain-scheduling control structure reduces to a traditional linear control law, thus increasing conservativeness of the design condition, possibly affecting the solution's feasibility and the efficiency of the ETC strategy.

The existing alternatives to cope with the asynchronism often assume given bounded deviations between the controller's and plant's parameters [2]. However, especially in the case of event-based implementations, ensuring these given bounds are not violated during operation is not an easy task and, in general, most of the works on ETC of TS fuzzy models do not concern this issue [2]. To deal with this drawback, the approach in [98] ensures the parameter's deviation enforcing a maximum allowable sampling period, while the approach in [103] introduces an extra condition into the event-triggering scheme to enforce the deviation bounds. However, the conservativeness of the co-design conditions in these works depends on the assumed deviation bounds, such that as long as the deviation bounds are reduced to obtain less conservative results, more transmissions are expected, which may lead to "unnecessary" transmissions. The triggering strategy proposed by [171] for discrete LPV systems deals with asynchronous parameters without assuming deviation bounds by incorporating information on the mismatch induced by the asynchronism into the trigger rule. Unfortunately, the method can not be directly applied to quasi-LPV systems, since no local convergence analysis is provided. More recently, considering a CETC with a maximum allowable sampling period, an exact discretization approach has been proposed by [172] to develop co-design conditions for continuous-time quasi-LPV systems avoiding the mismatch between the parameters. The enforced maximum allowable sampling period required to employ the exact discretization approach may also increase the number of transmissions. Thus, the third motivation of this work is:

- (iii) to propose a methodology to deal with the asynchronous phenomenon induced by the event-based sampling without assuming any pre-specified deviation bounds or maximum allowable sampling periods.

Finally, when quasi-LPV or TS fuzzy models are employed to design gain-scheduled controllers for local stabilization of nonlinear systems, it is of interest to obtain an estimation of the region of attraction inside the region in which both the polytopic model and the control law remain valid. However, the previously mentioned ETC co-design approaches for TS fuzzy models do not provide such a characterization, which may lead to implementation issues when the designed controller is employed to the actual nonlinear system, since there is no guarantee that the state trajectories will not evolve outside the modeling region [21, 20, 173] (see [174] for a deeper discussion on this topic). Moreover, in the case of network-induced delays affecting the communication, the first data packet is delivered to the plant with some delay, and during this time the state trajectory can also evolve outside the modeling region. In the worst case, it may even leave the actual region

of attraction of the closed-loop equilibrium. Thus, this phenomenon should be properly addressed to estimate the region of attraction. Then, the fourth motivation of this thesis is:

- (iv) to derive local co-design conditions for nonlinear systems equipped with dynamic ETC schemes represented by quasi-LPV models.

### 1.3 Objectives

Based on the aforementioned motivations, the general objective of this work is stated as follows:

*To propose dynamic event-triggered control strategies for local stabilization of nonlinear networked control systems represented by polytopic quasi-LPV models.*

As pointed out in Section 1.1, one of the crucial properties for the application of ETC strategies is the existence of a positive MIET to exclude the occurrence of Zeno behavior. Also, it was noticed a lack of ETC for nonlinear systems, especially concerning the co-design approach, even more in the case of dynamic ETC strategies. In the case of ETC design conditions formulated in the form of LMIs, it was discussed in Section 1.2 the demand for less conservative conditions and, within the context of event-triggered gain-scheduling control, the necessity of appropriately cope with the existing asynchronism between the scheduling functions and, consequently, the parameters of the gain-scheduled controller and the polytopic quasi-LPV model. Therefore, the following specific objectives are regarded:

- (i) To develop constructive and less conservative numerically implementable LMI-based conditions to perform the co-design of dynamic ETC schemes;
- (ii) To provide effective solutions to cope with the asynchronous phenomenon between the parameters of the gain-scheduled controller and the polytopic quasi-LPV model;
- (iii) Whenever possible, to consider the presence of network-induced delays affecting the communication network;
- (iv) To formulate convex optimization problems to introduce performance indexes in the ETC design aiming to reduce the number of transmissions;
- (v) To derive local co-design conditions to ensure the applicability of the dynamic ETC scheme for nonlinear systems represented by quasi-LPV models.

### 1.4 Thesis outline and contributions

The work's organization and the related contributions of each chapter are described as follows:

Chapter 2 concerns the problem of dynamic CETC of nonlinear systems represented by quasi-LPV models. A co-design condition is proposed to perform the design of a gain-scheduled controller and the dynamic ETM. The closed-loop system is represented as a perturbed model and the co-design condition is obtained based on the Lyapunov stability theory aiming to ensure the local asymptotic stability of the closed-loop system. By taking advantage of the continuous availability of the state measurement, the trigger-function is appropriately defined in order to cancel out the influence of asynchronous parameters, which allows to derive a less conservative LMI-based co-design condition. A convex optimization problem subject to LMI constraints is proposed to enlarge the inter-event times. For the proposed strategy, it is shown the existence of a positive MIET that prevents the occurrence of Zeno behavior and an estimate of the region of attraction of the closed-loop equilibrium is obtained, enabling the CETC implementation. The results presented in this chapter have been published in [Coutinho & Palhares \[175\]](#).

Chapter 3 concerns dynamic PETC of nonlinear systems represented by quasi-LPV models. By taking into account the effect of network-induced delays, the closed-loop system is represented by a time-delay model and the co-design is formulated regarding the Lyapunov-Krasovskii stability theory. A co-design condition is proposed to ensure the local stability of the closed-loop system by using the Wirtinger-based integral inequality and the delay-dependent reciprocally convex lemma, as it has been recently proposed in the PETC context by [Coutinho & Palhares \[176\]](#).

In both Chapters 2 and 3, convex optimization problems subject to LMI constraints are proposed to enlarge the inter-event times of the ETC system. Moreover, numerical simulations are performed to illustrate the effectiveness of the proposed co-design conditions.

Finally, the main contributions of this work are summarized and concluding remarks and suggestions for future work are provided in Chapter 4.

## 2 CANCELLATION-BASED DYNAMIC CETC

This chapter investigates the co-design of gain-scheduled state-feedback controllers and dynamic continuous ETMs for nonlinear NCS represented by quasi-LPV models. The co-design condition is derived based on the Lyapunov stability theory aiming to ensure the asymptotic stability of the closed-loop ETC system. To cope with the asynchronous phenomenon between the controller and quasi-LPV model parameters induced by the action of the ETM, the trigger-function of the dynamic CETC scheme is appropriately defined to cancel out the influence of asynchronous parameters, which allows deriving a less conservative LMI-based co-design condition. Moreover, a convex optimization problem subject to LMI constraints is proposed to enlarge the inter-event times. Also, for the proposed CETC, it is shown the existence of a MIET, which prevents the occurrence of Zeno behavior and enables its implementation. Numerical examples are provided to illustrate the advantages of the proposed dynamic CETC co-design approach over emulation-based approach and its static counterpart.

This chapter is organized as follows. The problem is formulated and stated in Section 2.1. The cancellation-based CETC, the proof of the existence of the MIET, the proposed dynamic CETC co-design condition, and its particularization for static CETC co-design are provided in Section 2.2. Numerical examples concerning two physical models are presented in Section 2.3 to illustrate the proposal's effectiveness. Finally, conclusions are presented in Section 2.4.

### 2.1 Problem formulation

Consider the following class of nonlinear systems

$$\dot{x}(t) = A(x(t))x(t) + B(x(t))u(t) \quad (2.1)$$

where  $x(t) \in \mathcal{D} \subset \mathbb{R}^n$  is the state,  $u(t) \in \mathbb{R}^m$  is the control input,  $A : \mathcal{D} \rightarrow \mathbb{R}^{n \times n}$  and  $B : \mathcal{D} \rightarrow \mathbb{R}^{n \times m}$ ,  $B(x) \neq 0, \forall x \in \mathcal{D}$ , are continuous matrix-valued functions. The nonlinear terms in the state-dependent coefficients of  $A(x)$  and  $B(x)$  are denoted by  $z_j : \mathcal{D} \rightarrow \mathbb{R}$ ,  $j \in \mathbb{N}_{\leq p}$ , and called scheduling functions. Furthermore,  $\mathcal{D} \subset \mathbb{R}^n$  is a convex polytope containing the origin. Notice that, without loss of generality, it is assumed that the origin is the equilibrium point of interest.

As the scheduling functions  $z_j(x)$ , are continuous functions and  $\mathcal{D}$  is a compact set, then there exist bounds such that:

$$z_j^0 \leq z_j(x) \leq z_j^1, \quad j \in \mathbb{N}_{\leq p}. \quad (2.2)$$

By following the sector-nonlinearity approach [159, 106, 107, 162], based on the bounds defined in (2.2), each scheduling function  $z_j(x)$  can be equivalently written as:

$$z_j(x) = w_0^j(x)z_j^0 + w_1^j(x)z_j^1 = \sum_{i_j=0}^1 w_{i_j}^j(x)z_j^{i_j}, \quad (2.3)$$

where the state-dependent weighting functions are defined by

$$w_0^j(x) := \frac{z_j^1 - z_j(x)}{z_j^1 - z_j^0}, \quad w_1^j(x) := 1 - w_0^j(x),$$

with  $0 \leq w_{i_j}^j(x) \leq 1$ ,  $i_j \in \mathbb{B}$ ,  $j \in \mathbb{N}_{\leq p}$ . Then, for all  $x \in \mathcal{D}$ , the nonlinear system (2.1) can be equivalently described by the following polytopic quasi-LPV model:

$$\dot{x}(t) = \sum_{\mathbf{i} \in \mathbb{B}^p} w_{\mathbf{i}}(x(t)) (A_{\mathbf{i}}x(t) + B_{\mathbf{i}}u(t)), \quad (2.4)$$

where the state-dependent parameters are defined by

$$w_{\mathbf{i}}(x) := \prod_{j=1}^p w_{i_j}^j(x), \quad (2.5)$$

being  $\mathbf{i} = (i_1, \dots, i_p) \in \mathbb{B}^p$ . By definition, notice that the convex sum property holds for the parameters:

$$\sum_{\mathbf{i} \in \mathbb{B}^p} w_{\mathbf{i}}(x) = 1, \quad 0 \leq w_{\mathbf{i}}(x) \leq 1, \quad \mathbf{i} \in \mathbb{B}^p,$$

such that the matrices

$$A_{\mathbf{i}} := A(x)|_{w_{\mathbf{i}}(x)=1}, \quad B_{\mathbf{i}} := B(x)|_{w_{\mathbf{i}}(x)=1},$$

define the vertices of the polytopic quasi-LPV model (2.4).

The following gain-scheduling state-feedback control law is considered to stabilize system (2.1):

$$u(t) = K(\hat{x}(t))\hat{x}(t) = \sum_{\mathbf{j} \in \mathbb{B}^p} w_{\mathbf{j}}(\hat{x}(t))K_{\mathbf{j}}\hat{x}(t), \quad (2.6)$$

where  $\hat{x}(t)$  is the state information available to the controller by the ETM, and the state-dependent matrix  $K : \mathcal{D} \rightarrow \mathbb{R}^{m \times n}$  is assumed to depend on the scheduling functions of (2.1) such that a gain-scheduled controller with gains  $K_{\mathbf{j}} = K(\hat{x})|_{w_{\mathbf{j}}(\hat{x})=1}$  can be parameterized in terms of the parameters  $w_{\mathbf{j}}(\hat{x})$ .

In this chapter it is considered the setup shown in Figure 1.3, where the plant  $\mathcal{P}$  is the nonlinear system (2.1), the triggering mechanism is connected to the controller  $\mathcal{C}$ , which in this case is the gain-scheduling control law (2.6), through a general-purpose network  $\mathcal{N}$ . The time sequence  $\{t_k\}_{k \in \mathbb{N}}$  when the state measurement is transmitted to the controller is determined online by the ETM.

### 2.1.1 Perturbed model of the closed-loop system

After substituting (2.6) into (2.1), the closed-loop system becomes

$$\dot{x}(t) = A(x(t))x(t) + B(x(t))K(\hat{x}(t))\hat{x}(t), \quad \forall t \in [t_k, t_{k+1}). \quad (2.7)$$

When a data sample is transmitted at the event time  $t_k$ , the state available to the controller is updated to  $\hat{x}(t) = x(t_k)$ ,  $\forall t \in [t_k, t_{k+1})$ . As a zero-order-hold is employed,  $\hat{x}(t)$  is kept constant until the next event time  $t_{k+1}$ , which induces the transmission error

$$e(t) = \hat{x}(t) - x(t), \quad \forall t \in [t_k, t_{k+1}).$$

Thus, the closed-loop system (2.7) can be equivalently rewritten in terms of the transmission error as follows

$$\begin{aligned} \dot{x}(t) = & [A(x(t)) + B(x(t))K(x(t))]x(t) + B(x(t))K(x(t))e(t) \\ & + B(x(t)) [K(x(t) + e(t)) - K(x(t))] (x(t) + e(t)), \quad \forall t \in [t_k, t_{k+1}). \end{aligned} \quad (2.8)$$

The influence of the asynchronous scheduling functions is put in evidence in the term  $K(x+e)$  of (2.8). The closed-loop dynamics in (2.8) can be interpreted as the composition of one part parameterized only in terms of  $x$ , and another one which depends on the asynchronous scheduling functions evaluated on  $\hat{x} = x + e$ . The structure derived in (2.8) is exploited in the next section to construct the proposed ETM.

**Remark 2.1.** *If a linear state-feedback control law  $u(t) = K\hat{x}(t)$  was employed, the closed-loop dynamics would be reduced to*

$$\dot{x}(t) = [A(x(t)) + B(x(t))K]x(t) + B(x(t))Ke(t), \quad \forall t \in [t_k, t_{k+1}).$$

*In this case, there is no asynchronous phenomenon affecting the closed-loop system, which makes the developments to obtain LMI-based co-design conditions amenable when compared to the case in (2.8). Although the use of linear state-feedback controllers is attractive from this point-of-view, it may introduce conservativeness to the design.*

As far as the control law (2.6) must be designed to ensure the origin of the closed-loop system (2.7) is asymptotically stable, it is of interest to determine the region of attraction of the origin. However, analytically obtaining that region is not an easy task [18, 42], for this reason, a problem of interest is to obtain an estimate of the region of attraction  $\mathcal{R}$  ensuring that closed-loop trajectories starting in  $\mathcal{R}$  converge asymptotically to the origin and do not evolve outside the domain  $\mathcal{D}$  in which the polytopic representation (2.4) is valid. Then, the control problem we are interested in is stated as follows.

**Problem 2.1.** *Design a gain-scheduled controller (2.6) and a dynamic continuous ETM such that:*

- (i) the origin of the closed-loop system (2.7) is asymptotically stable;
- (ii) the number of events generated by the dynamic continuous ETM is reduced as much as possible.

## 2.2 Main results

This section presents the proposed dynamic ETM and the formal proof of Zeno-freeness that allows its practical application. Then, a sufficient condition to perform the simultaneous design of the dynamic ETM and the gain-scheduled controller (2.6) is proposed, which solves item (i) of Problem 2.1. Finally, an optimization problem is proposed to enlarge the inter-event times, which solves the item (ii) of Problem 2.1.

### 2.2.1 Proposed dynamic CETC scheme

Consider the following dynamic continuous ETM

$$t_0 = 0, t_{k+1} = \inf\{t > t_k : \eta(t) + \theta\Gamma(x(t), e(t)) < 0\}, \forall k \in \mathbb{N}, \quad (2.9)$$

where  $\theta \in \mathbb{R}_{\geq 0}$  is a design parameter and the trigger function  $\Gamma(x, e)$  is defined as follows

$$\Gamma(x, e) = x^\top \Psi x - e^\top \Xi e - \zeta(x, e), \quad (2.10)$$

with

$$\zeta(x, e) = 2x^\top PB(x) (K(x + e) - K(x)) (x + e),$$

and  $\Xi, \Psi, P \in \mathbb{R}^{n \times n}$  are symmetric positive definite matrices. The term  $x^\top(t)\Psi x(t) - e^\top(t)\Xi e(t)$  can be viewed as a measure of deviation between the last sampled and the current states [51] and  $\zeta(x, e)$  is introduced to cope with the influence of asynchronous scheduling functions in the developments to derive an LMI-based co-design condition. The dynamics of the internal variable  $\eta(t)$  is defined as follows

$$\dot{\eta}(t) = -\lambda\eta(t) + \Gamma(x(t), e(t)), \quad (2.11)$$

where  $\eta(0) = \eta_0 \in \mathbb{R}_{\geq 0}$  is the initial condition and  $\lambda \in \mathbb{R}_{> 0}$  is a design parameter related to the decaying rate of  $\eta(t)$ .

The following lemma provides a result related to the positive definiteness of  $\eta(t)$ . This property will be crucial for the definition of an appropriate Lyapunov function candidate.

**Lemma 2.1.** *Given symmetric positive definite matrices  $\Xi, \Psi, P \in \mathbb{R}^{n \times n}$  and  $\eta_0, \theta \in \mathbb{R}_{\geq 0}$ , then  $\eta(t) \geq 0, \forall t \in [t_k, t_{k+1}), \forall k \in \mathbb{N}$ .*

*Proof.* The proof follows similar steps as [29, Lemma 2.2]. Consider the dynamic ETM (2.9). It directly ensures that  $\eta(t) + \theta\Gamma(x, e) \geq 0, \forall t \in [t_k, t_{k+1})$ . If  $\theta = 0$ , then  $\eta(t) \geq 0$  is ensured

from the last inequality. If  $\theta \neq 0$ , one has from (2.11) and (2.9) that  $\dot{\eta}(t) \geq -\left(\lambda + \frac{1}{\theta}\right)\eta(t)$ ,  $\eta(0) = \eta_0, \forall t \in [t_k, t_{k+1})$ . By the comparison lemma [42, Lemma 3.4], the solution  $\eta(t)$  is greater than or equal to the solution of  $\dot{\hat{\eta}} = -\left(\lambda + \frac{1}{\theta}\right)\hat{\eta}(t)$ , with  $\hat{\eta}(0) = \eta_0$ , which is  $\hat{\eta}(t) = \eta_0 e^{-(\lambda + \frac{1}{\theta})t}$ . As  $\hat{\eta}(t) \geq 0$ , then  $\eta(t) \geq 0$ , for all  $t \in [t_k, t_{k+1})$ ,  $\forall k \in \mathbb{N}$ . This concludes the proof.  $\square$

**Remark 2.2.** For a sufficiently large value of  $\theta$ , the dynamic ETM (2.9) reduces to the following static version which is completely independent of  $\eta(t)$

$$t_0 = 0, t_{k+1} = \inf\{t > t_k : \Gamma(x, e) < 0\}, \forall k \in \mathbb{N}, \quad (2.12)$$

with  $\Gamma(x, e)$  given in (2.10).

The existence of a MIET for the proposed dynamic CETC scheme is proved in the following lemma. It excludes the existence of Zeno behavior and enable the practical implementation of the proposed ETM.

**Lemma 2.2.** Consider the closed-loop nonlinear system (2.7) with the dynamic ETM (2.9)–(2.11). Given symmetric positive definite matrices  $\Xi, \Psi, P \in \mathbb{R}^{n \times n}$  and  $\eta_0, \theta \in \mathbb{R}_{\geq 0}$ , there exists a MIET  $\tau \in \mathbb{R}_{>0}$  such that  $t_{k+1} - t_k \geq \tau$ ,  $\forall k \in \mathbb{N}$ .

*Proof.* The lemma is proved in two parts. First, by using similar arguments as [29, Prop. 2.3], it is possible to prove that for a given  $x(t_k) \in \mathcal{D} \subset \mathbb{R}^n$  and  $\eta(t_k) \geq 0$ ,  $t_{k+1}^s \leq t_{k+1}^d$  holds, where  $t_{k+1}^s$  and  $t_{k+1}^d$  are the event instants determined by the static and dynamic rules given in (2.12) and (2.9), respectively. Then, in the sequel we prove that  $t_{k+1}^s - t_k^s \geq \tau$ , which implies that the inter-event times given by (2.9) are also lower bounded by  $\tau$ , i.e.,  $t_{k+1}^d - t_k^d \geq \tau$ .

By following similar arguments as [51, Theorem 3.2], consider the static triggering-mechanism (2.12) rewritten as

$$\mathcal{G}(x, e) > 1 - \mathcal{V}(x, e),$$

with  $\mathcal{G}(x, e) := (e^\top \Xi e) / (x^\top \Psi x)$ , and  $\mathcal{V}(x, e) := \zeta(x, e) / (x^\top \Psi x)$ . When a sample occurs at  $t = t_k$ , one has  $e = 0$  and  $\mathcal{G}(x, e) = \mathcal{V}(x, e) = 0$ . Before a new event is triggered,  $\mathcal{G}(x, e)$  must evolve from 0 to  $1 - \mathcal{V}(x, e)$ , or, alternatively, new events are not transmitted while  $\mathcal{G}(x, e) \leq 1 - \mathcal{V}(x, e)$ . Since  $\mathcal{G}(x, e) > 0, \forall t \in [t_k, t_{k+1})$ , then  $\mathcal{V}(x, e) < 1$  in the same time interval. Noticing that  $\mathcal{G}(x, e) \leq \Lambda \frac{\|e(t)\|^2}{\|x(t)\|^2}$ , with  $\Lambda = \frac{\lambda_{\max}(\Xi)}{\lambda_{\min}(\Psi)}$ , no event is triggered while

$$\frac{\|e(t)\|}{\|x(t)\|} \leq \frac{1}{\sqrt{\Lambda}} \sqrt{1 - \mathcal{V}(x, e)}.$$

By following similar steps as the proof of [28, Thm. III.1], the dynamics of  $\frac{\|e\|}{\|x\|}$  is bounded as follows

$$\begin{aligned} \frac{d}{dt} \left( \frac{\|e(t)\|}{\|x(t)\|} \right) &= -\frac{e^\top(t)\dot{x}(t)}{\|e(t)\|\|x(t)\|} - \frac{x^\top(t)\dot{x}(t)}{\|x(t)\|^2} \frac{\|e(t)\|}{\|x(t)\|} \\ &\leq \frac{\|e(t)\|\|\dot{x}(t)\|}{\|e(t)\|\|x(t)\|} + \frac{\|x(t)\|\|\dot{x}(t)\|}{\|x(t)\|^2} \frac{\|e(t)\|}{\|x(t)\|} \\ &\leq \left( 1 + \frac{\|e(t)\|}{\|x(t)\|} \right) \frac{\|\dot{x}(t)\|}{\|x(t)\|}. \end{aligned} \quad (2.13)$$

Since the state-dependent matrices  $A(x)$ ,  $B(x)$ , and  $K(\hat{x})$  are bounded for all  $x, \hat{x} \in \mathcal{D}$ , it is possible to find a constant  $L \in \mathbb{R}_{>0}$  such that

$$\|\dot{x}(t)\| = \|(A(x) + B(x)K(\hat{x}))x(t) + B(x)K(\hat{x})e(t)\| \leq L(\|x(t)\| + \|e(t)\|). \quad (2.14)$$

It follows from (2.13) and (2.14) that

$$\left( 1 + \frac{\|e(t)\|}{\|x(t)\|} \right) \frac{1}{\|x(t)\|} \|\dot{x}(t)\| \leq L \left( 1 + \frac{\|e(t)\|}{\|x(t)\|} \right)^2. \quad (2.15)$$

Then, by defining  $\varphi(t) = \frac{\|e(t)\|}{\|x(t)\|}$ , it follows from (2.13) and (2.15) the estimate

$$\dot{\varphi}(t) \leq L(1 + \varphi(t))^2, \quad (2.16)$$

from which it is possible to conclude that  $\varphi(t) \leq \psi(t, \psi_0)$ , where  $\psi(t, \psi_0)$  is the solution of the initial value problem  $\dot{\psi}(t) = L(1 + \psi(t))^2$ , with  $\psi(0, \psi_0) = \psi_0$ .

The following two cases are thus distinguished for the analysis:

(i)  $0 \leq \mathcal{V}(x, e) < 1$ : In this case, as  $\mathcal{G}(x, e) < 1$ ,  $\mathcal{G}(x, e)$  takes more time to evolve from 0 to  $1 - \mathcal{V}(x, e)$  than  $\psi(t, 0)$  to reach  $\frac{1}{\sqrt{\Lambda}}\sqrt{1 - \mathcal{V}(x, e)}$  for the first time.

(ii)  $\mathcal{V}(x, e) < 0$ : In this case,  $\psi(t, 0)$  take less time to evolve from 0 to  $\frac{1}{\sqrt{\Lambda}}$  than to  $\frac{1}{\sqrt{\Lambda}}\sqrt{1 - \mathcal{V}(x, e)}$ , since  $1 - \mathcal{V}(x, e) > 1$ . Thus, after an event is triggered,  $\mathcal{G}(x, e)$  takes more time to evolve from 0 to 1 than  $\psi(t, 0)$  to reach  $\frac{1}{\sqrt{\Lambda}}$ .

Then, the inter-event times are bounded by the time that  $\psi$  takes to evolve from 0 to  $\frac{\bar{\Lambda}}{\sqrt{\Lambda}}$ , where  $\bar{\Lambda} := \min \left( 1, \sqrt{1 - \mathcal{V}(x, e)} \right)$ . It means that the inter-event times are bounded by the solution  $\tau \in \mathbb{R}_{>0}$  of  $\psi(\tau, 0) = \frac{\bar{\Lambda}}{\sqrt{\Lambda}}$ . Since the solution of the initial value problem is  $\psi(\tau, 0) = \frac{\tau L}{1 - \tau L}$ , which is continuous at  $t = 0$ , it implies that

$$\tau = \frac{\bar{\Lambda}}{L\sqrt{\Lambda} + L\bar{\Lambda}}, \quad (2.17)$$

which is not null and there exists  $\epsilon \in \mathbb{R}_{>0}$  such that that  $t_{k+1}^s - t_k^s \geq \tau \geq \epsilon > 0$ . By invoking [29, Prop. 2.3], one can conclude that, for the same initial condition, the MIET of the dynamic ETM (2.9) is greater than or equal to that of the static ETM (2.12), thus excluding the existence of Zeno behavior. This concludes the proof.  $\square$

**Remark 2.3.** Notice from (2.17) that the MIET,  $\tau$ , has an inverse relation with  $\Lambda = \frac{\lambda_{\max}(\Xi)}{\lambda_{\min}(\Psi)}$ . Thus, if  $\lambda_{\max}(\Xi)$  is minimized and  $\lambda_{\min}(\Psi)$  is maximized, then  $\Lambda$  is reduced, possibly enlarging the inter-event times.

### 2.2.2 Co-design condition

The proposed sufficient condition to co-design the dynamic CETC scheme (2.9) and the gain-scheduled controller (2.6) is stated in the sequel.

**Theorem 2.1.** Given  $\theta, \eta_0 \in \mathbb{R}_{\geq 0}$ , and  $\lambda \in \mathbb{R}_{> 0}$ , if there exist matrices  $\tilde{K}_{\mathbf{j}} \in \mathbb{R}^{m \times n}$ ,  $\mathbf{j} \in \mathbb{B}^p$ , and symmetric positive definite matrices  $\tilde{\Xi}, \tilde{\Psi}, X \in \mathbb{R}^{n \times n}$ , such that the following LMIs are satisfied

$$\sum_{(\mathbf{i}, \mathbf{j}) \in \mathcal{P}(\mathbf{m}, \mathbf{n})} \Upsilon_{\mathbf{ij}} < 0, \quad \forall \mathbf{m}, \mathbf{n} \in \mathbb{B}^{p+}, \quad (2.18)$$

where

$$\Upsilon_{\mathbf{ij}} := \begin{bmatrix} \text{He} \left( A_{\mathbf{i}} X + B_{\mathbf{i}} \tilde{K}_{\mathbf{j}} \right) & B_{\mathbf{i}} \tilde{K}_{\mathbf{j}} & X \\ \star & -\tilde{\Xi} & 0 \\ \star & \star & -\tilde{\Psi} \end{bmatrix},$$

then, the origin of the closed-loop system (2.7) equipped with the dynamic CETC scheme (2.9)–(2.11) is asymptotically stable with  $K_{\mathbf{j}} = \tilde{K}_{\mathbf{j}} X^{-1}$ ,  $\mathbf{j} \in \mathbb{B}^p$ ,  $\Xi = X^{-1} \tilde{\Xi} X^{-1}$ ,  $\Psi = \tilde{\Psi}^{-1}$ ,  $P = X^{-1}$ , and Lyapunov function

$$W(x, \eta) = V(x) + \eta, \quad (2.19)$$

with  $V(x) = x^{\top} P x$ . In addition, a guaranteed region of attraction is given by the bounded region

$$\mathcal{R} = \{x \in \mathbb{R}^n, \eta \in \mathbb{R}_{\geq 0} : W(x, \eta) \leq c, c \in \mathbb{R}_{> 0}\}, \quad (2.20)$$

where the level set given by  $c \leq c^* = \max_{x \in \mathcal{D}} V(x)$  ensures that any state trajectory  $x(t)$  starting at

$$\mathcal{R}_0 = \{x \in \mathbb{R}^n : V(x) \leq c - \eta_0, \eta_0 \leq c\} \quad (2.21)$$

never leaves the region  $\mathcal{D}$ .

*Proof.* Assume that the LMIs (2.18) are feasible. From convexity of the state-dependent parameters, the LMIs in (2.18) imply [162, 21]:

$$\begin{aligned} & \sum_{\mathbf{i} \in \mathbb{B}^p} \sum_{\mathbf{j} \in \mathbb{B}^p} w_{\mathbf{i}}(x) w_{\mathbf{j}}(x) \Upsilon_{\mathbf{ij}} \\ &= \sum_{\mathbf{m} \in \mathbb{B}^{p+}} \sum_{\mathbf{n} \in \mathbb{B}^{p+}} w_{\mathbf{m}}(x) w_{\mathbf{n}}(x) \left( \sum_{(\mathbf{i}, \mathbf{j}) \in \mathcal{P}(\mathbf{m}, \mathbf{n})} \Upsilon_{\mathbf{ij}} \right) < 0. \end{aligned} \quad (2.22)$$

Since  $X$  is a nonsingular matrix, (2.22) can be multiplied by  $\text{diag}(X^{-1}, X^{-1}, I)$  on the left and on the right, which results in

$$\sum_{\mathbf{i} \in \mathbb{B}^p} \sum_{\mathbf{j} \in \mathbb{B}^p} \mathbf{w}_{\mathbf{i}}(x) \mathbf{w}_{\mathbf{j}}(x) \begin{bmatrix} \Theta_{\mathbf{ij}} & X^{-1} B_{\mathbf{i}} \widetilde{K}_{\mathbf{j}} X^{-1} & I \\ \star & -X^{-1} \widetilde{\Xi} X^{-1} & 0 \\ \star & \star & -\widetilde{\Psi} \end{bmatrix} < 0, \quad (2.23)$$

where  $\Theta_{\mathbf{ij}} = \text{He} \left( (X^{-1} A_{\mathbf{i}} + X^{-1} B_{\mathbf{i}} \widetilde{K}_{\mathbf{j}} X^{-1}) \right)$ . By performing the change of variables  $K_{\mathbf{j}} = \widetilde{K}_{\mathbf{j}} X^{-1}$ ,  $\mathbf{j} \in \mathbb{B}^p$ ,  $\Xi = X^{-1} \widetilde{\Xi} X^{-1}$ ,  $\Psi = \widetilde{\Psi}^{-1}$ ,  $P = X^{-1}$ , by Schur complement lemma, inequality (2.23) is equivalent to

$$\begin{bmatrix} \text{He}(PA(x) + PB(x)K(x)) + \Psi & PB(x)K(x) \\ \star & -\Xi \end{bmatrix} < 0. \quad (2.24)$$

By multiplying (2.24) by  $\begin{bmatrix} x^\top(t) & e^\top(t) \end{bmatrix}$  on the left and its transpose on the right, it follows that

$$\begin{aligned} & 2x^\top(t)P[(A(x) + B(x)K(x))x(t) + B(x)K(x)e(t)] \\ & - e^\top(t)\Xi e(t) + x^\top(t)\Psi x(t) < 0. \end{aligned} \quad (2.25)$$

For some given  $\eta_0, \theta \in \mathbb{R}_{\geq 0}$ , and  $\lambda \in \mathbb{R}_{> 0}$ , Lemma 2.1 ensures that  $\eta(t) \geq 0$ ,  $\forall t \in [t_k, t_{k+1})$ ,  $\forall k \in \mathbb{N}$ . Then, inequality (2.25) implies

$$\begin{aligned} & 2x^\top(t)P[(A(x) + B(x)K(x))x(t) + B(x)K(x)e(t)] \\ & - e^\top(t)\Xi e(t) + x^\top(t)\Psi x(t) - \lambda\eta(t) < 0. \end{aligned} \quad (2.26)$$

By adding the term  $\zeta(x, e)$  on both sides of (2.26), one has

$$\dot{x}^\top(t)Px(t) + x^\top(t)P\dot{x}(t) + \dot{\eta}(t) < 0, \quad (2.27)$$

where  $\dot{x}(t)$  and  $\dot{\eta}(t)$  are given in (2.8) and (2.11), respectively. Consider  $W(x, \eta)$  as in (2.19), from Lemma 2.1,  $W(x, \eta)$  is a positive definite and radially unbounded function and inequality (2.27) ensures  $\dot{W}(x, \eta) < 0$ . Therefore,  $W(x, \eta)$  is a Lyapunov function and the origin of the closed-loop system (2.7) with the dynamic ETM (2.9)–(2.11) is asymptotically stable. Let  $c \leq c^* = \max_{x \in \mathcal{D}} V(x)$ ,  $\mathcal{R}$  be as in (2.20) and  $\mathcal{R}_0$  be as in (2.21). As  $\mathcal{R}$  is bounded and contained in  $\mathcal{D} \times \mathbb{R}_{\geq 0}$ , then every trajectory  $(x, \eta)$  starting in  $\mathcal{R}$  remains inside it and converges asymptotically to the origin. Thus  $\mathcal{R}$  is an estimate of the region of attraction [42, Chpt.4]. Also, taking  $x(0) \in \mathcal{R}_0$ , then  $V(x(0)) \leq W(x(0), \eta_0) = V(x(0)) + \eta_0 \leq c$ , and the state  $x(t)$  never leaves  $\mathcal{D}$ . This concludes the proof.  $\square$

**Corollary 2.1.** *If there exist matrices  $\widetilde{K}_{\mathbf{j}} \in \mathbb{R}^{m \times n}$ ,  $\mathbf{j} \in \mathbb{B}^p$ , and symmetric positive definite matrices  $\widetilde{\Xi}, \widetilde{\Psi}$ ,  $X \in \mathbb{R}^{n \times n}$ , such that the LMIs (2.18) are feasible, then the origin of the*

closed-loop system (2.7) equipped with the static ETM (2.12) is asymptotically stable with  $K_{\mathbf{j}} = \tilde{K}_{\mathbf{j}}X^{-1}$ ,  $\mathbf{j} \in \mathbb{B}^p$ ,  $\Xi = X^{-1}\tilde{\Xi}X^{-1}$ ,  $\Psi = \tilde{\Psi}^{-1}$ , and  $P = X^{-1}$ , with Lyapunov function given by  $V(x) = x^\top Px$ . Furthermore, an estimate of its region of attraction is given by the bounded region  $\mathcal{R}_0$  in (2.21) with  $\eta_0 = 0$ .

*Proof.* The proof follows similar steps as the proof of Theorem 2.1 until inequality (2.25). Then, by adding  $\zeta(x, e)$  on both sides of (2.25), one has  $\dot{V}(x) < -\Gamma(x, e)$ , with  $V(x) = x^\top Px$  and  $\Gamma(x, e)$  given in (2.10). Since for all  $t \in [t_k, t_{k+1})$ ,  $\forall k \in \mathbb{N}$ , the triggering mechanism (2.12) ensures  $\Gamma(x, e) \geq 0$ , it implies that  $\dot{V}(x) < 0$ ,  $\forall t \in [t_k, t_{k+1})$ . Also, at  $t = t_k$ , one has  $\dot{V}(x) < -x^\top(t)\Psi x(t) < 0$ . Thus, the origin of the closed-loop system (2.7) with the static ETM (2.12) is asymptotically stable. This concludes the proof.  $\square$

**Remark 2.4.** If a linear state-feedback control law as  $u(t) = K\hat{x}(t)$  is considered, there is no asynchronous phenomenon affecting the closed-loop system (2.8), which makes the developments to obtain the LMI-based co-design conditions amenable when compared to the gain-scheduled case. Although the use of linear state-feedback controllers can be attractive from this point-of-view, it may introduce conservativeness to the co-design condition. Also notice that the relaxation in (2.22) can only be employed because the proposed ETM (2.9)–(2.11) can completely cancel out the influence of asynchronous scheduling functions. This relaxation allows to properly design the gain-scheduled controller (2.6) since it avoids checking the negativeness of the left-hand side of (2.22) for all vertices, preventing the gain-scheduled structure from reducing to a linear one, that is,  $K_{\mathbf{j}} = K, \forall \mathbf{j} \in \mathbb{B}^p$ .

### 2.2.3 Enlargement of inter-event times

As discussed in Remark 2.3, to obtain larger inter-event times and, consequently, reduce the number of generated events,  $\lambda_{\max}(\Xi)$  should be minimized and  $\lambda_{\min}(\Psi)$  maximized. To achieve this goal, by following a similar strategy to the one considered by [51, 52, 53], a convex optimization problem subject to LMI constraints is proposed as follows:

$$\min_{Q, X, \tilde{\Xi}, \tilde{\Psi}, \tilde{K}_{\mathbf{j}}} \text{tr}(\tilde{\Xi} + \tilde{\Psi} + Q) \quad (2.28)$$

$$\text{subject to } \begin{bmatrix} -Q & I \\ \star & -X \end{bmatrix} < 0 \quad (2.29)$$

and LMIs in (2.18),

where  $Q$  is a symmetric positive definite matrix. The objective function in (2.28) is defined aiming to minimize the eigenvalues of  $Q$ ,  $\tilde{\Xi}$ , and  $\tilde{\Psi}$ . From Schur complement lemma, one has that (2.29) is equivalent to  $X^{-1} < Q$ . Then, the minimization of  $\text{tr}(Q)$  implies the minimization of the eigenvalues of  $X^{-1}$ . Also, since the triggering matrices are given by  $\Xi = X^{-1}\tilde{\Xi}X^{-1}$  and  $\Psi = \tilde{\Psi}^{-1}$ , the solution of the optimization problem tends to reduce

$\Lambda = \frac{\lambda_{\max}(\Xi)}{\lambda_{\min}(\Psi)}$ , once  $\lambda_{\max}(\Xi)$  is minimized and  $\lambda_{\min}(\Psi)$  is maximized. From Remark 2.3, it is possible to argue that the inter-event times of the proposed dynamic and static CETC schemes can be enlarged.

#### 2.2.4 Estimate of the region of attraction

Once the optimization problem (2.28) has been solved, it is necessary to determine the estimate of the region of attraction  $\mathcal{R}$  given in (2.20). Consider the polytopic region  $\mathcal{X}$  in the half-space representation:

$$\mathcal{D} = \{x \in \mathbb{R}^n : |b_i^\top x| \leq 1, b_i \in \mathbb{R}^n, i \in \mathbb{N}_{\leq n_f}\}, \quad (2.30)$$

where  $n_f$  is half of the number of faces. The largest region  $\mathcal{R}$  is determined choosing [42, Chpt. 8]

$$c^* = \max_{x \in \mathcal{D}} V(x) < \min_{1 \leq i \leq n_f} \frac{1}{b_i^\top P^{-1} b_i}. \quad (2.31)$$

Notice that if  $\eta_0 = 0$ , the set of initial conditions  $\mathcal{R}_0$  in (2.21) is enlarged.

### 2.3 Numerical examples

In this section, two physically motivated numerical examples are provided to illustrate the effectiveness of the proposed co-design conditions.

#### 2.3.1 Example 1: van der Pol oscillator

Consider the forced van der Pol oscillator system [30]:

$$\begin{aligned} \dot{x}_1(t) &= x_2(t) \\ \dot{x}_2(t) &= (1 - x_1^2(t))x_2(t) - x_1(t) + u(t), \end{aligned} \quad (2.32)$$

where it is assumed the modeling region  $\mathcal{D} = \{x \in \mathbb{R}^2 : |x_i| \leq r_0, i \in \mathbb{N}_{\leq 2}\}$ . The set of differential equations (2.32) can be easily put in the format of (2.1) as follows:

$$\begin{bmatrix} \dot{x}_1(t) \\ \dot{x}_2(t) \end{bmatrix} = \begin{bmatrix} 0 & 1 \\ -1 & 1 - x_1^2(t) \end{bmatrix} \begin{bmatrix} x_1(t) \\ x_2(t) \end{bmatrix} + \begin{bmatrix} 0 \\ 1 \end{bmatrix} u(t). \quad (2.33)$$

By selecting the scheduling function  $z_1(x) = x_1^2$ , which is bounded within  $\mathcal{D}$  by  $z^0 = 0$  and  $z^1 = r_0^2$ , the matrices  $A(x)$  and  $B(x)$  can thus be written as:

$$A(x) = \begin{bmatrix} 0 & 1 \\ -1 & 1 \end{bmatrix} + z_1(x) \begin{bmatrix} 0 & 0 \\ 0 & -1 \end{bmatrix}, \quad \text{and} \quad B(x) = \begin{bmatrix} 0 \\ 1 \end{bmatrix} + z_1(x) \begin{bmatrix} 0 \\ 0 \end{bmatrix},$$

from where it is clear their affine dependence with respect to  $z_1(x)$ .

Then, by following the sector-nonlinearity approach, the system (2.33) can be equivalently represented within  $\mathcal{D}$  by the following polytopic quasi-LPV model as (2.4)

$$\dot{x}(t) = w_0(x) (A_0 x(t) + B_0 u(t)) + w_1(x) (A_1 x(t) + B_1 u(t)),$$

where the state-dependent parameters are

$$w_0(x) = \frac{r_0^2 - x_1^2(t)}{r_0^2}, \quad w_1(x) = 1 - w_0(x),$$

and the vertices matrices are

$$\begin{aligned} A_0 &= \begin{bmatrix} 0 & 1 \\ -1 & 1 \end{bmatrix}, & B_0 &= \begin{bmatrix} 0 \\ 1 \end{bmatrix}, \\ A_1 &= \begin{bmatrix} 0 & 1 \\ -1 & 1 - r_0^2 \end{bmatrix}, & B_1 &= \begin{bmatrix} 0 \\ 1 \end{bmatrix}. \end{aligned} \tag{2.34}$$

Here, the modeling region is defined with  $r_0 = 5$ . By solving<sup>1</sup> the optimization problem (2.28), the following control gains and triggering matrices are obtained

$$\begin{aligned} K_0 &= \begin{bmatrix} -0.559 & -3.5 \end{bmatrix}, \quad K_1 = \begin{bmatrix} -6.05 & -3.01 \end{bmatrix}, \\ \Xi &= \begin{bmatrix} 1.36 & 1.34 \\ 1.34 & 6.39 \end{bmatrix}, \quad \Psi = \begin{bmatrix} 0.951 & 0.333 \\ 0.333 & 1.81 \end{bmatrix}, \quad P = \begin{bmatrix} 2.08 & 0.41 \\ 0.41 & 1.83 \end{bmatrix}. \end{aligned} \tag{2.35}$$

On the other hand, for a linear state feedback control law, the optimization problem (2.28) is feasible with

$$K = \begin{bmatrix} -1.698 & -3.435 \end{bmatrix}, \quad P = \begin{bmatrix} 3.22 & 0.253 \\ 0.253 & 1.46 \end{bmatrix}.$$

Also, consider the emulation condition [177, Corollary 5.2] for sampled-data nonlinear systems in the polytopic representation (2.4) with a linear control law  $u(t) = Kx(t)$ . By solving it with  $\alpha = 0.01$  and the control gain obtained, the closed-loop stability is certified with a maximum sampling interval of 0.242s.

The proposed ETC co-design approach is compared with the sampled-data emulation approach in [177, Corollary 5.2]. Let  $\mathcal{R}_{0,1}$  and  $\mathcal{R}_{0,2}$  denote, respectively, the sets of state initial conditions for the ETM system with the gain-scheduled controller and the linear controller, both with  $\eta_0 = 0$ ; and  $\mathcal{R}_{0,3}$  the set with the emulation condition in [177, Corollary 5.2]. Based on (2.31), the largest set of initial conditions  $\mathcal{R}_{0,1}$  is obtained with  $c_1^* = 43.759$ ,  $\mathcal{R}_{0,2}$  is achieved with  $c_2^* = 36.039$ , and  $\mathcal{R}_{0,3}$  with  $c_3^* = 21.802$ . These regions are depicted in Fig. 2.1, in which it is clearly observed that  $\mathcal{R}_{0,1}$  is larger than  $\mathcal{R}_{0,2}$  and  $\mathcal{R}_{0,3}$ , and also  $\mathcal{R}_{0,3} \subset \mathcal{R}_{0,2}$ . This illustrates the conservativeness reduction provided by

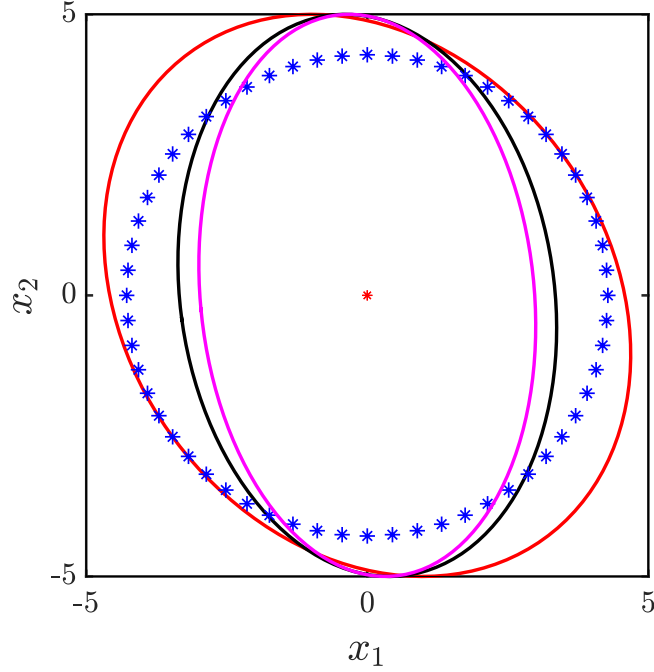


**Figure 2.1** – Regions of state initial conditions  $\mathcal{R}_{0,1}$  (in red),  $\mathcal{R}_{0,2}$  (in black), and  $\mathcal{R}_{0,3}$  (in magenta) obtained with [177, Corollary 5.2]. The initial conditions are denoted by ‘\*’.

the gain-scheduling structure (as discussed in Remark 2.4) and by the proposed co-design approach when compared to an emulation approach.

The effectiveness of the proposed co-design approach is also evaluated in terms of average inter-event times computed<sup>2</sup> from 60 simulations performed with the initial conditions  $x(0) = \left[ 4.28 \cos\left(\frac{2\pi}{60}i\right) \ 4.28 \sin\left(\frac{2\pi}{60}i\right) \right]^\top$ ,  $i \in \mathbb{N}_{\leq 60}$ ,  $\eta_0 = 0$ , as shown in Figure 2.1, and simulation time of 30s. Notice that only the origin of the closed-loop system, using the gain-scheduled controller, has the asymptotic stability ensured for these initial conditions. The proposed static and dynamic ETC co-design approaches are compared with the static ETM proposed by [28] designed as in [30] by following the emulation-based approach with  $V(x) = 0.0058679x_1^2 + 0.0040791x_1x_2 + 0.0063684x_2^2$ ,  $u = -x_2 - (1 - x_1^2)x_2$ , and  $W(e) = 2.222e^2$ , with  $e = \hat{u} - u$ . In this case, the triggering rule is  $W(e) \geq V(x)$ . The results are presented in Table 2.1.

Notice that the proposed static and dynamic ETMs designed with the co-design approach provided larger average inter-event times than the emulation-based approach [28]. Moreover, the average inter-event times of the proposed ETC approaches are larger than the maximum sampling interval of 0.242s obtained with the time-triggered approach

<sup>1</sup> The optimization problem is solved in MATLAB environment using the LMI parser YALMIP [153] and the semidefinite programming solver Mosek.

<sup>2</sup> The average inter-event time is the relation between the simulation time and the total number of events.

**Table 2.1** – Mean of average inter-event times, in seconds, for the different approaches.

Static ETC			
ETM [28]	0.0301		
Corollary 2.1 - gain-scheduling	0.6915		
Dynamic ETC	$\lambda = 0.1$	$\lambda = 0.3$	$\lambda = 0.5$
Theorem 2.1 ( $\theta = 1$ )	0.8540	0.7643	0.7159
Theorem 2.1 ( $\theta = 10$ )	0.8671	0.8157	0.7301
Theorem 2.1 ( $\theta = 10^2$ )	0.8842	0.8261	0.7227
Theorem 2.1 ( $\theta = 10^5$ )	0.8290	0.7594	0.7324

[177, Corollary 5.2]. It can also be noticed that the design parameters  $\theta$  and  $\lambda$  can be adjusted to reduce the network usage, in particular, it is verified that the different dynamic ETC setups could provide larger average inter-event times than the static ETC. Notice that as  $\lambda$  increases,  $\eta(t)$  tends faster to the origin, which reduces the average inter-event times. Also, as  $\theta$  increases, the average inter-event times increases when  $\theta = 10^2$ , then it is reduced when  $\theta = 10^5$  because the dynamic ETM (2.9) tends to the static one (2.12), as stated in Remark 2.2. Thus, the reported results illustrate that the dynamic ETC saves more communication resources when compared to its static counterpart.

To illustrate the application of the proposed CETC co-design approach, consider the implementation of the static CETC scheme given in (2.12) with the control gains and triggering parameters in (2.35). Figure 2.2 depicts the simulation performed during 30 s with initial condition is  $x(0) = [4.2467 \ 1.1155]^\top$ . From Figure 2.2(a), it is possible to notice that the states converge asymptotically to the equilibrium  $x = 0$ . The functions  $\mathcal{G}(x, e)$  and  $1 - \mathcal{V}(x, e)$  defined in the proof of the existence of a MIET in Lemma 2.2 are shown in Figure 2.2(b). The arguments provided in Lemma 2.2 can be clearly observed since always that  $\mathcal{G}(x, e) = 1 - \mathcal{V}(x, e)$  a new event is transmitted, as it can be observed in Figure 2.2(c). To conclude, the control input signal  $u(t)$  is shown in Figure 2.2(d), where it is clear the effect of the ZOH in the compute of  $u(t)$ .

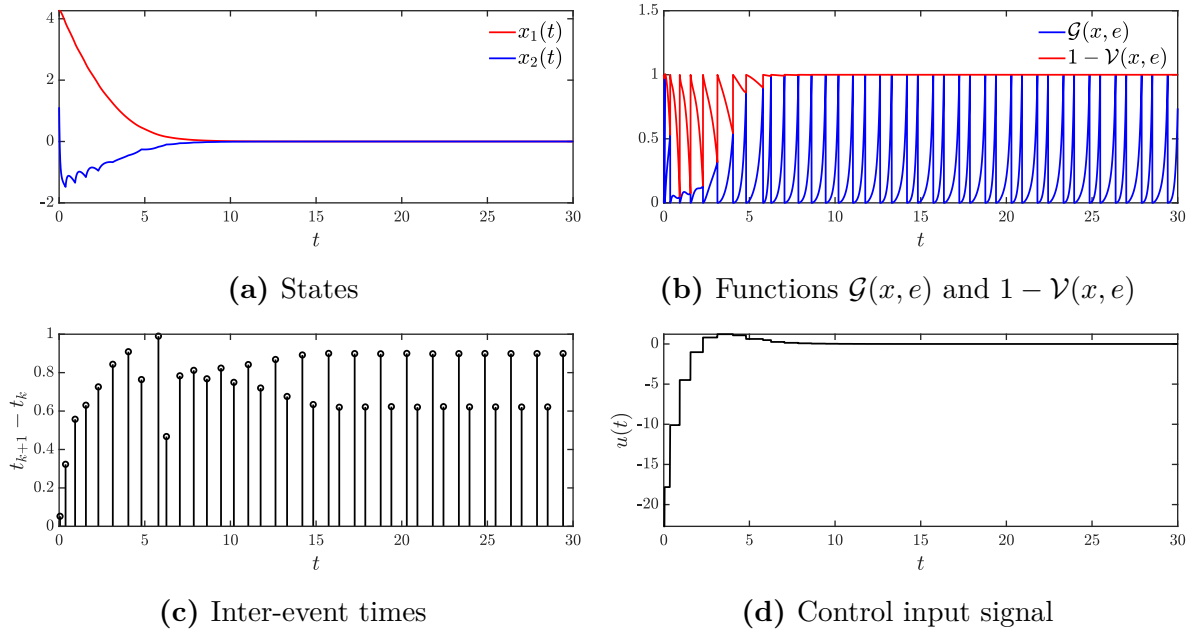


**Figure 2.2** – Simulation of the closed-loop system (2.32) with the gain-scheduling control law (2.6) under the static ETM (2.12).

The simulation for the dynamic CETC co-design approach is shown in Figure 2.3. In particular, the time-series of the internal variable  $\eta(t)$  is shown in Figure 2.3(a) together with the state  $x(t)$ . Notice that  $\eta(t)$  is non-negative for all  $t$ , as expected from Lemma 2.1, and it converges to the equilibrium  $\eta = 0$ . The effect of  $\eta(t)$  produces the enlargement of the inter-event times, as shown in Figure 2.2(b), because it can be seen as a buffer that stores unnecessary decrease of  $V(x) = x^\top P x$ . In this case, 30 events are generated and the maximum inter-event time is 3.421s, while the one for the static CETC is only 0.99s. The control input signal  $u(t)$  is shown in Figure 2.2(c).

### 2.3.2 Example 2: rotational motion of a cart with an inverted pendulum

Consider the following rotational motion of a cart with an inverted pendulum system [178]

$$\begin{aligned}\dot{x}_1(t) &= x_2(t) \\ \dot{x}_2(t) &= \sin(x_1(t)) - x_2(t) - \cos(x_1(t))u(t),\end{aligned}\tag{2.36}$$

where  $x_1(t)$  is the pendulum angle with respect to the vertical axis and  $x_2(t)$  is the angular velocity. As the trigonometric nonlinear terms  $\sin(x_1(t))$  and  $\cos(x_1(t))$  depend on the state  $x_1(t)$ , one can define the following modeling region  $\mathcal{D} = \{x \in \mathbb{R}^2 : |x_1| \leq \theta_0, |x_2| \leq 2\}$ . However, this system can not be put directly in the form (2.1). For that purpose, the trigonometric function  $\sin(x_1(t))$  is expanded in Maclaurin series, which results the factorization

$$\sin(x_1(t)) = z_1(x)x_1(t),$$

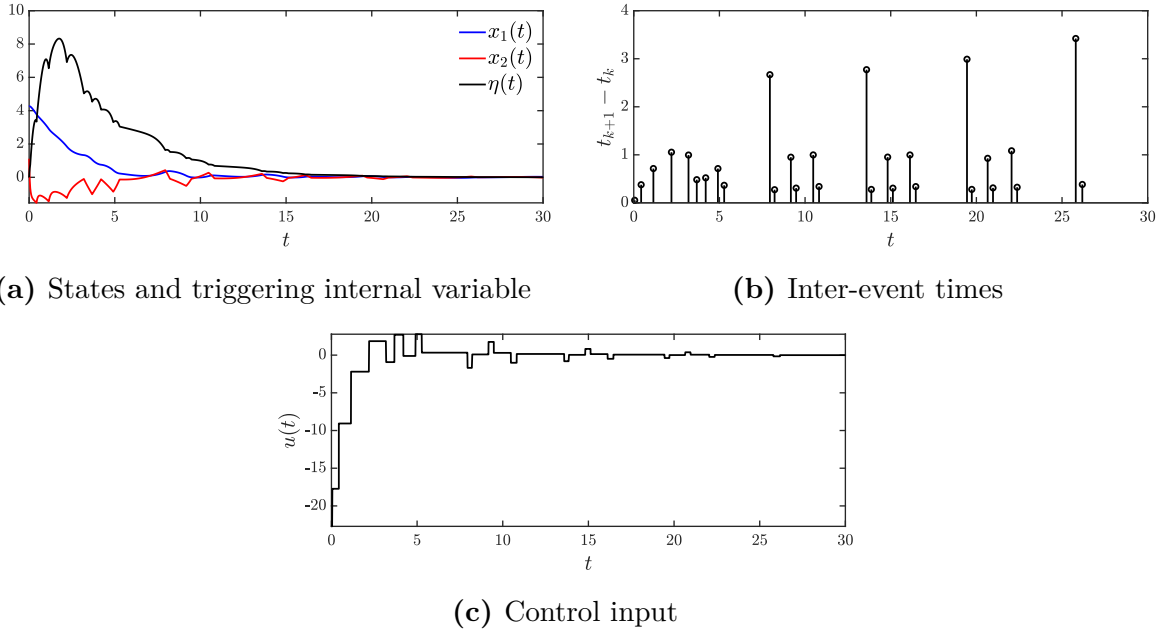


**Figure 2.3** – Simulation of the closed-loop system (2.32) with the gain-scheduling control law (2.6) under the dynamic ETM (2.9)–(2.11).

where

$$z_1(x) = \sum_{i=0}^{\infty} \frac{(-1)^i}{(2i+1)!} x_1^{2i}(t).$$

Then, (2.36) can be written as (2.1) as follows:

$$\begin{bmatrix} \dot{x}_1(t) \\ \dot{x}_2(t) \end{bmatrix} = \begin{bmatrix} 0 & 1 \\ z_1(x) & -1 \end{bmatrix} \begin{bmatrix} x_1(t) \\ x_2(t) \end{bmatrix} + \begin{bmatrix} 0 \\ -\cos(x_1(t)) \end{bmatrix} u(t).$$

By selecting the scheduling functions  $z_1(x) \in [\sin(\theta_0)/\theta_0, 1]$  and  $z_2(x) = \cos(x_1) \in [\cos(\theta_0), 1]$ ,  $\forall x \in \mathcal{D}$ , the matrices  $A(x)$  and  $B(x)$  can be written with an affine dependence with respect to  $z_1(x)$  and  $z_2(x)$ :

$$A(x) = \begin{bmatrix} 0 & 1 \\ z_1(x) & -1 \end{bmatrix} \quad B(x) = \begin{bmatrix} 0 \\ -z_2(x) \end{bmatrix}.$$

Then, the polytopic quasi-LPV model (2.4) is thus defined by the state-dependent parameters

$$\begin{aligned} w_{00}(x) &= w_0^1(x)w_0^2(x), & w_{01}(x) &= w_0^1(x)w_1^2(x), \\ w_{10}(x) &= w_1^1(x)w_0^2(x), & w_{11}(x) &= w_1^1(x)w_1^2(x), \end{aligned}$$

with  $w_0^1(x) = (1 - z_1(x)) / \left(1 - \frac{\sin(\theta_0)}{\theta_0}\right)$ ,  $w_1^1(x) = 1 - w_0^1(x)$ ,  $w_0^2(x) = (1 - z_2(x)) / (1 - \cos(\theta_0))$ ,  $w_1^2(x) = 1 - w_0^2(x)$ , and the following vertices

$$\begin{aligned} A_{00} = A_{01} &= \begin{bmatrix} 0 & 1 \\ \frac{\sin(\theta_0)}{\theta_0} & -1 \end{bmatrix}, & B_{00} = B_{10} &= \begin{bmatrix} 0 \\ -\cos(\theta_0) \end{bmatrix}, \\ A_{10} = A_{11} &= \begin{bmatrix} 0 & 1 \\ 1 & -1 \end{bmatrix}, & B_{01} = B_{11} &= \begin{bmatrix} 0 \\ -1 \end{bmatrix}. \end{aligned} \tag{2.37}$$

Notice that this system can not be modeled as a Lur'e-type system [144] nor a system with cone-bounded nonlinear inputs [179, 52] since both matrices  $A(x)$  and  $B(x)$  are state-dependent. This indicates that the proposed co-design approach can be employed in a broader class of nonlinear systems.

By solving the optimization problem (2.28) for  $\theta_0 = 4\pi/9$ , the following control gains and triggering matrices are obtained:

$$\begin{aligned} K_{00} &= \begin{bmatrix} 9.51 & 6.26 \end{bmatrix}, K_{01} = \begin{bmatrix} 1.52 & 1.0 \end{bmatrix}, \\ K_{10} &= \begin{bmatrix} 11.1 & 7.28 \end{bmatrix}, K_{11} = \begin{bmatrix} 2.96 & 1.95 \end{bmatrix}, \\ \Xi &= \begin{bmatrix} 6.15 & 4.05 \\ 4.05 & 2.67 \end{bmatrix}, \Psi = \begin{bmatrix} 1.24 & 0.416 \\ 0.416 & 1.23 \end{bmatrix}, P = \begin{bmatrix} 2.13 & 1.0 \\ 1.0 & 1.01 \end{bmatrix}. \end{aligned}$$

Both the proposed static and dynamic ETC schemes are applied. The dynamic ETC parameters are  $\theta = 10$ ,  $\lambda = 0.8$ , and  $\eta_0 = 0$ . According to (2.31), for  $\eta_0 = 0$ , the level set that leads to the largest region  $\mathcal{R}_0$  inside the modeling region is  $c^* = 2.158$ . The region  $\mathcal{R}_0 \subset \mathcal{D}$  is shown in Fig. 2.4, where are also shown several trajectories of the closed-loop system (2.7) equipped with the dynamic ETM (2.9)–(2.11) for initial conditions inside and outside the modeling region. Notice that there are some trajectories starting inside of  $\mathcal{D}$  that converge but evolve outside of  $\mathcal{R}_0$ , while some others even diverge. This illustrates the importance of determining an estimate of the region of attraction.

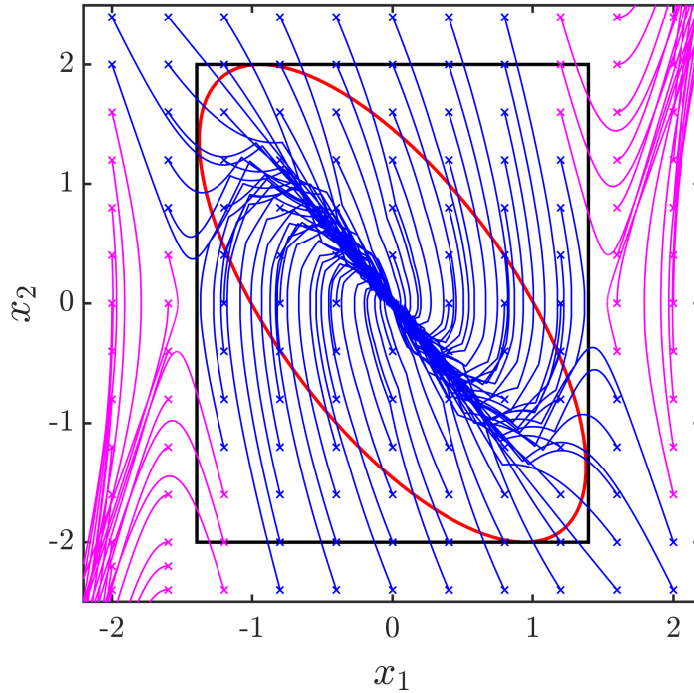


**Figure 2.4** – Region of state initial conditions  $\mathcal{R}_0$  (in red) of the origin of the closed-loop system (2.7) with the dynamic ETM (2.9)–(2.11). The region  $\mathcal{R}_0$  is contained in the polytopic region  $\mathcal{D}$  (in black). The convergent (in blue) and divergent (in magenta) trajectories are also depicted considering initial conditions denoted by “ $\times$ ”.

Here, both proposed static and dynamic ETC schemes are applied. The dynamic ETC parameters are  $\theta = 10$ ,  $\lambda = 0.8$ , and  $\eta_0 = 0$ . Consider the initial condition  $x(0) = [-0.1392 \ 1.5903]^\top \in \mathcal{R}_0$  and simulation time of 15 s. The simulation for the closed-loop system with the static CETC scheme is depicted in Figure 2.5. In particular, as shown in Figure 2.5(b), in this example the function  $1 - \mathcal{V}(x, e)$  is larger than 1, illustrating the case (ii) in the proof of Lemma 2.2. In this case, 23 events are transmitted, and the average inter-event time is 0.6699 s.

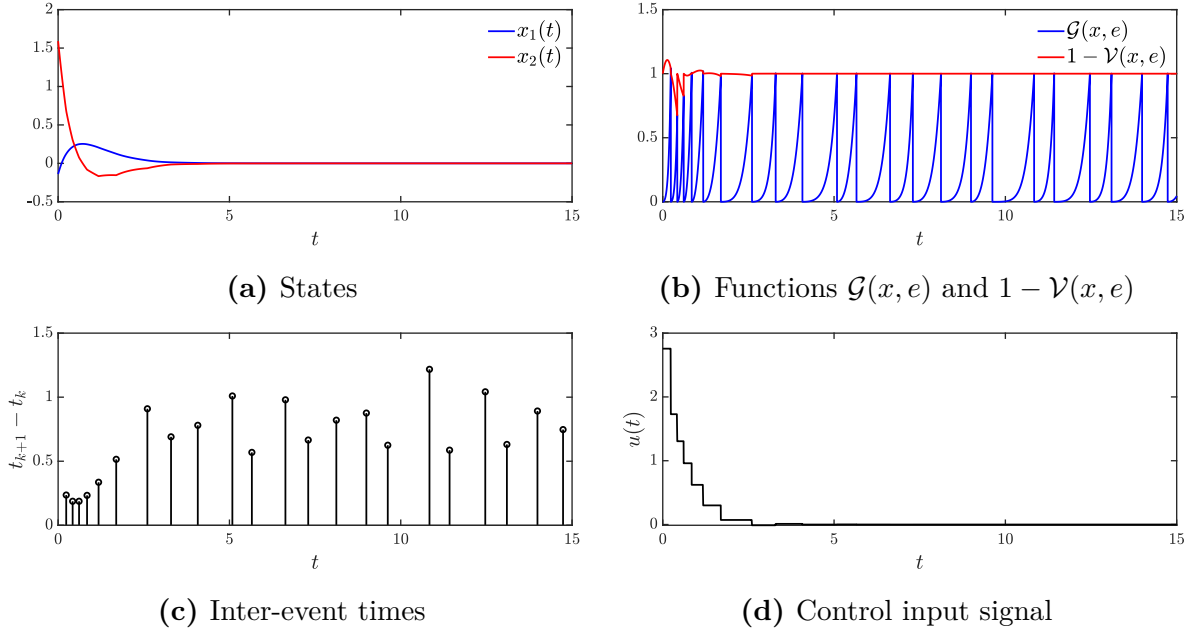


**Figure 2.5** – Simulation of the closed-loop system (2.36) with the gain-scheduling control law (2.6) equipped with the static ETC scheme (2.12).

The simulation for the closed-loop system with the dynamic CETC scheme is depicted in Figure 2.6. In contrast to the static CETC scheme, the number of events with the dynamic ETC is reduced to 17 and the average inter-event time is enlarged to 0.8511 s. Moreover, the minimum and maximum inter-event times are 0.1975 s and 2.2965 s, respectively, which illustrates the Zeno-freeness ensured by Lemma 2.2. This confirms the advantage of the dynamic ETC in saving network resources over the static counterpart. It can be observed from Figure 2.6(a) that both system state  $x(t)$  and trigger internal variable  $\eta(t)$  converge asymptotically to the equilibrium  $(x, \eta) = (0, 0)$ . However, even  $\eta(t)$  converging to zero, its effect in the triggering mechanism is clearly illustrated in Figure 2.6(b), where the function  $1 - \mathcal{V}(x, e) + \frac{1}{\theta} \frac{\eta(t)}{x^\top(t) \Psi x(t)}$  is shown instead of  $1 - \mathcal{V}(x, e)$  for the static case. Notice that as  $x(t)$  converge to the origin, the function  $1 - \mathcal{V}(x, e) + \frac{1}{\theta} \frac{\eta(t)}{x^\top(t) \Psi x(t)}$  does not converge to 1, as the function  $1 - \mathcal{V}(x, e)$ , which may postpone the occurrence of transmissions, as one can observe in Figure 2.6(c).

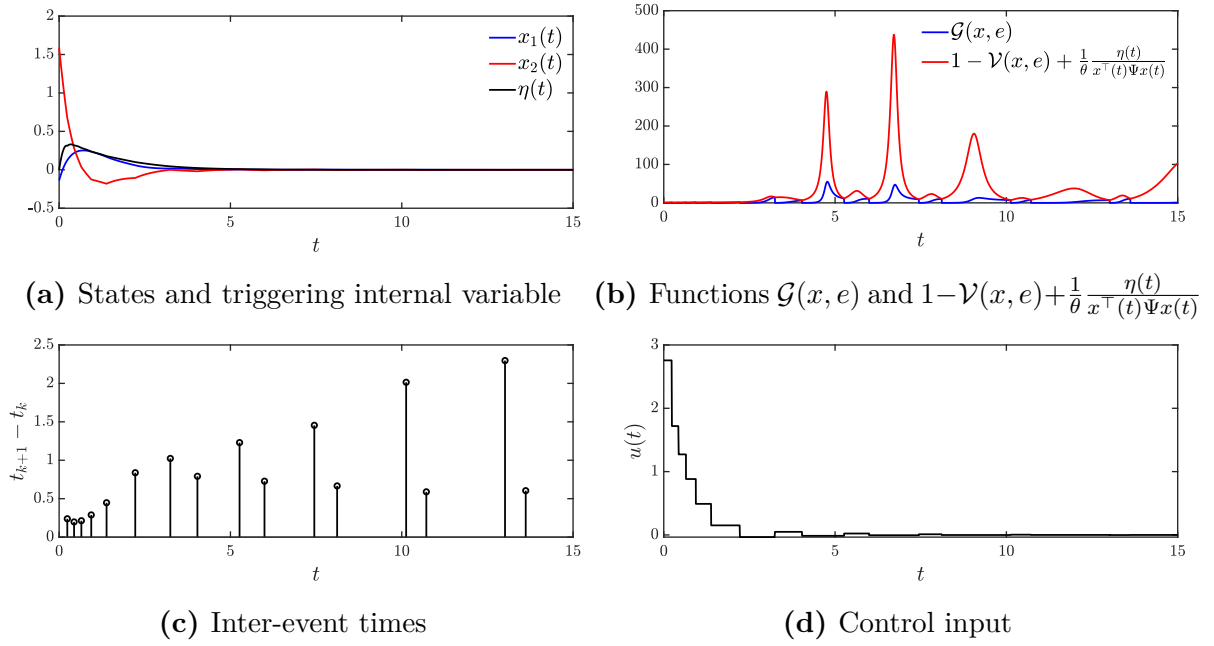


**Figure 2.6** – Simulation of the closed-loop system (2.36) with the gain-scheduling control law (2.6) equipped with the dynamic ETC scheme (2.9)–(2.11).

## 2.4 Conclusion

This chapter has investigated the co-design problem of dynamic continuous ETMs and gain-scheduled state-feedback controllers for a class of nonlinear systems represented by quasi-LPV models. Based on the quasi-LPV representation, a convex optimization problem subject to LMI constraints was proposed to systematically perform the co-design and to enlarge the inter-event times. The proposed trigger function was effective to cancel out the influence of asynchronous scheduling functions and a less conservative LMI-based co-design condition has been derived by means of the Lyapunov stability theory. Also, a formal proof of the existence of a MIET was provided, which excluded the existence of Zeno solutions. Numerical examples have been provided to illustrate the effectiveness of the proposal in providing larger average inter-event times than an emulation-based ETC scheme and the static counterpart of the proposed dynamic CETC. From the implementation point-of-view, the main advantage of the dynamic scheme is the reduction of transmissions, corresponding to more communication resources economy. On the other hand, in comparison with the static scheme, the dynamic requires the solution of a differential equation to determine the evolution of the internal variable.

### 3 DYNAMIC PETC WITH NETWORK-INDUCED DELAYS

This chapter investigates the co-design of dynamic periodic ETMs and state feedback controllers for nonlinear networked control systems. The considered class of nonlinear systems is such that an equivalent local quasi-LPV model is obtained. Initially, a local stability analysis condition is provided for general input-affine nonlinear systems. Then, an improved co-design condition is proposed to ensure the local asymptotic stability of the closed-loop system by using the Wirtinger-based integral inequality and the delay-dependent reciprocally convex combination lemma. Numerical examples illustrate the advantages of the proposed dynamic PETC co-design approach over its static counterpart.

This chapter is organized as follows. Preliminary results are revisited in Section 3.1. The problem is formulated in Section 3.2. The proposed local stability analysis and the dynamic PETC co-design condition are presented in Section 3.3. As a direct consequence, the particularization of the co-design condition is derived for the static PETC case. Numerical examples are presented in Section 3.4 to illustrate the condition's effectiveness. Finally, conclusions are presented in Section 3.5.

#### 3.1 Preliminary results

This section presents useful technical lemmas for obtaining the proposed dynamic PETC co-design conditions. The delay-dependent reciprocally convex inequality employed here has been studied by [165, 167, 180] (not in the context of ETC) and it contains the standard version proposed by [146] as a particular case.

**Lemma 3.1.** *Let  $n \in \mathbb{N}$ , and  $R_1, R_2 \in \mathbb{R}^{n \times n}$  be symmetric positive definite matrices. If there exist symmetric matrices  $X_1, X_2 \in \mathbb{R}^{n \times n}$  and matrices  $Y_1, Y_2 \in \mathbb{R}^{n \times n}$  such that*

$$\begin{bmatrix} R_1 & 0 \\ 0 & R_2 \end{bmatrix} - \alpha \begin{bmatrix} X_1 & Y_1 \\ Y_1^\top & 0 \end{bmatrix} - (1 - \alpha) \begin{bmatrix} 0 & Y_2 \\ Y_2^\top & X_2 \end{bmatrix} \geq 0, \quad (3.1)$$

*holds for  $\alpha \in \mathbb{B}$ . Then, the following inequality holds for all  $\alpha \in (0, 1) \subset \mathbb{R}$ :*

$$\begin{bmatrix} \frac{1}{\alpha} R_1 & 0 \\ 0 & \frac{1}{1-\alpha} R_2 \end{bmatrix} \geq \begin{bmatrix} R_1 & 0 \\ 0 & R_2 \end{bmatrix} + (1 - \alpha) \begin{bmatrix} X_1 & Y_2 \\ Y_2^\top & 0 \end{bmatrix} + \alpha \begin{bmatrix} 0 & Y_1 \\ Y_1^\top & X_2 \end{bmatrix}.$$

*Proof.* The proof can be found in [165, 180]. □

**Remark 3.1.** *As remarked by [165, 180], the improved version of the reciprocally convex inequality lemma given in Lemma 3.1 allows deriving delay-dependent conditions due to the dependence on the parameter  $\alpha$ , which will be related to the time-varying network-induced delay. Notice also that, in contrast to the standard version given by [146] and largely*

employed in the ETC literature, see [100, 101, 102, 105, 121] and references therein, Lemma 3.1 has the additional variables  $X_1$  and  $X_2$ . However, in order to reduce the number of involved decision variables and reduce the numerical complexity, one can select  $X_1 = R_1 - Y_1 R_2^{-1} Y_1^\top$  and  $X_2 = R_2 - Y_2^\top R_1^{-1} Y_2$ , which is also a valid choice for condition (3.1). Finally, notice that the particular choices  $X_1 = X_2 = 0$  and  $Y_1 = Y_2$  reduce Lemma 3.1 to the standard version of the reciprocally convex inequality [146].

To take advantage of the delay-dependent reciprocally convex inequality, the Wirtinger-based integral inequality is employed to reduce the design conservativeness. It is stated as follows.

**Lemma 3.2** (Wirtinger-based integral inequality [147]). *For any symmetric positive definite matrix  $R \in \mathbb{R}^{n \times n}$ , the following inequality holds for all continuously differentiable function  $\omega \in [a, b] \rightarrow \mathbb{R}^n$ :*

$$(b-a) \int_a^b \dot{\omega}^\top(s) R \dot{\omega}(s) ds \geq (\omega(b) - \omega(a))^\top R (\omega(b) - \omega(a)) + 3\tilde{\Omega}^\top R \tilde{\Omega}, \quad (3.2)$$

where  $\tilde{\Omega} = \omega(b) + \omega(a) - \frac{2}{b-a} \int_a^b \omega(s) ds$ .

### 3.2 Problem formulation

The PETC setup is shown in Figure 3.1, where the state information measured from the plant is transmitted to the controller via a multi-purpose communication network, whose transmission instants are determined by an ETM.

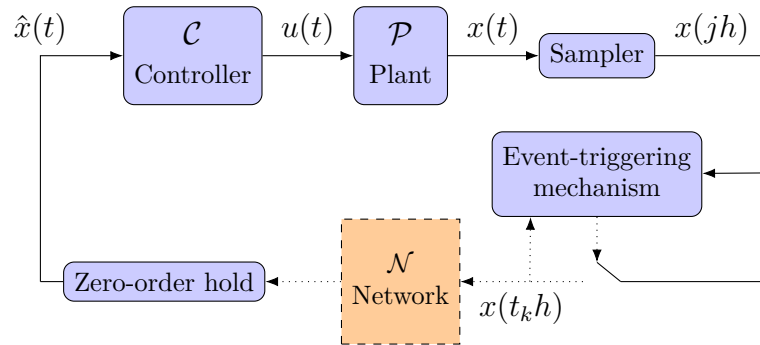


**Figure 3.1** – Representation of the PETC control setup, where  $\mathcal{P}$  is the continuous-time plant,  $\mathcal{C}$  is a static state feedback controller,  $\mathcal{N}$  is the communication channel,  $x(t)$  is the continuous state measurement,  $x(jh)$  is the sampled state measurement,  $x(t_k h)$  is the most recently transmitted state measurement,  $\hat{x}(t)$  is  $x(t_k h)$  affected by network-induced delays, and  $u(t)$  is the control input.

Consider the plant given by the following class of continuous-time nonlinear systems:

$$\dot{x}(t) = f(x(t)) + g(x(t))u(t), \quad x(0) = x_0 \text{ given}, \quad (3.3)$$

where  $x(t) \in \mathbb{R}^n$  is the state,  $u(t) \in \mathbb{R}^m$  is the control input,  $f : \mathcal{D} \rightarrow \mathbb{R}^n$ , with  $f(0) = 0$ , is a continuously differentiable function,  $g : \mathcal{D} \rightarrow \mathbb{R}^{n \times m}$ , with  $g(x) \neq 0, \forall x \in \mathcal{D}$ , is a continuous function. The region  $\mathcal{D} \subset \mathbb{R}^n$  is assumed to be a convex polytope containing the origin  $x = 0$  and it admits the following half-space representation:

$$\mathcal{D} = \{x \in \mathbb{R}^n : b_j^\top x \leq 1, \forall j \in \mathbb{N}_{\leq n_f}\}, \quad (3.4)$$

where  $b_j \in \mathbb{R}^n, \forall j \in \mathbb{N}_{\leq n_f}$ , define the hyperplanes.

The following state feedback control law is considered:

$$u(t) = k(\hat{x}(t)), \quad (3.5)$$

where  $\hat{x} \in \mathcal{D}$  is the most recent state information available to the controller,  $k : \mathcal{D} \rightarrow \mathbb{R}^m$ , with  $k(0) = 0$ , is a continuously differentiable function, and  $u(t) = 0, \forall t < 0$ .

In the PETC setup in Figure 3.1, the sampled state measurement  $x(jh)$  is available to the ETM to determine the next transmission instant, where the periodic sampling sequence  $\mathcal{S} = \{s_j\}_{j \in \mathbb{N}_0}$ , with  $s_j = jh$ , is determined with a fixed sampling time  $h \in \mathbb{R}_{>0}$ . After a transmission instant is determined, the discrete signal is converted by the ZOH mechanism into a piecewise constant signal to be available to the controller. The dotted lines indicate that data are transmitted only at the transmission instants  $\{t_k h\}_{k \in \mathbb{N}}$ ,  $t_k \in \mathbb{N}_0$ , determined by the ETM, which is a sub-sequence of the sampling sequence  $\mathcal{S}$ . As the communication network may not be used exclusively for the control task, it is considered that bounded time-varying delays are induced during transmission [33]. Then, the information of  $x(t)$  available to the controller is

$$\hat{x}(t) = x(t_k h), \quad t \in [t_k h + \tau_k, t_{k+1} h + \tau_{k+1}), \quad (3.6)$$

where  $\tau_k$  is a bounded delay induced at  $t = t_k h$ .

By assuming the sampling sequence is initiated at  $t = 0$  as  $s_0 = 0$ , the sequence of event times  $\{t_k h\}_{k \in \mathbb{N}}$  satisfies to

$$t_0 h = 0, \quad (t_{k+1} - t_k)h \geq h, \quad \forall k \in \mathbb{N}, \quad (3.7)$$

which directly enforces an MIET of  $h$  time units and it ensures the exclusion of Zeno behavior. To reduce the use of communication resources, the following dynamic periodic ETM is proposed to determine the event times:

$$t_{k+1} h = \min\{t > t_k h : \eta(t) + \theta \Gamma(x(t), x(t_k h)) \leq 0, t \in \mathcal{S}\}, \quad (3.8)$$

where  $\theta \in \mathbb{R}_{\geq 0}$  is a design parameter,

$$\Gamma(x, \hat{x}) := \sigma \alpha(\|x\|) - \gamma(\|\hat{x} - x\|), \quad (3.9)$$

with  $\alpha, \gamma \in \mathcal{K}_\infty$ ,  $\sigma \in (0, 1) \subset \mathbb{R}$ , and  $\eta(t) \in \mathbb{R}_{\geq 0}$  is the internal variable of the dynamic periodic ETM which evolves according to the following dynamics:

$$\dot{\eta}(t) = -\lambda\eta(t) + \Gamma(x(s_j), x(t_k h)), \quad t \in [s_j, s_{j+1}), \quad (3.10)$$

where  $\eta(0) = \eta_0 \in \mathbb{R}_{\geq 0}$  is the initial condition, and  $\lambda \in \mathbb{R}_{>0}$  is a design parameter related to the decaying rate of  $\eta(t)$ .

**Lemma 3.3.** *Let  $\alpha, \gamma \in \mathcal{K}_\infty$ ,  $\sigma \in (0, 1) \subset \mathbb{R}$ ,  $\eta_0 \in \mathbb{R}_{\geq 0}$ . If  $\theta \geq \frac{1}{\lambda}(e^{\lambda h} - 1)$ , then  $\eta(t) > 0$ ,  $\forall t \in [s_j, s_{j+1})$ ,  $\forall j \in \mathbb{N}$ .*

*Proof.* The proof follows similar steps as [87, Lemma 2] and [176]. Consider the dynamic periodic ETM (3.8). The solution of the differential equation (3.10) with initial condition  $\eta(s_j)$  is

$$\eta(t) = e^{-\lambda(t-s_j)}\eta(s_j) + \frac{1}{\lambda} \left(1 - e^{-\lambda(t-s_j)}\right) \Gamma(x(s_j), x(t_k h)), \quad \forall t \in [s_j, s_{j+1}). \quad (3.11)$$

From the dynamic ETM in (3.8), one has  $\Gamma(x(t), x(t_k h)) > -\frac{1}{\theta}\eta(s_j)$ . Given that  $\eta(s_0) = \eta_0 > 0$ , the solution of (3.10) in (3.11) implies  $\eta(t) > [e^{-\lambda(t-s_0)} - \frac{1}{\theta\lambda}(1 - e^{-\lambda(t-s_0)})]\eta(s_0)$ . Also, since  $s_{j+1} - s_j = h$ , it follows that

$$\eta(t) > \left(e^{-\lambda h} - \frac{1}{\theta\lambda}(1 - e^{-\lambda h})\right) \eta(s_0).$$

Therefore, by taking  $\theta \geq \frac{1}{\lambda}(e^{\lambda h} - 1)$ , it ensures that  $\eta(t) > 0$  for all  $t \in [s_0, s_1)$ . From continuity of  $\eta(t)$ , one has  $\eta(s_1) > 0$ . Finally, by induction, one can conclude that  $\eta(t) > 0$ , for all  $t \in \mathbb{R}_{\geq 0}$ .  $\square$

**Remark 3.2.** *Notice that the continuous counterpart of the PETC in (3.8) is obtained by taking  $h \rightarrow 0$ . In this case, the condition of Lemma 3.3 is satisfied for any  $\theta \in \mathbb{R}_{\geq 0}$ , as in [29], which ensures the positive definiteness of  $\eta$  for any  $\theta \in \mathbb{R}_{\geq 0}$ .*

**Remark 3.3.** *For sufficiently large values of  $\theta$  the dynamic periodic ETM (3.8) is independent of  $\eta(t)$ , which reduces it to the following static counterpart*

$$t_0 h = 0, \quad t_{k+1} h = \min\{t > t_k h : \Gamma(x(t), x(t_k h)) \leq 0, t \in \mathcal{S}\}. \quad (3.12)$$

with  $\Gamma(x, \hat{x})$  given in (3.9).

### 3.2.1 Perturbed time-delay model of PETC systems

To ensure that each data packet arrives the controller node before a new event is transmitted, similar to [6], the following assumption is made.

**Assumption 3.1.** *The transmission delays induced by the network satisfy to  $0 \leq \tau_k \leq \bar{\tau} \leq h$ ,  $k \in \mathbb{N}_0$ , where  $\bar{\tau} \in \mathbb{R}_{\geq 0}$  is the maximum allowable delay and  $h \in \mathbb{R}_{>0}$  is the sampling period.*

Similar as in [176], since the network-induced delays are bounded, there exists a scalar  $\delta \in \mathbb{N}$  such that

$$t_k h + \delta h + \bar{\tau} < t_{k+1} h + \tau_{k+1} \leq t_k h + \delta h + h + \bar{\tau}. \quad (3.13)$$

Then, by defining the intervals

$$\mathcal{I}_i = \begin{cases} [t_k h + \tau_k, t_k h + h + \bar{\tau}), & i = 0, \\ [t_k h + i h + \bar{\tau}, t_k h + i h + h + \bar{\tau}), & i \in \mathbb{N}_{\leq \delta-1}, \\ [t_k h + \delta h + \bar{\tau}, t_{k+1} h + \tau_{k+1}), & i = \delta \end{cases}$$

the transmission interval can be partitioned as follows

$$[t_k h + \tau_k, t_{k+1} h + \tau_{k+1}) = \bigcup_{i=0}^{\delta} \mathcal{I}_i.$$

Then, by defining the artificial delay

$$\tau(t) := t - t_k h - i h, \quad \forall t \in \mathcal{I}_i, i \in \{0, \dots, \delta\},$$

such that

$$\begin{cases} \tau_k \leq \tau(t) \leq h + \bar{\tau}, & \forall t \in \mathcal{I}_0, \\ \tau_k \leq \bar{\tau} \leq \tau(t) \leq h + \bar{\tau}, & \forall t \in \mathcal{I}_i, i \in \mathbb{N}_{\leq \delta}, \end{cases}$$

it follows that  $\tau(t)$  is a bounded time-varying delay

$$0 \leq \tau_k \leq \tau(t) \leq h + \bar{\tau} = d, \quad \forall t \in [t_k h + \tau_k, t_{k+1} h + \tau_{k+1}), \quad (3.14)$$

satisfying to  $\dot{\tau}(t) = 1$  for all  $t \neq t_k h$ . Thus, the transmission error is defined as follows:

$$e(t) := x(t_k h) - x(t_k h + i h) \quad (3.15)$$

$$= \hat{x}(t) - x(t - \tau(t)), \quad \forall t \in \mathcal{I}_i, i \in \{0, \dots, \delta\}. \quad (3.16)$$

As far as it is assumed that  $u(t) = 0, \forall t < 0$ , due to the network-induced delay, the state information transmitted at  $t_0 = 0$ , that is  $x(0) = x_0$ , will be available to the controller whenever  $t - \tau_0 \geq 0$ , otherwise the control input signal  $u(t)$  is set to zero. In particular, since the input delay at  $t = 0$  is bounded by  $\tau_0 \leq \bar{\tau}$ , there exists a unique time  $t_0^* \leq \bar{\tau}$  such that  $t - \tau_0 < 0, \forall t \in [0, t_0^*)$ , and  $t - \tau_0 \geq 0, \forall t \geq t_0^*$ . Then, it can be noticed that  $u(t) = 0, \forall t < t_0^*$ , and the system operates in open-loop in the time interval  $t \in [0, t_0^*)$ . Thus, the closed-loop dynamic PETC system can be rewritten as follows:

$$\dot{x}(t) = \begin{cases} f(x(t)), & t \in [0, t_0^*) \\ f(x(t)) + g(x(t))k(x_\tau(t) + e(t)), & t \geq t_0^* \end{cases} \quad (3.17a)$$

$$\dot{\eta}(t) = \begin{cases} -\lambda \eta(t) + \Gamma(x_\tau(t), 0), & t \in [0, t_0^*) \\ -\lambda \eta(t) + \Gamma(x_\tau(t), e(t)), & t \geq t_0^* \end{cases} \quad (3.17b)$$

$$x(0) = x_0, \quad \eta(0) = \eta_0 \quad \text{given,}$$

where  $x_\tau(t) := x(t - \tau(t))$ . As within the time interval  $t \in [0, t_0^*)$  the system (3.17a) operates in open-loop, it is necessary to explicitly take into account the system's behavior at that interval, especially when the equilibrium  $x = 0$  of the unforced system is unstable, since in this case the trajectories starting at  $x_0$  can move away from the equilibrium point, eventually leaving the region of attraction of the closed-loop equilibrium before the control input starts to be applied at  $t = t_0^*$ . To properly address this behavior, similar as the local stability characterization of equilibrium points of input-delayed nonlinear systems proposed by [181], the following definition is considered in this work.

**Definition 3.1.** *Consider the nonlinear system in (3.3), a given stabilizing state feedback control law (3.5), and the dynamic periodic ETM in (3.8)–(3.10). The equilibrium point  $x = 0$  of the plant (3.3) is locally asymptotically stable if there exist two compact sets  $\mathcal{R}_0$  and  $\mathcal{R}$  satisfying  $\mathcal{R}_0 \subset \mathcal{R} \subset \mathcal{D}$ , with  $\mathcal{R}_0$  containing  $x = 0$ , such that for any  $x_0 \in \mathcal{R}_0$ , the state trajectory  $x(t)$  remains confined in  $\mathcal{R}$ , for all  $t \geq 0$ , and  $x(t) \rightarrow 0$  as  $t \rightarrow +\infty$ .*

### 3.3 Main results

The main results of this chapter are presented here. First, based on an appropriate LKF candidate, a local stability analysis condition is proposed for the closed-loop system (3.17) equipped with the dynamic PETC in (3.8). In the sequel, by employing the delay-dependent reciprocally convex combination lemma and the Wirtinger-based integral inequality, a delay-dependent co-design condition is derived to perform the co-design for a class of quasi-LPV models of the nonlinear plant (3.3).

#### 3.3.1 Local analysis of dynamic PETC systems

This section presents an extension of the approaches proposed in [181, 182] for input-delayed systems to the case of dynamic PETC systems represented by a time-delay system as in (3.17). More specifically, the following problem is addressed here.

**Problem 3.1.** *Given a stabilizing control law (3.5) for the nonlinear plant (3.3), determine conditions to ensure that the origin of the closed-loop system (3.17) equipped with the dynamic periodic ETM in (3.8)–(3.10) is locally asymptotically stable in the sense of Definition 3.1.*

The conditions are derived based on the following LKF candidate:

$$W(x_t, \dot{x}_t, \eta) = V(x_t, \dot{x}_t) + \eta(t), \quad (3.18)$$

where  $x_t \in \mathcal{C}_{[-d, 0]}^n$  is a segment of the function  $x_t(s) = x(t + s)$ ,  $\forall s \in [-d, 0]$ ,

$$V(x_t, \dot{x}_t) = V_1(x_t) + V_2(x_t) + V_3(\dot{x}_t) \quad (3.19)$$

with

$$\begin{aligned} V_1(x_t) &= \begin{bmatrix} x(t) \\ \int_{t-d}^t x(s)ds \end{bmatrix}^\top \begin{bmatrix} P & M \\ M^\top & S \end{bmatrix} \begin{bmatrix} x(t) \\ \int_{t-d}^t x(s)ds \end{bmatrix} \\ V_2(x_t) &= \int_{t-d}^t x^\top(s)Qx(s)ds \\ V_3(\dot{x}_t) &= d \int_{-d}^0 \int_{t+s}^t \dot{x}^\top(v)R\dot{x}(v)dvds, \end{aligned}$$

being  $P, Q, R, S$  symmetric matrices and  $M$  is a full matrix, all belonging to  $\mathbb{R}^n$ .

**Theorem 3.1.** *Consider the closed-loop system (3.17) and the LKF candidate given in (3.18). Let the sets*

$$\mathcal{R}_0 = \{x \in \mathbb{R}^n : V_0(x) \leq c - \eta_0/\beta\}, \quad (3.20)$$

$$\mathcal{R} = \{x \in \mathbb{R}^n : V_0(x) \leq c^*\}, \quad (3.21)$$

with

$$V_0(x) = x^\top Px, \quad (3.22)$$

and the scalars  $\sigma \in (0, 1)$ ,  $d, \mu, \lambda, \rho \in \mathbb{R}_{>0}$ ,  $\eta_0 \in \mathbb{R}_{\geq 0}$ . If the following conditions hold:

$$\begin{bmatrix} P & M \\ M^\top & S \end{bmatrix} > 0, \quad Q > 0, \quad R > 0, \quad (3.23)$$

and

$$\dot{V}(x_t, \dot{x}_t) < -\sigma\alpha(\|x_\tau(t)\|) + \gamma(\|e(t)\|), \quad \forall x_t \in \mathcal{D}_a, \quad t \geq t_0^* \quad (3.24)$$

$$\dot{V}_0(x(t)) - 2\rho V_0(x(t)) \leq 0, \quad \forall x \in \mathcal{D}, \quad t \in [0, t_0^*) \quad (3.25)$$

$$\dot{V}(x_t, \dot{x}_t) \leq -\sigma\alpha(\|x_\tau(t)\|) + 2\rho V_0(x(t)), \quad \forall x_t \in \mathcal{D}_a, \quad t \in [0, t_0^*) \quad (3.26)$$

$$\mu P - d^2 S - d(Q + M + M^\top) \geq 0 \quad (3.27)$$

$$\mathcal{R} \subset \mathcal{D}, \text{ with } c^* = c\beta, \beta = \mu + e^{2\rho\bar{c}}, c \leq \bar{c} - \eta_0/\beta, \quad (3.28)$$

where  $\bar{c} = \max_{x \in \mathcal{D}} \frac{1}{\beta} V_0(x)$ , and

$$\mathcal{D}_a = \{\phi \in \mathcal{C}_{[-d,0]}^n : \phi(s) \in \mathcal{D}, \forall s \in [-d, 0]\}. \quad (3.29)$$

Then, for every initial condition  $x_0 \in \mathcal{R}_0$ , the state trajectory  $(x(t), \eta(t))$  converges asymptotically to the origin and remains confined in the region

$$\widetilde{\mathcal{R}} = \{x_t \in \mathcal{C}_{[-d,0]}^n, \eta \in \mathbb{R}_{\geq 0} : W(x_t, \dot{x}_t, \eta) \leq c^*\} \quad (3.30)$$

and  $x(t)$  is confined in  $\mathcal{R} \subset \mathcal{D}$ , for all  $t \geq 0$ .

*Proof.* Consider the LKF candidate in (3.18). From condition (3.23), it is possible to conclude that the functional  $V(x_t, \dot{x}_t)$  is positive definite for all  $x_t \in \mathcal{D}_a \setminus \{0\}$ . Since Lemma 3.3 ensures that  $\eta(t)$  is positive definite for all  $t \in \mathbb{R}_{\geq 0}$  for a given  $\eta_0 \in \mathbb{R}_{>0}$ , then the functional (3.18) is positive definite.

Consider the time-derivative of the functional (3.18) along the trajectories of the closed-loop system (3.17):

$$\begin{aligned}\dot{W}(x_t, \dot{x}_t, \eta) &= \dot{V}(x_t, \dot{x}_t) + \dot{\eta}(t) \\ &= \dot{V}(x_t, \dot{x}_t) + \sigma\alpha(\|x_\tau(t)\|) - \gamma(\|e(t)\|) - \lambda\eta(t).\end{aligned}$$

From condition (3.24), one has that

$$\dot{W}(x_t, \dot{x}_t, \eta) < 0, \quad \forall t \geq t_0^*,$$

which ensures the asymptotic stability of the origin of the closed-loop system (3.17) for all  $t \in \mathbb{R}_{\geq 0}$ , provided that the state trajectory  $(x(t), \eta(t))$ , for any  $t \in [0, t_0^*)$ , is confined in the region  $\widetilde{\mathcal{R}}$  defined in (3.30) for some  $c^* \in \mathbb{R}_{>0}$  and  $\widetilde{\mathcal{R}} \subset \mathcal{D}_a \times \mathbb{R}_{\geq 0}$ . In the sequel it is shown that conditions (3.25)–(3.27) ensure that any state trajectory  $x(t)$  lies inside the region  $\mathcal{R} \subset \mathcal{D}$ , with  $c^*$  given by (3.28), for all  $t \in [0, t_0^*)$ .

Based on the Comparison Lemma [42, Chapter 3], the condition (3.25) implies

$$V_0(x(t)) \leq e^{2\rho t} V_0(x_0), \quad \forall t \in [0, t_0^*). \quad (3.31)$$

For all  $t \in [0, t_0^*)$ , the time-derivative of the functional (3.18) is

$$\dot{W}(x_t, \dot{x}_t, \eta) - 2\rho V_0(x(t)) = \dot{V}(x_t, \dot{x}_t) + \sigma\alpha(\|x_\tau(t)\|) - \lambda\eta(t) - 2\rho V_0(x(t)).$$

From condition (3.26), it follows that

$$\dot{W}(x_t, \dot{x}_t, \eta) - 2\rho V_0(x(t)) \leq 0, \quad \forall x_t \in \mathcal{D}_a, t \in [0, t_0^*),$$

which implies

$$\overline{W}(t) \leq \overline{W}(0) + 2\rho \int_0^t V_0(x(s)) ds, \quad \forall t \in [0, t_0^*),$$

where  $\overline{W}(t) := W(x_t, \dot{x}_t, \eta)$  is defined to simplify the notation. Thus, it follows from (3.31) that

$$\overline{W}(t) \leq \overline{W}(0) + V_0(x_0) (e^{2\rho t} - 1), \quad \forall t \in [0, t_0^*). \quad (3.32)$$

Now, an upper bound is derived to  $\overline{W}(0)$  based on (3.18). By assuming that  $x(s) = x_0, \forall s \in [-d, 0]$ , the solution of (3.17) does not depend on  $x(s)$  for  $s \in [-d, 0]$ . Thus, the

following relation is obtained:

$$\begin{aligned}\bar{W}(0) &= \begin{bmatrix} x_0 \\ \int_{-d}^0 x(s) ds \end{bmatrix}^\top \begin{bmatrix} P & M \\ M^\top & S \end{bmatrix} \begin{bmatrix} x_0 \\ \int_{-d}^0 x(s) ds \end{bmatrix} \\ &\quad + \int_{-d}^0 x_0^\top Q x_0 ds + \eta_0 \\ &= x_0^\top \left[ P + d^2 S + d(Q + M + M^\top) \right] x_0 + \eta_0,\end{aligned}\tag{3.33}$$

for  $x(s) = x_0, \forall s \in [d, 0]$ , and  $\eta(0) = \eta_0$  given. From (3.32), (3.33), and the condition in (3.27), one has that:

$$W(x_t, \dot{x}_t, \eta) \leq (\mu + e^{2\rho t}) x_0^\top P x_0 + \eta_0, \quad \forall t \in [0, t_0^*].$$

Thus, if  $x_0 \in \mathcal{R}_0$  and since  $t_0^* \leq \bar{\tau}$ , it follows that:

$$W(x_t, \dot{x}_t, \eta) \leq c^*, \quad \forall t \in [0, t_0^*],\tag{3.34}$$

with  $c^* = c\beta$ ,  $\beta = \mu + e^{2\rho\bar{\tau}}$ . Since from (3.18) one has  $W(x_t, \dot{x}_t, \eta) \geq V_0(x)$ , then:

$$V_0(x) \leq W(x_t, \dot{x}_t, \eta) \leq c^*, \quad \forall t \in [0, t_0^*].\tag{3.35}$$

Given that  $x_0 \in \mathcal{R}_0$ , with  $\mathcal{R}_0$  given as in (3.20), inequality (3.35) ensures that  $x(t) \in \mathcal{R}$  for all  $t \in [0, t_0^*]$ , with  $\mathcal{R}$  given as in (3.21), and hence  $V_0(x(t)) \leq \bar{W}(t) \leq \bar{W}(t_0^*) \leq c^*$ , for all  $t \geq t_0^*$ . Finally, from condition (3.28), if  $c$  is taken such that  $c \leq \bar{c}$ , where  $\bar{c} = \max_{x \in \mathcal{D}} \frac{1}{\beta} V_0(x)$ , then  $\mathcal{R} \subset \mathcal{D}$  and the state trajectory  $(x_t, \eta)$  remains confined in  $\widetilde{\mathcal{R}} \subset \mathcal{D}_a \times \mathbb{R}_{\geq 0}$  for all  $t \in \mathbb{R}_{\geq 0}$  and thus  $x_t \in \mathcal{D}_a$ , which ensures that  $(x(t), \eta(t)) \rightarrow 0$  as  $t \rightarrow +\infty$ . This concludes the proof.  $\square$

### 3.3.2 Delay-dependent co-design condition

Consider the following class of nonlinear systems:

$$\dot{x}(t) = A(x(t))x(t) + B(x(t))u(t),\tag{3.36}$$

where  $A : \mathcal{D} \rightarrow \mathbb{R}^{n \times n}$ ,  $B : \mathcal{D} \rightarrow \mathbb{R}^{n \times m}$ ,  $B(x) \neq 0, \forall x \in \mathcal{D}$ , are continuous mappings. The following linear state feedback control law is considered:

$$u(t) = K\hat{x}(t),\tag{3.37}$$

where  $K \in \mathbb{R}^{m \times n}$  is a control gain to be designed and  $u(t) = 0, \forall t < 0$ . The nonlinear terms in the coefficients of the state-dependent matrices  $A(x)$  and  $B(x)$  are denoted as  $z_j : \mathcal{D} \rightarrow \mathbb{R}, j \in \mathbb{N}_{\leq p}$ , and called scheduling functions. As  $\mathcal{D}$  is a compact set, by definition, and the scheduling functions  $z_j(x), j \in \mathbb{N}_{\leq p}$ , are continuous, then there exist bounds  $z_j^0, z_j^1 \in \mathbb{R}, j \in \mathbb{N}_{\leq p}$ , such that

$$z_j^0 \leq z_j(x) \leq z_j^1, \quad \forall x \in \mathcal{D}, \forall j \in \mathbb{N}_{\leq p}.\tag{3.38}$$

From the bounds in (3.38), each scheduling function can be equivalently written as  $z_j(x) = z_j^0 w_0^j(x) + z_j^1 w_1^j(x)$ , where

$$w_0^j(x) = \frac{z_j^1 - z_j(x)}{z_j^1 - z_j^0}, \quad w_1^j(x) = 1 - w_0^j(x),$$

Then, the nonlinear system (3.36) can be equivalently written as the following polytopic quasi-LPV model:

$$\dot{x}(t) = \sum_{\mathbf{i} \in \mathbb{B}^p} \mathbf{w}_{\mathbf{i}}(x(t)) (A_{\mathbf{i}}x(t) + B_{\mathbf{i}}u(t)), \quad (3.39)$$

where

$$\mathbf{w}_{\mathbf{i}}(x) = \prod_{j=1}^p w_{i_j}^j(x), \quad i_j \in \mathbb{B}, \quad j \in \mathbb{N}_{\leq p},$$

are parameters that satisfy to the following properties:

$$\sum_{\mathbf{i} \in \mathbb{B}^p} \mathbf{w}_{\mathbf{i}}(x) = 1, \quad \mathbf{w}_{\mathbf{i}}(x) \geq 0, \quad \forall \mathbf{i} \in \mathbb{B}^p. \quad (3.40)$$

**Remark 3.4.** Given a nonlinear system as in (3.3), there exists a possibly non-unique factorization such that (3.3) can be written as (3.36) [183]. Then, based on the sector nonlinearity approach [106], it is possible to properly select scheduling functions from the state-dependent coefficient matrices to obtain locally equivalent quasi-LPV representations as in (3.39) for (3.36) or, alternatively, for (3.3).

To reduce the number of transmissions, the following trigger function is considered for the dynamic ETM defined in (3.8), (3.10):

$$\Gamma(x_{\tau}(t), e(t)) := x^{\top}(t - \tau(t))\Theta x(t - \tau(t)) - e^{\top}(t)\Xi e(t), \quad (3.41)$$

where  $\Theta, \Xi \in \mathbb{R}^{n \times n}$  are symmetric positive definite matrices. The trigger function (3.41) can be viewed as the weighted deviation between the current state measurement  $x(t - \tau(t))$  and the latest transmitted state  $x(t_k h)$ .

Based on the transmission error defined in (3.15), the closed-loop system (3.17) for (3.36) with the control law (3.37) can be written as:

$$\dot{x}(t) = \begin{cases} A(x(t))x(t), & t \in [0, t_0^*) \\ A(x(t))x(t) + B(x(t))K(x_{\tau}(t) + e(t)), & t \geq t_0^* \end{cases} \quad (3.42a)$$

$$\dot{\eta}(t) = \begin{cases} -\lambda\eta(t) + \Gamma(x_{\tau}(t), 0), & t \in [0, t_0^*) \\ -\lambda\eta(t) + \Gamma(x_{\tau}(t), e(t)), & t \geq t_0^* \end{cases} \quad (3.42b)$$

with  $x(0) = x_0$ ,  $\eta(0) = \eta_0$  given, and  $\Gamma(x_{\tau}, e)$  given in (3.41).

**Problem 3.2.** Consider the nonlinear plant (3.36) equipped with the dynamic periodic ETM defined in (3.8), (3.10) with the trigger function (3.41). Based on a local quasi-LPV representation as in (3.39), determine constructive co-design conditions to design the stabilizing control law (3.37) and the parameters of the dynamic periodic ETM rule (3.41) such that the following requirements are fulfilled:

- (i) the time-delay closed-loop system (3.42a)-(3.42b) is asymptotically stable;
- (ii) the number of events generated by the dynamic periodic ETM is reduced as much as possible.

Before stating the solution to Problem 3.2, two auxiliary results are introduced. First, the following lemma introduces a constructive condition to check condition (3.24) of Theorem 3.1 for the closed-loop system (3.42a)–(3.42b).

**Lemma 3.4.** Consider the system (3.42) and let scalars  $h, \epsilon \in \mathbb{R}_{>0}$ ,  $\eta_0, \bar{\tau} \in \mathbb{R}_{\geq 0}$ ,  $\bar{\tau} \leq h$ , and  $d = h + \bar{\tau}$  be given. If there exist symmetric matrices  $\tilde{P}, \tilde{S}, \tilde{Q}, \tilde{R}, \tilde{\Xi}, \tilde{\Theta} \in \mathbb{R}^{n \times n}$ , and matrices  $\tilde{K} \in \mathbb{R}^{m \times n}$ ,  $\tilde{M}, X \in \mathbb{R}^{n \times n}$ ,  $\tilde{Y}_1, \tilde{Y}_2 \in \mathbb{R}^{2n \times 2n}$ , such that the following inequalities hold

$$\tilde{\mathcal{P}} > 0 \quad (3.43a)$$

$$\tilde{Q} > 0, \quad \tilde{R} > 0, \quad \tilde{\Xi} > 0 \quad (3.43b)$$

$$\tilde{\Upsilon}_i(0) = \begin{bmatrix} \tilde{\Phi}_i(0) - \Omega^\top \tilde{\Psi}(0) \Omega & \star & \star \\ [\tilde{Y}_1^\top \ 0] \Omega & -\tilde{\mathcal{R}} & \star \\ X v_3 & 0 & -\tilde{\Theta} \end{bmatrix} < 0, \quad (3.43c)$$

$$\tilde{\Upsilon}_i(d) = \begin{bmatrix} \tilde{\Phi}_i(d) - \Omega^\top \tilde{\Psi}(d) \Omega & \star & \star \\ [0 \ \tilde{Y}_2] \Omega & -\tilde{\mathcal{R}} & \star \\ X v_3 & 0 & -\tilde{\Theta} \end{bmatrix} < 0, \quad (3.43d)$$

for all  $i \in \mathbb{B}^p$ , where

$$\begin{aligned} \tilde{\Phi}_i(\tau) &= \text{He}(G_1^\top(\tau) \tilde{\mathcal{P}} G_0) + v_1^\top \tilde{Q} v_1 - v_4^\top \tilde{Q} v_4 + d^2 v_2^\top \tilde{R} v_2 - v_7^\top \tilde{\Xi} v_7 + \text{He}(\tilde{\mathcal{X}} \tilde{F}_i), \\ \tilde{\Psi}(\tau) &= \begin{bmatrix} \tilde{\mathcal{R}} & 0 \\ 0 & \tilde{\mathcal{R}} \end{bmatrix} + \frac{d-\tau}{d} \begin{bmatrix} \tilde{\mathcal{R}} & \tilde{Y}_2 \\ \tilde{Y}_2^\top & 0 \end{bmatrix} + \frac{\tau}{d} \begin{bmatrix} 0 & \tilde{Y}_1 \\ \tilde{Y}_1^\top & \tilde{\mathcal{R}} \end{bmatrix}, \\ G_0 &= \begin{bmatrix} v_2 \\ v_1 - v_4 \end{bmatrix}, \quad G_1(\tau) = \begin{bmatrix} v_1 \\ \tau v_5 + (d-\tau)v_6 \end{bmatrix}, \end{aligned}$$

$$\begin{aligned}
G_2 &= \begin{bmatrix} v_1 - v_3 \\ v_1 + v_3 - 2v_5 \end{bmatrix}, \quad G_3 = \begin{bmatrix} v_3 - v_4 \\ v_3 + v_4 - 2v_6 \end{bmatrix}, \quad \Omega = \begin{bmatrix} G_2 \\ G_3 \end{bmatrix}, \\
\tilde{\mathcal{X}} &= v_1^\top + \epsilon v_2^\top + \epsilon v_3^\top, \\
\tilde{F}_i &= A_i X v_1 - X v_2 + B_i \tilde{K} v_3 + B_i \tilde{K} v_7, \\
\tilde{\mathcal{R}} &= \begin{bmatrix} \tilde{R} & 0 \\ 0 & 3\tilde{R} \end{bmatrix}, \quad \tilde{\mathcal{P}} = \begin{bmatrix} \tilde{P} & \tilde{M} \\ \tilde{M}^\top & \tilde{S} \end{bmatrix}, \\
v_i &= \begin{bmatrix} 0_{n \times (i-1)n} & I_n & 0_{n \times (7-i)n} \end{bmatrix}.
\end{aligned}$$

Then, the time-derivative of the functional (3.19) along the trajectories of the closed-loop system (3.42) satisfies

$$\dot{V}(x_t, \dot{x}_t) \leq -\Gamma(x_\tau(t), e(t)), \quad \forall x_t \in \mathcal{D}_a, \quad t \geq t_0^*, \quad (3.44)$$

where  $\mathcal{D}_a$  is defined in (3.29) and  $\Gamma(x_\tau, e)$  is given in (3.41) with

$$\begin{aligned}
P &= X^{-\top} \tilde{P} X^{-1}, \quad M = X^{-\top} \tilde{M} X^{-1}, \quad S = X^{-\top} \tilde{S} X^{-1}, \\
Q &= X^{-\top} \tilde{Q} X^{-1}, \quad R = X^{-\top} \tilde{R} X^{-1}, \quad K = \tilde{K} X^{-1}, \\
\Xi &= X^{-\top} \tilde{\Xi} X^{-1}, \quad \Theta = \tilde{\Theta}^{-1}.
\end{aligned} \quad (3.45)$$

*Proof.* Assume that conditions (3.43a)–(3.43d) hold. By pre-multiplying inequality (3.43a) by  $I_2 \otimes X^{-\top}$  and post-multiplying it by its transpose, it ensures that  $\mathcal{P} > 0$ , where

$$\mathcal{P} = \begin{bmatrix} P & M \\ M^\top & S \end{bmatrix}. \quad (3.46)$$

Moreover, by pre-multiplying inequalities (3.43b) by  $X^{-\top}$  and post-multiplying them by its transpose, it ensures that  $Q > 0$ ,  $R > 0$ , and  $\Xi > 0$ . These inequalities ensure the positive-definiteness of the functional (3.19).

From Schur complement, inequalities (3.43c)–(3.43d) imply

$$\begin{bmatrix} \tilde{\Phi}_i(0) - \Omega^\top \tilde{\Psi}(0) \Omega + v_3^\top X^\top \tilde{\Theta}^{-1} X v_3 & \star \\ [\tilde{Y}_1^\top & 0] \Omega & -\tilde{\mathcal{R}} \end{bmatrix} < 0, \quad (3.47a)$$

$$\begin{bmatrix} \tilde{\Phi}_i(d) - \Omega^\top \tilde{\Psi}(d) \Omega + v_3^\top X^\top \tilde{\Theta}^{-1} X v_3 & \star \\ [0 & \tilde{Y}_2] \Omega & -\tilde{\mathcal{R}} \end{bmatrix} < 0, \quad (3.47b)$$

for all  $i \in \mathbb{B}^p$ . By pre-multiplying the inequalities in (3.47a)–(3.47b) by  $I_9 \otimes X^{-\top}$  and post-multiplying them by its transpose, it results

$$\Upsilon_i(0) = \begin{bmatrix} \Phi_i(0) - \Omega^\top \Psi(0) \Omega + v_3^\top \Theta v_3 & \star \\ [Y_1^\top & 0] \Omega & -\mathcal{R} \end{bmatrix} < 0, \quad (3.48a)$$

$$\Upsilon_i(d) = \begin{bmatrix} \Phi_i(d) - \Omega^\top \Psi(d) \Omega + v_3^\top \Theta v_3 & \star \\ [0 & Y_2] \Omega & -\mathcal{R} \end{bmatrix} < 0, \quad (3.48b)$$

for all  $\mathbf{i} \in \mathbb{B}^p$ , where

$$\begin{aligned}\Phi_{\mathbf{i}}(\tau) &= \text{He}(G_1^\top(\tau)\mathcal{P}G_0) + v_1^\top Q v_1 - v_4^\top Q v_4 + d^2 v_2^\top R v_2 - v_7^\top \Xi v_7 + \text{He}(\mathcal{X}F_{\mathbf{i}}), \\ \Psi(\tau) &= \begin{bmatrix} \mathcal{R} & 0 \\ 0 & \mathcal{R} \end{bmatrix} + \frac{d-\tau}{d} \begin{bmatrix} \mathcal{R} & Y_2 \\ Y_2^\top & 0 \end{bmatrix} + \frac{\tau}{d} \begin{bmatrix} 0 & Y_1 \\ Y_1^\top & \mathcal{R} \end{bmatrix}, \\ \mathcal{X} &= v_1^\top X^{-\top} + \epsilon v_2^\top X^{-\top} + \epsilon v_3^\top X^{-\top}, \\ F_{\mathbf{i}} &= A_{\mathbf{i}} v_1 - X v_2 + B_{\mathbf{i}} K v_3 + B_{\mathbf{i}} K v_7, \\ \mathcal{R} &= \begin{bmatrix} R & 0 \\ 0 & 3R \end{bmatrix}, \quad Y_i = (I_2 \otimes X^{-\top}) \tilde{Y}_i (I_2 \otimes X^{-1}), \quad i \in \mathbb{N}_{\leq 2},\end{aligned}\tag{3.49}$$

and matrices  $P, M, S, Q, R, K, \Xi$ , and  $\Theta$  defined in (3.45). From convexity property of the state-dependent parameters in (3.40), it implies that

$$\Upsilon(x, \tau) = \sum_{\mathbf{i} \in \mathbb{B}^p} w_{\mathbf{i}}(x) \Upsilon_{\mathbf{i}}(\tau) < 0, \quad \tau \in \{0, d\}.\tag{3.50}$$

Thus, it follows from (3.48a)–(3.48b) and (3.50) that

$$\Phi(x, \tau) + v_3^\top \Theta v_3 - \Omega^\top (\Psi(\tau) - \Psi_0(\tau)) \Omega < 0,\tag{3.51}$$

where

$$\Psi_0(\tau) = \begin{bmatrix} \frac{d-\tau}{d} Y_1 \mathcal{R}^{-1} Y_1^\top & 0 \\ 0 & \frac{\tau}{d} Y_2^\top \mathcal{R}^{-1} Y_2 \end{bmatrix}.$$

By defining  $\alpha(t) = \tau(t)/d \in [0, 1]$ , regarding the delay-dependent reciprocally convex combination lemma (see Lemma 3.1), it implies from (3.50) that

$$\Phi(x(t), \tau(t)) + v_3^\top \Theta v_3 - \Omega^\top \hat{\Psi}(\tau(t)) \Omega < 0,\tag{3.52}$$

where

$$\hat{\Psi}(\tau) = \begin{bmatrix} \frac{1}{\alpha(t)} \mathcal{R} & 0 \\ 0 & \frac{1}{1-\alpha(t)} \mathcal{R} \end{bmatrix}.$$

By defining the augmented vector

$$\xi(t) = \begin{bmatrix} x(t) \\ \dot{x}(t) \\ x(t - \tau(t)) \\ x(t - d) \\ \frac{1}{\tau(t)} \int_{t-\tau(t)}^t x(s) \, ds \\ \frac{1}{d-\tau(t)} \int_{t-d}^{t-\tau(t)} x(s) \, ds \\ e(t) \end{bmatrix},$$

the inequality in (3.52) implies that

$$\xi^\top(t) \left( \Phi(x(t), \tau(t)) + v_3^\top \Theta v_3 - \Omega^\top \hat{\Psi}(\tau(t)) \Omega \right) \xi(t) < 0.\tag{3.53}$$

Given that  $2\xi^\top(t)\mathcal{X}F(x(t))\xi(t) = 0$  and considering the Wirtinger-based integral inequality (see Lemma 3.2), condition (3.53) ensures that (3.44) holds. This concludes the proof.  $\square$

The following lemma introduces a constructive condition to check condition (3.26) of Theorem 3.1 for the closed-loop system (3.42a)–(3.42b).

**Lemma 3.5.** *Consider the system (3.42) and let scalars  $h, \epsilon, \rho \in \mathbb{R}_{>0}$ ,  $\bar{\tau} \in \mathbb{R}_{\geq 0}$ ,  $\bar{\tau} \leq h$ , and  $d = h + \bar{\tau}$  be given. If there exist symmetric matrices  $\tilde{P}, \tilde{S}, \tilde{Q}, \tilde{R} \in \mathbb{R}^{n \times n}$ , and matrices  $\tilde{M} \in \mathbb{R}^{n \times n}$ ,  $X \in \mathbb{R}^{n \times n}$ , such that (3.43a)–(3.43b) and the following inequalities hold*

$$\tilde{\Pi}_i = \begin{bmatrix} \tilde{\Lambda}_i & \ell_3^\top X^\top \\ X \ell_3 & -\tilde{\Theta} \end{bmatrix} < 0, \quad \forall i \in \mathbb{B}^p, \quad (3.54)$$

where

$$\begin{aligned} \tilde{\Lambda}_i &= \text{He}(H_1^\top \tilde{P} H_0) + \ell_1^\top \tilde{Q} \ell_1 - \ell_3^\top \tilde{Q} \ell_3 + d^2 \ell_4^\top \tilde{R} \ell_4 - H_2^\top \tilde{\mathcal{R}} H_2 + \text{He}(\tilde{\mathcal{Z}} \tilde{J}_i) - 2\rho \ell_1^\top \tilde{P} \ell_1, \\ H_0 &= \begin{bmatrix} \ell_2 \\ \ell_1 - \ell_3 \end{bmatrix}, \quad H_1 = \begin{bmatrix} \ell_1 \\ d \ell_4 \end{bmatrix}, \quad H_2 = \begin{bmatrix} \ell_1 - \ell_3 \\ \ell_1 + \ell_3 - 2\ell_4 \end{bmatrix}, \\ \tilde{\mathcal{Z}} &= \ell_1^\top + \epsilon \ell_2^\top + \epsilon \ell_3^\top, \quad \tilde{J}_i = A_i X \ell_1 - X \ell_2, \\ \ell_i &= \begin{bmatrix} 0_{n \times (i-1)n} & I_n & 0_{n \times (4-i)n} \end{bmatrix}, \end{aligned}$$

$\tilde{P}, \tilde{\mathcal{R}}$ , and  $\tilde{\Theta}$  defined as in (3.43). Then, the time-derivative of the functional (3.19) along the trajectories of the closed-loop system (3.42) satisfies

$$\dot{V}(x_t, \dot{x}_t) \leq -\Gamma(x_\tau(t), 0) + 2\rho V_0(x(t)), \quad \forall x_t \in \mathcal{D}_a, \quad t \in [0, t_0^*), \quad (3.55)$$

where  $\Gamma(x_\tau, e)$  is given in (3.41),  $\mathcal{D}_a$  in (3.29), and matrices  $P, M, S, Q, R$ , and  $\Theta$  are defined as in (3.45).

*Proof.* From conditions (3.43a)–(3.43b), similar as the arguments employed in the proof of Lemma 3.4, the positive-definiteness of the functional (3.19) is ensured. Then, assume that inequalities (3.54) hold. From Schur complement, these inequalities imply

$$\tilde{\Lambda}_i + \ell_3^\top X^\top \tilde{\Theta}^{-1} X \ell_3 < 0, \quad \forall i \in \mathbb{B}^p. \quad (3.56)$$

By pre-multiplying the inequalities in (3.56) by  $I_4 \otimes X^{-\top}$  and post-multiplying them by its transpose, it results

$$\Lambda_i + \ell_3^\top \Theta \ell_3 < 0, \quad \forall i \in \mathbb{B}^p, \quad (3.57)$$

where

$$\begin{aligned} \Lambda_i &= \text{He}(H_1^\top \mathcal{P} H_0) + \ell_1^\top Q \ell_1 - \ell_3^\top Q \ell_3 + d^2 \ell_4^\top R \ell_4 - H_2^\top \mathcal{R} H_2 + \text{He}(\mathcal{Z} J_i) - 2\rho \ell_1^\top P \ell_1, \\ \mathcal{Z} &= \ell_1^\top X^\top + \epsilon \ell_2^\top X^\top + \epsilon \ell_3^\top X^\top, \\ J_i &= A_i \ell_1 - \ell_2, \end{aligned}$$

with  $\mathcal{P}$  and  $\mathcal{R}$  given in (3.46) and (3.49), respectively, and matrices  $P$ ,  $M$ ,  $S$ ,  $Q$ ,  $R$ , and  $\Theta$  defined in (3.45). From convexity property of the state-dependent parameters in (3.40), it implies that

$$\Lambda(x) = \sum_{\mathbf{i} \in \mathbb{B}^p} w_{\mathbf{i}}(x) \Lambda_{\mathbf{i}} < 0, \quad (3.58)$$

then, conditions in (3.57) and (3.58) imply

$$\Lambda(x) + \ell_3^\top \Theta \ell_3 < 0. \quad (3.59)$$

By defining the augmented vector

$$\zeta(t) = \begin{bmatrix} x(t) \\ \dot{x}(t) \\ x_0 \\ \frac{1}{d-\tau(t)} \int_{t-d}^t x(s) \, ds \end{bmatrix},$$

the inequality in (3.59) implies that

$$\zeta^\top(t) \left( \Lambda(x) + \ell_3^\top \Theta \ell_3 \right) \zeta(t) < 0. \quad (3.60)$$

Given that  $2\zeta^\top(t) \mathcal{Z} J(x) \zeta(t) = 0$  and considering the Wirtinger-based integral inequality (see Lemma 3.2), condition (3.60) ensures that (3.55) holds. This concludes the proof.  $\square$

**Theorem 3.2.** *Consider the system (3.42) and let scalars  $h, \epsilon, \mu, \rho, \lambda \in \mathbb{R}_{>0}$ ,  $\eta_0, \bar{\tau} \in \mathbb{R}_{\geq 0}$ ,  $\bar{\tau} \leq h$ , and  $d = h + \bar{\tau}$  be given. If there exist symmetric matrices  $\tilde{P}, \tilde{S}, \tilde{Q}, \tilde{R}, \tilde{\Xi}, \tilde{\Theta} \in \mathbb{R}^{n \times n}$ , and matrices  $\tilde{K} \in \mathbb{R}^{m \times n}$ ,  $\tilde{M}, X \in \mathbb{R}^{n \times n}$ ,  $\tilde{Y}_1, \tilde{Y}_2 \in \mathbb{R}^{2n \times 2n}$ , such that (3.43a)–(3.43b) and the following inequalities hold*

$$\tilde{\Upsilon}_{\mathbf{i}}(0) < 0, \quad \tilde{\Upsilon}_{\mathbf{i}}(d) < 0, \quad \forall \mathbf{i} \in \mathbb{B}^p, \quad (3.61)$$

$$\begin{bmatrix} -2\rho\tilde{P} + \text{He}(A_{\mathbf{i}}X) & \star \\ \tilde{P} - X^\top + \epsilon A_{\mathbf{i}}X & -\epsilon \text{He}(X) \end{bmatrix} < 0, \quad (3.62)$$

$$\tilde{\Pi}_{\mathbf{i}} < 0, \quad \forall \mathbf{i} \in \mathbb{B}^p, \quad (3.63)$$

$$\mu\tilde{P} - d^2\tilde{S} - d(\tilde{Q} + \tilde{M} + \tilde{M}^\top) \geq 0, \quad (3.64)$$

where  $\tilde{\Upsilon}_{\mathbf{i}}(\tau)$ ,  $\forall \mathbf{i} \in \mathbb{B}^p$ ,  $\tau \in \{0, d\}$ , are defined in (3.43c)–(3.43d) and  $\tilde{\Pi}_{\mathbf{i}}$ ,  $\forall \mathbf{i} \in \mathbb{B}^p$ , are defined in (3.54). Then, for every initial condition  $x_0 \in \mathcal{R}_0$  defined as in (3.20), with the level sets  $c^*$  and  $c$  selected satisfying to (3.28) with

$$\bar{c} = \min_{1 \leq j \leq n_f} \frac{1}{\beta b_j^\top P^{-1} b_j}, \quad (3.65)$$

where  $\beta = \mu + e^{2\rho\bar{\tau}}$ ,  $P$ ,  $M$ ,  $S$ ,  $Q$ ,  $R$ ,  $\Theta$ , and  $\Xi$  defined as in (3.45), the state trajectory  $(x(t), \eta(t))$ , for all  $t \geq 0$ , converges asymptotically to the origin and it remains confined in the region  $\tilde{\mathcal{R}}$ , defined in (3.30), and  $x(t)$  is confined in  $\mathcal{R} \subset \mathcal{D}$ , defined in (3.21), for all  $t \geq 0$ .

*Proof.* From conditions (3.43a)–(3.43b) and given  $\eta_0 \in \mathbb{R}_{>0}$ , similar as the arguments in Lemma 3.4 and Theorem 3.1, the positive-definiteness of the functional (3.18) is ensured.

If the inequalities in (3.61) hold, Lemma 3.4 ensures that condition (3.55) holds, which means that (3.24) in Theorem 3.1 holds with  $V(x_t, \dot{x}_t)$  defined in (3.19) and  $\Gamma(x_t, e)$  given in (3.41) along the trajectories of the closed-loop system (3.42), with matrices defining the functional (3.18) and the trigger function (3.41) as in (3.45).

If (3.62) holds, by pre-multiplying it by  $I_2 \otimes X^{-\top}$  and post-multiplying it by its transpose, it leads to

$$\begin{bmatrix} -2\rho P + \text{He}(X^{-\top} A_i) & \star \\ P - X^{-1} + \epsilon X^{-\top} A_i & -\epsilon \text{He}(X^{-1}) \end{bmatrix} < 0, \quad \forall i \in \mathbb{B}^p, \quad (3.66)$$

where  $P$  is defined as in (3.45). Then, by pre-multiplying (3.66) by  $[I \quad -A_i^\top]$  and post-multiplying it by its transpose, yields

$$A_i^\top P + P A_i - 2\rho P < 0, \quad \forall i \in \mathbb{B}^p,$$

which follows from the convexity property of the state-dependent parameters in (3.40) that

$$A^\top(x(t))P + P A(x(t)) < 2\rho P,$$

which after pre-multiplied by  $x^\top(t)$  and post-multiplied by  $x(t)$ , it implies that (3.25) in Theorem 3.1 holds with  $V_0(x)$  given as in (3.22) along the trajectories of (3.42).

If (3.63) holds, Lemma 3.5 ensures that condition (3.55) holds, which means that (3.26) in Theorem 3.1 holds with  $V(x_t, \dot{x}_t)$  defined in (3.19) with  $\Gamma(x_\tau, e)$  given in (3.41) along the trajectories of (3.42).

If condition (3.64) holds, by pre-multiplying it by  $X^{-\top}$  and post-multiplying it by  $X^{-1}$ , it ensures that condition (3.27) in Theorem 3.1 holds.

Finally, if conditions (3.61)–(3.64) hold, a matrix  $P$  is determined as in (3.45) and the largest level set that ensures that  $\mathcal{R} \subset \mathcal{D}$ , given by  $\bar{c} = \max_{x \in \mathcal{D}} \frac{1}{\beta} V_0(x)$ , is determined based on (3.65) [42, Chapter 8]. Then, condition (3.28) in Theorem 3.1 holds.

Thus, the closed-loop trajectory  $(x_t, \eta)$  of (3.42) remains confined in  $\widetilde{\mathcal{R}} \subset \mathcal{D}_a \times \mathbb{R}_{\geq 0}$  for all  $t \in \mathbb{R}_{\geq 0}$  and then  $x(t) \in \mathcal{R}$ ,  $\forall t \in \mathbb{R}_{\geq 0}$ , and  $(x(t), \eta(t)) \rightarrow (0, 0)$  as  $t \rightarrow +\infty$ . This concludes the proof.  $\square$

The next result states a co-design condition for static PETC and it can be readily deduced from Theorem 3.2.

**Corollary 3.1.** *Consider the system (3.42a) equipped with the static PETC in (3.12) and let scalars  $h, \epsilon, \mu, \rho \in \mathbb{R}_{>0}$ ,  $\bar{\tau} \in \mathbb{R}_{\geq 0}$ ,  $\bar{\tau} \leq h$ , and  $d = h + \bar{\tau}$  be given. If there exist symmetric*

matrices  $\tilde{P}, \tilde{S}, \tilde{Q}, \tilde{R}, \tilde{\Xi}, \tilde{\Theta} \in \mathbb{R}^{n \times n}$ , and matrices  $\tilde{K} \in \mathbb{R}^{m \times n}$ ,  $\tilde{M}, X \in \mathbb{R}^{n \times n}$ ,  $\tilde{Y}_1, \tilde{Y}_2 \in \mathbb{R}^{2n \times 2n}$ , such that (3.43a)–(3.43b) and the inequalities (3.61)–(3.64) in Theorem 3.2 hold. Then, for every initial condition  $x_0 \in \mathcal{R}_0$  defined as in (3.20) with  $\eta_0 = 0$ , the state trajectory  $x(t)$ , for all  $t \geq 0$ , converges asymptotically to the origin and it remains confined in the region  $\mathcal{R} \subset \mathcal{D}$  defined as in (3.21) with  $\eta_0 = 0$ , for all  $t \geq 0$ .

*Proof.* Considering the LKF candidate given in (3.19), the proof follows similar steps as the proof of Theorem 3.2  $\square$

### 3.3.3 Enlargement of inter-event times

This section describes a criterion considered to enlarge the inter-event times provided by the PETC scheme. To address this problem, from the trigger rule in (3.8) with the trigger function (3.41), new transmissions are triggered when:

$$\lambda_{\min}(\Theta)\|x_\tau(t)\|^2 - \lambda_{\max}(\Xi)\|e(t)\|^2 + \frac{1}{\theta}\eta(t) \leq 0,$$

which, in the worst case, it implies that

$$\mathcal{G}(x_\tau(t), e(t)) \leq 1 + \mathcal{V}(x_\tau(t), \eta(t)),$$

where

$$\mathcal{G}(x_t, e) = \frac{\lambda_{\max}(\Xi)\|e\|^2}{\lambda_{\min}(\Theta)\|x_t\|^2}, \quad \mathcal{V}(x_t, \eta) = \frac{1}{\theta} \frac{\eta(t)}{\lambda_{\min}(\Theta)\|x_t\|^2}.$$

Thus, the idea is maximizing the eigenvalues of  $\Theta$  and minimizing the eigenvalues of  $\Xi$  such that the minimum time required for  $\mathcal{G}(x_t, e)$  to evolve from 0 to  $1 + \mathcal{V}(x_t, \eta)$  is enlarged. For that, similar to [51], the following optimization problem is considered:

$$\begin{aligned} & \text{minimize} && \beta \text{tr}(\tilde{\Xi} + \tilde{\Theta}) \\ & \text{subject to} && (3.43a)–(3.43b), (3.61)–(3.64), \\ & && \tilde{P} \geq I \end{aligned} \tag{3.67}$$

The minimization of  $\text{tr}(\tilde{\Xi} + \tilde{\Theta})$  tends to maximize the eigenvalues of  $\Theta$  and to minimize the eigenvalues of  $\Xi$ , which tends to enlarge the inter-event times. The last constraint is introduced for well conditioning purposes. Notice that the given scalar  $\beta = \mu + e^{2\rho\bar{\tau}}$  is related to the size of the set of admissible initial conditions  $\mathcal{R}_0$  such that as the parameters  $\rho$  or  $\bar{\tau}$  increase,  $\mathcal{R}_0$  tends to reduce. Thus,  $\beta$  is included into the objective function to introduce a trade-off between the size of the set of admissible of initial conditions and the number of inter-event times. Hence, if the optimization problem in (3.67) is feasible, the condition (3.65) of Theorem 3.2 is directly applied to obtain the largest estimate of the region of attraction.

### 3.4 Numerical examples

Numerical examples are presented in this section to illustrate the effectiveness of the proposed delay-dependent co-design condition.

#### 3.4.1 Example 1: van der Pol oscillator

Consider the van der Pol oscillator system described in (2.32). For  $r_0 = 2$ , the vertices of the quasi-LPV model (3.39) can be obtained as in (2.34) and the validity region is given by  $\mathcal{D} = \{x \in \mathbb{R}^n : |x_1| \leq 2, |x_2| \leq 2\}$ . Initially, the influence of parameters  $\rho$  and  $\epsilon$  over the solution of the optimization problem (3.67) is evaluated. For that, consider  $\mu = 0.01$  and  $h = \bar{\tau} = 0.15$ , which leads to  $d = h + \bar{\tau} = 0.30$ . The behavior of the objective function of (3.67) with respect to  $\rho$  for different values of  $\epsilon$  is illustrated in Figure 3.2.

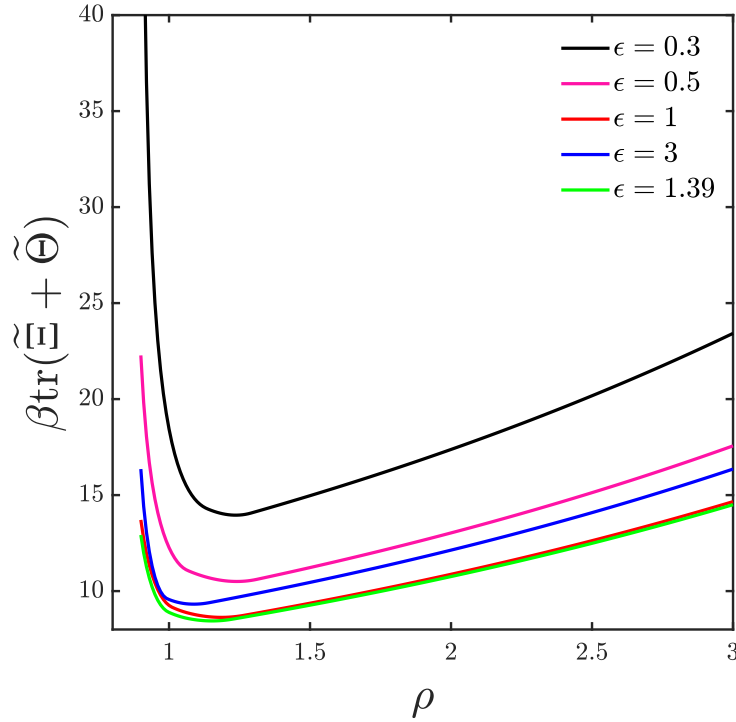


**Figure 3.2** – Objective function  $\beta\text{tr}(\tilde{\Xi} + \tilde{\Theta})$  of (3.67) with respect to  $\rho$  for different values of  $\epsilon$ .

For all the considered values of  $\epsilon$ , as  $\rho$  increases, the objective function decreases up to achieve a minimum then it tends to increase again due to the exponential relation of  $\beta$  with respect to  $\rho$ . On the other hand, the values of the objective function with respect to  $\rho$  are bigger for smaller values of  $\epsilon$ , as  $\epsilon$  increases, a minimum is achieved and then the objective function tends to increase again as  $\epsilon$  increases. By employing a grid search algorithm<sup>1</sup>, the minimum value of  $\beta\text{tr}(\tilde{\Xi} + \tilde{\Theta})$  has been achieved with  $\epsilon = 1.39$  and  $\rho = 1.15$ , as illustrated in Figure 3.2.

<sup>1</sup> The Box's evolutionary optimization method [184, Section 3.3.1] has been employed to perform the grid search in the space  $(\epsilon, \rho)$ .

Another aspect evaluated here is the feasibility of the optimization problem (3.67) for different values of the delay  $d$ . For  $\mu = 10^{-5}$  and a fixed  $\bar{\tau} = 0.1\text{s}$ , the optimization problem is solved for different values of  $h$  and the grid search algorithm is employed to determine the values of  $\rho = \rho^*$  and  $\epsilon = \epsilon^*$  that minimize the cost of (3.67). The results are presented in Table 3.1. Notice that the value of the cost increases as the delay  $d = h + \bar{\tau}$  increases, which indicates that more transmissions are required to ensure the closed-loop stability for larger values of delay.

**Table 3.1** – Minimum objective function  $\beta\text{tr}(\tilde{\Xi} + \tilde{\Theta})$  and the related values of  $\epsilon^*$  and  $\rho^*$  for different values of  $h$  in seconds.

$h$ (s)	0.1	0.15	0.2	0.25	0.3	0.33
$\beta\text{tr}(\tilde{\Xi} + \tilde{\Theta})$	3.148	4.634	7.465	14.538	49.206	1010.8
$\epsilon^*$	2.815	1.960	1.335	1.005	0.780	0.805
$\rho^*$	1.475	1.300	1.175	1.125	1.10	1.375

For  $h = \bar{\tau} = 0.15\text{s}$ , that is  $d = 0.30\text{s}$ , and  $\mu = 10^{-5}$ , the values of  $\rho = 1.15$  and  $\epsilon = 1.41$  obtained from the grid search algorithm lead to the minimum cost of the optimization problem in (3.67). The obtained solution is:

$$K = \begin{bmatrix} 0.4340 & -1.6720 \end{bmatrix}, P = \begin{bmatrix} 28.8593 & -2.1502 \\ -2.1502 & 25.1086 \end{bmatrix},$$

$$\Theta = \begin{bmatrix} 1.2428 & -0.2049 \\ -0.2049 & 1.7569 \end{bmatrix}, \Xi = \begin{bmatrix} 6.5483 & -25.2249 \\ -25.2249 & 97.1732 \end{bmatrix}.$$

In this case, the condition (3.65) in Theorem 3.2 provides  $\bar{c} = 70.675$ . For  $\eta_0 = 0$ ,  $\lambda = 0.5$ ,  $\theta = \frac{1}{\lambda}(e^{\lambda h} - 1)$  and a simulation time of 10s, simulations are performed regarding closed-loop trajectories with initial conditions at the border of  $\mathcal{R}_0$ . In the conducted simulations, the delay induced during communication is given by  $\tau_k = \frac{\bar{\tau}}{2}(1 + \cos(\pi t_k h))$ , notice that at  $t = t_0 h = 0$ , the delay is maximum, since  $\tau_0 = \bar{\tau} = t_0^*$ . The sets  $\mathcal{R}_0$  and  $\mathcal{R}$ , given in (3.20) and (3.21), respectively, and the closed-loop trajectories initiating in  $\mathcal{R}_0$  are shown in Figure 3.3. It can be noticed that for  $t \in [0, t_0^*)$ , when  $u(t) = 0$ , some of the trajectories leave the region  $\mathcal{R}_0$  due to the unstable behavior of the unforced equilibrium, but they remain inside the region  $\mathcal{R}$  and converge to the equilibrium when the control signal starts to be applied at  $t = t_0^* = \bar{\tau}$ . It illustrates the effectiveness of the proposed local co-design condition.

### 3.4.2 Example 2: rotational motion of a cart with an inverted pendulum

Consider the rotational motion of a cart with an inverted pendulum system described in (2.32). For  $\theta_0 = \frac{\pi}{3}$ , the vertices of the quasi-LPV model (3.39) can be obtained as in (2.37) and the validity region is given by  $\mathcal{D} = \{x \in \mathbb{R}^n : |x_1| \leq \frac{\pi}{3}, |x_2| \leq 2\}$ . For  $h = \bar{\tau} = 0.20\text{s}$ , which leads to  $d = 0.40\text{s}$ , and  $\mu = 10^{-5}$ , the values of  $\rho = 1.025$  and

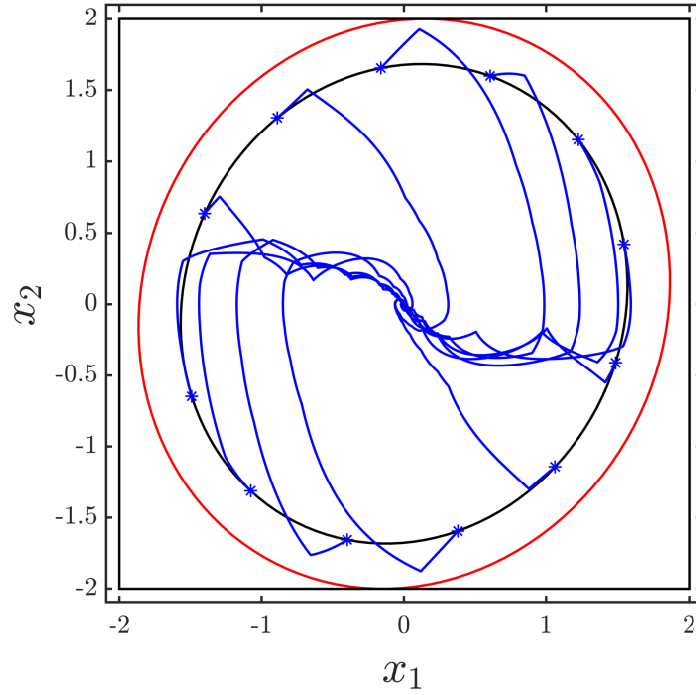


**Figure 3.3** – Sets  $\mathcal{R}_0$  (in black) and  $\mathcal{R}$  (in red) and convergent closed-loop trajectories (in blue) initiating in  $\mathcal{R}_0$ .

$\epsilon = 5.875$  are obtained from the grid search algorithm. In this case, the optimization problem in (3.67) leads to:

$$K = \begin{bmatrix} 2.4912 & 1.5451 \end{bmatrix}, P = \begin{bmatrix} 227.9599 & 129.9538 \\ 129.9538 & 89.1168 \end{bmatrix},$$

$$\Theta = \begin{bmatrix} 5.9399 & 0.2186 \\ 0.2186 & 8.8055 \end{bmatrix}, \Xi = \begin{bmatrix} 293.8745 & 182.2648 \\ 182.2648 & 113.0430 \end{bmatrix}.$$

Based on condition (3.65) in Theorem 3.2,  $\bar{c} = 27.987$  is obtained. For  $\eta_0 = 0$ ,  $\lambda = 0.1$ ,  $\theta = 10$ ,  $\tau_k = \frac{\bar{\tau}}{2}(1 + \cos(\frac{\pi}{2}t_k h))$  and a simulation time of 15s, the simulations are performed regarding several closed-loop trajectories initiating inside and outside of  $\mathcal{D}$ . The sets  $\mathcal{R}_0$  and  $\mathcal{R}$ , and the closed-loop trajectories are shown in Figure 3.4.

Notice that there are some trajectories initiating inside of the convex set  $\mathcal{D}$  that diverge while some others converge but evolve outside of  $\mathcal{D}$  before approaching to the equilibrium. It illustrates the importance of determining an estimate of the region of attraction for the closed-loop equilibrium. The average number of events for the trajectories initiating inside of  $\mathcal{R}_0$  is 11, while for the same initial conditions the average number of events obtained from the static counterpart (3.12) is 39.31. This corresponds to an economy provided by the dynamic PETC scheme of 72.02% with respect to the static PETC and 85.33% with respect to a standard periodic time-triggered scheme. In particular, for the initial condition  $x_0 = (0.7057, -1.3440)$ , the simulation results are shown in Figure 3.5.

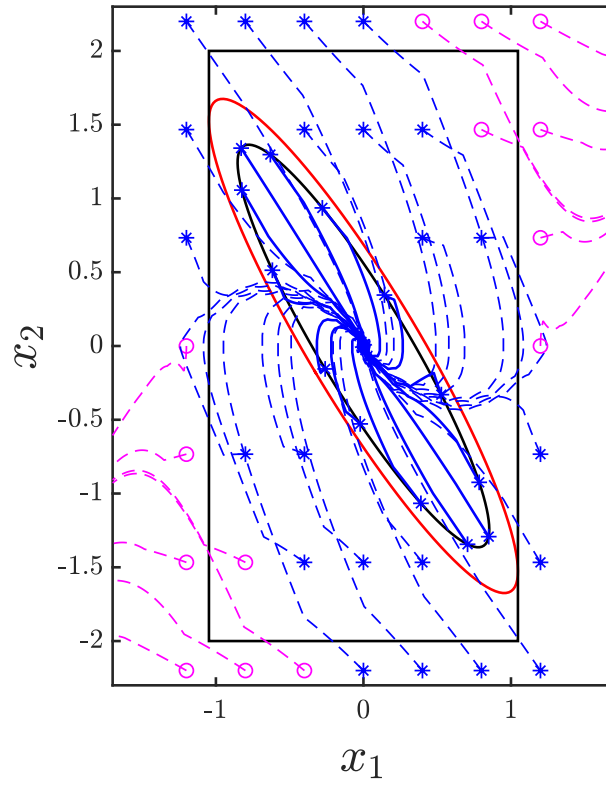


**Figure 3.4** – Sets  $\mathcal{R}_0$  (in black) and  $\mathcal{R}$  (in red) and convergent (starting at points “\*”) and divergent (starting at points “o”) closed-loop trajectories (in blue).

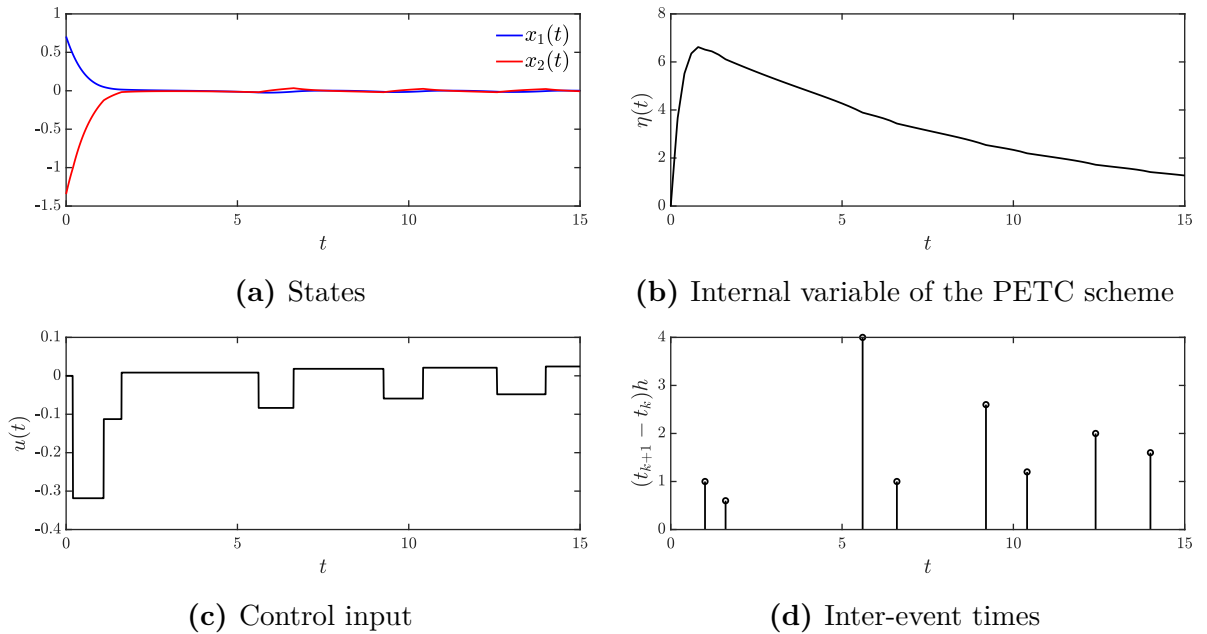


**Figure 3.5** – Simulation of the closed-loop system (2.36) with the control law (3.37) equipped with the dynamic PETC scheme (3.8), (3.10), (3.41).

In this simulation, 9 events are generated with the dynamic PETC scheme while 48 events are generated with the static counterpart. From Figures 3.5(a) and 3.5(b), it

can be noticed the asymptotic convergence of the pair  $(x, \eta)$  to the zero equilibrium. In particular, from Figure 3.5(c), it is possible to observe that the control input  $u(t)$  is set to zero until the state information starts to be transmitted to the controller at  $t = t_0^* = 0.20\text{s}$ . The inter event times are shown in Figure 3.5(d).

### 3.5 Conclusion

This chapter has addressed the co-design of dynamic periodic ETM and state feedback controllers for nonlinear systems represented by a polytopic quasi-LPV model. An improved co-design condition has been derived by employing the Wirtinger-based integral inequality and the delay-dependent reciprocally convex combination lemma. To ensure the application of the proposed method, an estimate of the region of attraction has been obtained, ensuring the convergence in the presence of network-induced delays. Numerical examples illustrated the effectiveness of the proposed dynamic ETM in ensuring local stability of the closed-loop system requiring fewer events than its static counterpart, which is largely employed in the related literature.

## 4 CONCLUDING REMARKS

This thesis has addressed the dynamic ETC of nonlinear systems represented by quasi-LPV models. By following the co-design approach, the controller and the parameters of the dynamic ETM have been simultaneously designed. In contrast to emulation-based approaches, in which the controller and the ETM are designed in a two-step procedure that may limit the effectiveness of the ETC implementation, co-design approaches can increase the efficiency of ETC reducing the number of transmissions and consequently saving communication resources in NCS. Regarding Lyapunov-based stability techniques, constructive and numerically implementable co-design conditions have been derived in terms of sufficient LMI-based conditions. Moreover, to ensure the applicability of the ETC design, estimates of the region of attraction have been obtained inside the modeling region in which the quasi-LPV is built.

More precisely, the main results of this thesis are listed as follows:

- a) Chapter 2 focused on dynamic CETC co-design for nonlinear systems represented by quasi-LPV models. From an appropriate formulation of the perturbed closed-loop ETC system, a novel dynamic CETC scheme has been proposed and the formal proof of the existence of a positive MIET has been provided to ensure the applicability of the CETC. The proposed trigger-function has been defined such that the influence of asynchronous parameters in the gain-scheduling control law was completely canceled from the Lyapunov analysis to derive LMI-based co-design conditions. As a result, an effective LMI relaxation often employed in the context of traditional gain-scheduling control synthesis could be applied. Also, a convex optimization problem has been defined aiming to enlarge the inter-execution times provided by the proposed CETC strategy.
- b) Chapter 3 focused on dynamic PETC co-design for nonlinear systems represented by quasi-LPV models. The closed-loop ETC system subject to network-induced delays is represented by a time-delay model. As far as a PETC strategy is concerned, Zeno behavior is naturally excluded. Based on the use of Wirtinger-based integral inequality and the delay-dependent reciprocally convex lemma, an improved co-design condition has been proposed to provide a less conservative co-design condition. Finally, a convex optimization problem has been formulated to enlarge the inter-event times provided by the proposed PETC strategy.
- c) In both Chapters 2 and 3, estimates of the region of attraction have been obtained to ensure the applicability of both the dynamic CETC and dynamic PETC schemes, respectively. Finally, the applicability of the proposed dynamic ETC schemes has been illustrated considering two physically-motivated examples and

their effectiveness over emulation-based and static ETC strategies have been demonstrated since it was shown that the proposed dynamic ETC methods were able to reduce the usage of communication resources due to the reduction of data transmissions. One aspect that can be improved in the proposed approaches is the introduction of the parameters  $\lambda$  and  $\theta$  of the dynamic event-triggering scheme into the co-design conditions. It might be helpful to further reducing the number of transmissions.

#### 4.1 Future research

Some suggestions of possible next steps for this doctoral research are discussed in this section. They are based on the further development of the main objective of this thesis: to propose dynamic event-triggered control strategies for local stabilization of nonlinear networked control systems represented by polytopic quasi-LPV models. The further steps are listed as follows:

- a) To improve robustness of continuous event-triggered control strategies with time-regularization:

The inclusion of a positive waiting (or dwell-)time is an effective alternative to improve the robustness of CETC schemes, leading to the CETC with time-regularization. In this case, Zeno behavior is naturally excluded because the MIET is ensured by the enforced waiting time. As a result, asymptotic stability and  $\mathcal{L}_p$  stability conditions [6] can be derived for this event-based strategy. Co-design approaches for CETC with time-regularization strategies have been mainly developed for linear systems [145, 48, 143, 49, 50, 72, 74] and specific classes of nonlinear systems [52]. Thus, further investigations on co-design approaches for CETC with time-regularization of nonlinear systems represented by quasi-LPV models are recommended considering a looped-functional approach as in [185].

- b) Conservativeness reduction of the proposed local dynamic PETC strategy:

The use of Bessel-Legendre inequalities has been proved to be effective to provide less conservative results in the context of dynamic PETC of quasi-LPV models [176]. However, the condition in [176] does not provide estimates of the region of attraction of the closed-loop equilibrium, which may lead to implementation issues, as discussed in Chapter 3. Motivated by the developments proposed in Chapter 3, local PETC co-design conditions can be derived considering the Bessel-Legendre inequality together with the delay-dependent reciprocally convex lemma.

- c) Output-based and decentralized event-triggering control strategies:

In practical applications, frequently only output information is available instead of full state measurement. For this reason, it is recommended to develop output-based event-triggering gain-scheduling control co-design strategies [68, 63, 72, 6, 179, 52]. One of the main challenges in this case is that the scheduling functions may depend on unmeasured states. As a result, it is necessary to develop appropriate strategies to deal with such unmeasured scheduling functions by indirect estimation via state observers [186, 187, 188].

Moreover, in NCS data may be transmitted over multiple networks that operate asynchronously and independently. In this case, due to the unavailability of global information for each node, decentralized [189, 75, 6, 84] ETC strategies might be developed.

- d) To consider more effects of network-induced phenomena into the analysis:

In most of ETC strategies, only part of the network-induced phenomena is considered [13], such as network-induced time-delays, as addressed in Chapter 3. However, in practical applications, more than one network-induced phenomenon may appear simultaneously. For this reason, it is recommended to derive co-design conditions considering other phenomena, such as packet dropouts [137] and quantization effects [52].

## 4.2 Publications

During the period in which this doctoral research was developed, contributions related to the topics of event-triggered control, sampled-data control, and stabilization of (quasi-)LPV/TS fuzzy models have been attained. The publications related to the specific topic of this thesis are listed below:

- a) **COUTINHO, P. H. S.**; PALHARES, R. M. Dynamic periodic event-triggered gain-scheduling control co-design for quasi-LPV systems. **Nonlinear Analysis: Hybrid Systems**, Elsevier, v. 41, p. 101044, 2021.  
doi: <https://doi.org/10.1016/j.nahs.2021.101044>
- b) **COUTINHO, P. H. S.**; PALHARES, R. M. Co-design of dynamic event-triggered gain-scheduling control for a class of nonlinear systems. **IEEE Transactions on Automatic Control**, IEEE, 2021.  
doi: <https://doi.org/10.1109/TAC.2021.3108498>

The publications on sampled-data control systems, a topic closely related with the main subject of this doctoral research, are listed below:

- c) **COUTINHO, P. H. S.**; BERNAL, M.; PALHARES, R. M. Robust sampled-data controller design for uncertain nonlinear systems via Euler discretization. **International Journal of Robust and Nonlinear Control**, Wiley Online

Library, v. 30, n. 18, p. 8244–8258, 2020.

doi: <https://doi.org/10.1002/rnc.5234>

- d) **COUTINHO, P. H. S.**; PEIXOTO, M. L. C.; BERNAL, M.; NGUYEN, A.-T.; PALHARES, R. M. Local sampled-data gain-scheduling control of quasi-LPV systems. In: 4th IFAC Conference on Embedded Systems, Computational Intelligence and Telematics in Control (CESCIT 2021), 2021, p. 86–91.  
doi: <https://doi.org/10.1016/j.ifacol.2021.10.015>
- e) **COUTINHO, P. H. S.**; CHAGAS, T. P.; TORRES, L. A.; PALHARES, R. M. Robust eigenvalue assignment via sampled state-feedback for linear polytopic discrete-time periodic systems. In: 14<sup>o</sup> Simpósio Brasileiro de Automação Inteligente. Ouro Preto, 2019, p. 1–6.  
doi: <https://doi.org/10.17648/sbai-2019-111239>.

Finally, the publications on stabilization of TS fuzzy models and LPV systems are listed below:

- f) PEIXOTO, M. L. C.; **COUTINHO, P. H. S.**; PALHARES, R. M. Improved robust gain-scheduling static output-feedback control for discrete-time LPV systems. **European Journal of Control**, v. 58, p. 11-16, 2021.  
doi: <https://doi.org/10.1016/j.ejcon.2020.12.006>
- g) ARAÚJO, R. F.; **COUTINHO, P. H. S.**; NGUYEN, A.-T.; PALHARES, R. M.. Delayed nonquadratic  $\mathcal{L}_2$ -stabilization of continuous-time nonlinear Takagi–Sugeno fuzzy models. **Information Sciences**, v. 563, p. 59-69, 2021.  
doi: <https://doi.org/10.1016/j.ins.2021.01.007>
- h) **COUTINHO, P. H. S.**; ARAÚJO, R. F.; NGUYEN, A.-T.; PALHARES, R. M. A multiple-parameterization approach for local stabilization of constrained Takagi-Sugeno fuzzy systems with nonlinear consequents. **Information Sciences**, v. 506, p. 295–307, 2020.  
doi: <https://doi.org/10.1016/j.ins.2019.08.008>
- i) **COUTINHO, P. H. S.**; PEIXOTO, M. L.; LACERDA, M. J.; BERNAL, M.; PALHARES, R. M. Generalized non-monotonic Lyapunov functions for analysis and synthesis of Takagi-Sugeno fuzzy systems. **Journal of Intelligent & Fuzzy Systems**, v. 39, n. 3, p. 4147-4158, 2020.  
doi: <https://doi.org/10.3233/JIFS-200262>

## BIBLIOGRAPHY

- [1] LIU, K.; S., A.; FRIDMAN, E. Survey on time-delay approach to networked control. **Annual Reviews in Control**, Elsevier, 2019. Pages 15, 16, 19, and 29.
- [2] QIU, J.; GAO, H.; DING, S. X. Recent advances on fuzzy-model-based nonlinear networked control systems: A survey. **IEEE Transactions on Industrial Electronics**, IEEE, v. 63, n. 2, p. 1207–1217, 2015. Pages 15, 22, and 31.
- [3] BRAGA, M. F.; MORAIS, C. F.; TOGNETTI, E. S.; OLIVEIRA, R. C. L. F.; PERES, P. L. D. Discretization and event triggered digital output feedback control of LPV systems. **Systems & Control Letters**, Elsevier, v. 86, p. 54–65, 2015. Pages 15 and 22.
- [4] HESPANHA, J. P.; NAGHSHTABRIZI, P.; XU, Y. A survey of recent results in networked control systems. **Proceedings of the IEEE**, IEEE, v. 95, n. 1, p. 138–162, 2007. Page 15.
- [5] BORGES, R. A.; OLIVEIRA, R. C. L. F.; ABDALLAH, C. T.; PERES, P. L. D. Robust  $\mathcal{H}_\infty$  networked control for systems with uncertain sampling rates. **IET Control Theory & Applications**, IET, v. 4, n. 1, p. 50–60, 2010. Pages 15 and 16.
- [6] DOLK, V. S.; BORGERS, D. P.; HEEMELS, W. P. M. H. Output-based and decentralized dynamic event-triggered control with guaranteed  $\mathcal{L}_p$ -gain performance and zeno-freeness. **IEEE Transactions on Automatic Control**, IEEE, v. 62, n. 1, p. 34–49, 2017. Pages 15, 19, 21, 25, 26, 55, 75, and 76.
- [7] JOHANSSON, K. H.; TÖRNGREN, M.; NIELSEN, L. Vehicle applications of controller area network. In: **Handbook of Networked and Embedded Control Systems**. New York: Birkhäuser Basel, 2005. p. 741–765. Page 15.
- [8] MAHMOUD, M. S.; HUSSAIN, S. A.; ABIDO, M. A. Modeling and control of microgrid: An overview. **Journal of the Franklin Institute**, Elsevier, v. 351, n. 5, p. 2822–2859, 2014. Page 15.
- [9] DE LIMA, M. V.; MOZELLI, L. A.; NETO, A. A.; SOUZA, F. O. A simple algebraic criterion for stability of bilateral teleoperation systems under time-varying delays. **Mechanical Systems and Signal Processing**, Elsevier, v. 137, p. 106217, 2020. Page 15.
- [10] WANG, Y.-L.; HAN, Q.-L. Network-based modelling and dynamic output feedback control for unmanned marine vehicles in network environments. **Automatica**, Elsevier, v. 91, p. 43–53, 2018. Page 15.
- [11] ZHANG, D.; SHI, P.; WANG, Q.-G.; YU, L. Analysis and synthesis of networked control systems: A survey of recent advances and challenges. **ISA Transactions**, Elsevier, v. 66, p. 376–392, 2017. Page 15.
- [12] ZHANG, X.-M.; HAN, Q.-L.; GE, X.; DING, D.; DING, L.; YUE, D.; PENG, C. Networked control systems: a survey of trends and techniques. **IEEE/CAA Journal of Automatica Sinica**, IEEE, v. 7, n. 1, p. 1–17, 2019. Page 15.

- [13] HEEMELS, W. P. M. H.; TEEL, A. R.; VAN DE WOUW, N.; NEŠIĆ, D. Networked control systems with communication constraints: Tradeoffs between transmission intervals, delays and performance. **IEEE Transactions on Automatic control**, IEEE, v. 55, n. 8, p. 1781–1796, 2010. Pages 15 and 76.
- [14] CARNEVALE, D.; TEEL, A. R.; NEŠIĆ, D. A Lyapunov proof of an improved maximum allowable transfer interval for networked control systems. **IEEE Transactions on Automatic Control**, IEEE, v. 52, n. 5, p. 892–897, 2007. Page 16.
- [15] HEIJMANS, S. H. J.; POSTOYAN, R.; NEŠIĆ, D.; HEEMELS, W. P. M. H. Computing minimal and maximal allowable transmission intervals for networked control systems using the hybrid systems approach. **IEEE Control Systems Letters**, IEEE, v. 1, n. 1, p. 56–61, 2017. Page 16.
- [16] HEIJMANS, S. H. J.; BORGERS, Do. P.; HEEMELS, W. P. M. H. Stability and performance analysis of spatially invariant systems with networked communication. **IEEE Transactions on Automatic Control**, IEEE, v. 62, n. 10, p. 4994–5009, 2017. Page 16.
- [17] HETEL, L.; FITER, C.; OMRAN, H.; SEURET, A.; FRIDMAN, E.; RICHARD, J.-P.; NICULESCU, S. I. Recent developments on the stability of systems with aperiodic sampling: An overview. **Automatica**, Elsevier, v. 76, p. 309–335, 2017. Page 16.
- [18] PALMEIRA, A. H. K.; GOMES DA SILVA JR, J. M.; FLORES, J. V. Regional stability analysis of nonlinear sampled-data control systems: a quasi-LPV approach. In: **IEEE EUROPEAN CONTROL CONFERENCE**. Limassol, 2018. p. 2016–2021. Pages 16, 29, and 36.
- [19] GOMES DA SILVA JR, J. M.; PALMEIRA, A. H. K.; MORAES, V. M.; FLORES, J. V.  $\mathcal{L}_2$ -disturbance attenuation for lpv systems under sampled-data control. **International Journal of Robust and Nonlinear Control**, Wiley Online Library, v. 28, n. 16, p. 5019–5032, 2018. Pages 16 and 29.
- [20] PALMEIRA, A. H. K.; GOMES DA SILVA JR, J. M.; FLORES, J. V. Regional stabilization of nonlinear sampled-data control systems: A quasi-LPV approach. **European Journal of Control**, Elsevier, v. 59, p. 301–312, 2021. Pages 16 and 31.
- [21] COUTINHO, P. H. S.; BERNAL, M.; PALHARES, R. M. Robust sampled-data controller design for uncertain nonlinear systems via Euler discretization. **International Journal of Robust and Nonlinear Control**, Wiley Online Library, v. 30, n. 18, p. 8244–8258, 2020. DOI: <<https://doi.org/10.1002/rnc.5234>>. Pages 16, 31, and 40.
- [22] ZHANG, X.-M.; HAN, Q.-L.; YU, X. Survey on recent advances in networked control systems. **IEEE Transactions on Industrial Informatics**, IEEE, v. 12, n. 5, p. 1740–1752, 2015. Page 16.
- [23] DE PERSIS, Claudio; TESI, Pietro. A comparison among deterministic packet-dropouts models in networked control systems. **IEEE Control Systems Letters**, IEEE, v. 2, n. 1, p. 109–114, 2017. Page 16.
- [24] BROCKETT, R. W.; LIBERZON, D. Quantized feedback stabilization of linear systems. **IEEE Transactions on Automatic Control**, IEEE, v. 45, n. 7, p. 1279–1289, 2000. Pages 16 and 19.

- [25] LIBERZON, D. Quantization, time delays, and nonlinear stabilization. **IEEE Transactions on Automatic Control**, IEEE, v. 51, n. 7, p. 1190–1195, 2006. Page 16.
- [26] ELIA, N.; MITTER, S. K. Stabilization of linear systems with limited information. **IEEE Transactions on Automatic Control**, IEEE, v. 46, n. 9, p. 1384–1400, 2001. Pages 16 and 19.
- [27] HEEMELS, W. P. M. H.; JOHANSSON, K. H.; TABUADA, P. An introduction to event-triggered and self-triggered control. In: 51st IEEE CONFERENCE ON DECISION AND CONTROL. Maui, 2012. p. 3270–3285. Pages 17, 20, 21, and 27.
- [28] TABUADA, P. Event-triggered real-time scheduling of stabilizing control tasks. **IEEE Transactions on Automatic Control**, Citeseer, v. 52, n. 9, p. 1680–1685, 2007. Pages 17, 19, 20, 21, 22, 24, 39, 45, and 46.
- [29] GIRARD, A. Dynamic triggering mechanisms for event-triggered control. **IEEE Transactions on Automatic Control**, IEEE, v. 60, n. 7, p. 1992–1997, 2015. Pages 17, 19, 20, 24, 25, 37, 38, 39, and 55.
- [30] POSTOYAN, R.; TABUADA, P.; NEŠIĆ, D.; ANTA, A. A framework for the event-triggered stabilization of nonlinear systems. **IEEE Transactions on Automatic Control**, IEEE, v. 60, n. 4, p. 982–996, 2015. Pages 17, 19, 24, 25, 43, and 45.
- [31] ANTA, A.; TABUADA, P. To sample or not to sample: Self-triggered control for nonlinear systems. **IEEE Transactions on Automatic Control**, IEEE, v. 55, n. 9, p. 2030–2042, 2010. Page 17.
- [32] BRUNNER, F. D.; HEEMELS, W. P. M. H.; ALLGÖWER, F. Event-triggered and self-triggered control for linear systems based on reachable sets. **Automatica**, Elsevier, v. 101, p. 15–26, 2019. Page 17.
- [33] LUNZE, J. Event-based control: Introduction and survey. In: **Event-Based Control and Signal Processing**. San Francisco: CRC Press, 2018. p. 3–20. Pages 18 and 54.
- [34] ÅSTRÖM, K. J.; BERNHARDSSON, B. Comparison of periodic and event based sampling for first-order stochastic systems. **IFAC Proceedings Volumes**, Elsevier, v. 32, n. 2, p. 5006–5011, 1999. Page 18.
- [35] POLAK, E. Stability and graphical analysis of first-order pulse-width-modulated sampled-data regulator systems. **IRE Transactions on Automatic Control**, IEEE, v. 6, n. 3, p. 276–282, 1961. Page 18.
- [36] SIRA-RAMIREZ, H.; LISCHINSKY-ARENAS, P. Dynamical discontinuous feedback control of nonlinear systems. **IEEE Transactions on Automatic Control**, v. 35, n. 12, p. 1373–1378, 1990. Page 18.
- [37] ÅARZÉN, K.-E. A simple event-based PID controller. **IFAC Proceedings Volumes**, Elsevier, v. 32, n. 2, p. 8687–8692, 1999. Page 18.
- [38] MOLIN, A.; HIRCHE, S. On the optimality of certainty equivalence for event-triggered control systems. **IEEE Transactions on Automatic Control**, IEEE, v. 58, n. 2, p. 470–474, 2012. Page 18.

- [39] ANTUNES, D.; HEEMELS, W. P. M. H. Rollout event-triggered control: Beyond periodic control performance. **IEEE Transactions on Automatic Control**, IEEE, v. 59, n. 12, p. 3296–3311, 2014. Page 18.
- [40] RAMESH, C.; SANDBERG, H.; JOHANSSON, K. H. Performance analysis of a network of event-based systems. **IEEE Transactions on Automatic Control**, IEEE, v. 61, n. 11, p. 3568–3573, 2016. Page 18.
- [41] KHASHOOEI, B. A.; ANTUNES, D. J.; HEEMELS, W. P. M. H. Output-based event-triggered control with performance guarantees. **IEEE Transactions on Automatic Control**, IEEE, v. 62, n. 7, p. 3646–3652, 2017. Page 18.
- [42] KHALIL, H. K.; GRIZZLE, J. W. **Nonlinear systems**. Upper Saddle River, New Jersey, USA: Prentice Hall, 2002. v. 3. Pages 18, 36, 38, 41, 43, 59, and 67.
- [43] PENG, C.; LI, F. A survey on recent advances in event-triggered communication and control. **Information Sciences**, Elsevier, v. 457, p. 113–125, 2018. Pages 19 and 27.
- [44] BORGERS, D. P. N.; HEEMELS, W. P. M. H. Event-separation properties of event-triggered control systems. **IEEE Transactions on Automatic Control**, IEEE, v. 59, n. 10, p. 2644–2656, 2014. Pages 19 and 21.
- [45] DOLK, V. S.; BORGERS, D. P.; HEEMELS, W. P. M. H. Dynamic event-triggered control: Tradeoffs between transmission intervals and performance. In: 53rd IEEE CONFERENCE ON DECISION AND CONTROL. Los Angeles, 2014. p. 2764–2769. Pages 19, 21, and 25.
- [46] ABDELRAHIM, M.; POSTOYAN, R.; DAAFOUZ, J.; NEŠIĆ, D. Robust event-triggered output feedback controllers for nonlinear systems. **Automatica**, Elsevier, v. 75, p. 96–108, 2017. Pages 19 and 21.
- [47] BORGERS, D. P.; DOLK, V. S.; HEEMELS, W. P. M. H. Dynamic periodic event-triggered control for linear systems. In: 20th INTERNATIONAL CONFERENCE ON HYBRID SYSTEMS: COMPUTATION AND CONTROL. Pittsburgh, 2017. p. 179–186. Pages 19, 20, 22, and 26.
- [48] ABDELRAHIM, M.; POSTOYAN, R.; DAAFOUZ, J.; NEŠIĆ, D.; HEEMELS, W. P. M. H. Co-design of output feedback laws and event-triggering conditions for the  $\mathcal{L}_2$ -stabilization of linear systems. **Automatica**, Elsevier, v. 87, p. 337–344, 2018. Pages 19, 21, 27, and 75.
- [49] SEURET, A.; PRIEUR, C.; TARBOURIECH, S.; ZACCARIAN, L. LQ-based event-triggered controller co-design for saturated linear systems. **Automatica**, Elsevier, v. 74, p. 47–54, 2016. Pages 19, 27, and 75.
- [50] MOREIRA, L. G.; GROFF, L. B.; GOMES DA SILVA JR, J. M. Event-triggered state-feedback control for continuous-time plants subject to input saturation. **Journal of Control, Automation and Electrical Systems**, Springer, v. 27, n. 5, p. 473–484, 2016. Pages 19, 20, 27, and 75.
- [51] MOREIRA, L. G.; GROFF, L. B.; GOMES DA SILVA JR., J. M.; TARBOURIECH, S. PI event-triggered control under saturating actuators. **International Journal of Control**, Taylor & Francis, v. 92, n. 7, p. 1634–1644, 2019. Pages 19, 21, 37, 38, 42, and 68.

- [52] MOREIRA, L. G.; TARBOURIECH, S.; SEURET, A.; GOMES DA SILVA JR, J. M. Observer-based event-triggered control in the presence of cone-bounded nonlinear inputs. **Nonlinear Analysis: Hybrid Systems**, Elsevier, v. 33, p. 17–32, 2019. Pages [19](#), [21](#), [28](#), [42](#), [49](#), [75](#), and [76](#).
- [53] MOREIRA, L. G.; GROFF, L. B.; GOMES DA SILVA JR, J. M.; COUTINHO, D. F. Event-triggered control for nonlinear rational systems. **IFAC-PapersOnLine**, Elsevier, v. 50, n. 1, p. 15307–15312, 2017. Pages [19](#), [20](#), and [42](#).
- [54] PENG, C.; YANG, T. C. Event-triggered communication and  $H_\infty$  control co-design for networked control systems. **Automatica**, Elsevier, v. 49, n. 5, p. 1326–1332, 2013. Pages [19](#) and [28](#).
- [55] YUE, D.; TIAN, E.; HAN, Q.-L. A delay system method for designing event-triggered controllers of networked control systems. **IEEE Transactions on Automatic Control**, IEEE, v. 58, n. 2, p. 475–481, 2013. Pages [19](#), [22](#), [28](#), and [29](#).
- [56] OLIVEIRA, T. G.; PALHARES, R. M.; CAMPOS, V. C. S.; QUEIROZ, P. S.; GONÇALVES, E. N. Improved Takagi-Sugeno fuzzy output tracking control for nonlinear networked control systems. **Journal of the Franklin Institute**, Elsevier, v. 354, n. 16, p. 7280–7305, 2017. Pages [19](#), [22](#), [28](#), and [30](#).
- [57] NAIR, G. N.; EVANS, R. J. Stabilization with data-rate-limited feedback: Tightest attainable bounds. **Systems & Control Letters**, Elsevier, v. 41, n. 1, p. 49–56, 2000. Page [19](#).
- [58] GOEDEL, R.; SANFELICE, R. G.; TEEL, A. R. **Hybrid Dynamical Systems: Modeling, Stability, and Robustness**. Princeton: Princeton University Press, 2012. Page [19](#).
- [59] ARANDA-ESCOLÁSTICO, E.; GUINALDO, M.; HERADIO, R.; CHACON, J.; VARGAS, H.; SÁNCHEZ, J.; DORMIDO, S. Event-based control: A bibliometric analysis of twenty years of research. **IEEE Access**, IEEE, v. 8, p. 47188–47208, 2020. Page [20](#).
- [60] HEEMELS, W. P. M. H.; DONKERS, M. C. F.; TEEL, A. R. Periodic event-triggered control for linear systems. **IEEE Transactions on Automatic Control**, IEEE, v. 58, n. 4, p. 847–861, 2013. Pages [20](#) and [22](#).
- [61] LUNZE, J.; LEHMANN, D. A state-feedback approach to event-based control. **Automatica**, Elsevier, v. 46, n. 1, p. 211–215, 2010. Pages [20](#) and [21](#).
- [62] GARCIA, E.; ANTSAKLIS, P. J. Model-based event-triggered control for systems with quantization and time-varying network delays. **IEEE Transactions on Automatic Control**, IEEE, v. 58, n. 2, p. 422–434, 2012. Pages [20](#) and [21](#).
- [63] DONKERS, M. C. F.; HEEMELS, W. P. M. H. Output-based event-triggered control with guaranteed  $\mathcal{L}_\infty$ -gain and improved and decentralized event-triggering. **IEEE Transactions on Automatic Control**, v. 57, n. 6, p. 1362–1376, 2012. Pages [20](#), [21](#), and [76](#).
- [64] DE PERSIS, C.; SAILER, R.; WIRTH, F. Parsimonious event-triggered distributed control: A Zeno free approach. **Automatica**, Elsevier, v. 49, n. 7, p. 2116–2124, 2013. Page [20](#).

- [65] LEHMANN, D.; LUNZE, J. Event-based control with communication delays and packet losses. **International Journal of Control**, Taylor & Francis, v. 85, n. 5, p. 563–577, 2012. Page 20.
- [66] WANG, X.; LEMMON, M. D. Event-triggering in distributed networked control systems. **IEEE Transactions on Automatic Control**, IEEE, v. 56, n. 3, p. 586–601, 2010. Page 21.
- [67] YU, H.; ANTSAKLIS, P. J. Event-triggered output feedback control for networked control systems using passivity: Achieving  $\mathcal{L}_2$  stability in the presence of communication delays and signal quantization. **Automatica**, Elsevier, v. 49, n. 1, p. 30–38, 2013. Page 21.
- [68] DONKERS, M. C. F.; HEEMELS, W. P. M. H. Output-based event-triggered control with guaranteed  $\mathcal{L}_\infty$ -gain and improved event-triggering. In: 49th IEEE CONFERENCE ON DECISION AND CONTROL. Atlanta, 2010. p. 3246–3251. Pages 21 and 76.
- [69] SOUZA, M.; FIORAVANTI, A. R.; CORLESS, M.; SHORTEN, R. N. Switching controller design with dwell-times and sampling. **IEEE Transactions on Automatic Control**, IEEE, v. 62, n. 11, p. 5837–5843, 2016. Pages 21 and 28.
- [70] TALLAPRAGADA, P.; CHOPRA, N. Event-triggered dynamic output feedback control for LTI systems. In: 51st IEEE CONFERENCE ON DECISION AND CONTROL. Maui, 2012. p. 6597–6602. Page 21.
- [71] FORNI, F.; GALEANI, S.; NEŠIĆ, D.; ZACCARIAN, L. Event-triggered transmission for linear control over communication channels. **Automatica**, Elsevier, v. 50, n. 2, p. 490–498, 2014. Page 21.
- [72] TARBOURIECH, S.; SEURET, A.; GOMES DA SILVA JR, J. M.I; SBARBARO, D. Observer-based event-triggered control co-design for linear systems. **IET Control Theory & Applications**, IET, v. 10, n. 18, p. 2466–2473, 2016. Pages 21, 28, 75, and 76.
- [73] BORGERS, D. P.; DOLK, V. S.; HEEMELS, W. P. M. H. Riccati-based design of event-triggered controllers for linear systems with delays. **IEEE Transactions on Automatic Control**, IEEE, v. 63, n. 1, p. 174–188, 2017. Pages 21, 25, and 26.
- [74] TARBOURIECH, S.; GIRARD, A. LMI-based design of dynamic event-triggering mechanism for linear systems. In: 57th IEEE CONFERENCE ON DECISION AND CONTROL. Miami Beach, 2018. p. 121–126. Pages 21, 25, 26, 28, and 75.
- [75] TALLAPRAGADA, P.; CHOPRA, N. Decentralized event-triggering for control of nonlinear systems. **IEEE Transactions on Automatic Control**, IEEE, v. 59, n. 12, p. 3312–3324, 2014. Pages 21 and 76.
- [76] ABDELRAHIM, M.; POSTOYAN, R.; DAAFOUZ, J.; NEŠIĆ, D. Stabilization of nonlinear systems using event-triggered output feedback controllers. **IEEE Transactions on Automatic Control**, IEEE, v. 61, n. 9, p. 2682–2687, 2015. Page 21.
- [77] GAO, Y.-F.; DU, X.; MA, Y.; SUN, X.-M. Stabilization of nonlinear systems using event-triggered controllers with dwell times. **Information Sciences**, Elsevier, v. 457, p. 156–165, 2018. Page 21.

- [78] SELIVANOV, A.; FRIDMAN, E. A switching approach to event-triggered control. In: 54th IEEE CONFERENCE ON DECISION AND CONTROL. Osaka, 2015. p. 5468–5473. Page 21.
- [79] SELIVANOV, A.; FRIDMAN, E. Event-triggered  $H_\infty$  control: A switching approach. **IEEE Transactions on Automatic Control**, IEEE, v. 61, n. 10, p. 3221–3226, 2016. Page 21.
- [80] HEEMELS, W. P. M. H.; POSTOYAN, R.; DONKERS, M. C. F.; TEEL, A. R.; ANTA, A.; TABUADA, P.; NEŠIĆ, D. Periodic event-triggered control. In: **Event-Based Control and Signal Processing**. Boca Raton: CRC Press, 2015. p. 105–119. Page 22.
- [81] PENG, C.; YUE, D.; FEI, M.-R. Relaxed stability and stabilization conditions of networked fuzzy control systems subject to asynchronous grades of membership. **IEEE Transactions on Fuzzy Systems**, IEEE, v. 22, n. 5, p. 1101–1112, 2014. Pages 22 and 28.
- [82] CHEN, X.; HAO, F. Periodic event-triggered state-feedback and output-feedback control for linear systems. **International Journal of Control, Automation and Systems**, Springer, v. 13, n. 4, p. 779–787, 2015. Page 22.
- [83] ARANDA-ESCOLÁSTICO, E.; RODRÍGUEZ, C.; GUINALDO, M.; GUZMÁN, J. L.; DORMIDO, S. Asynchronous periodic event-triggered control with dynamical controllers. **Journal of the Franklin Institute**, Elsevier, v. 355, n. 8, p. 3455–3469, 2018. Page 22.
- [84] FU, A.; MAZO JR., M. Decentralized periodic event-triggered control with quantization and asynchronous communication. **Automatica**, Elsevier, v. 94, p. 294–299, 2018. Pages 22 and 76.
- [85] LINSSENMAYER, S.; DIMAROGONAS, D. V.; ALLGÖWER, F. Periodic event-triggered control for networked control systems based on non-monotonic lyapunov functions. **Automatica**, Elsevier, v. 106, p. 35–46, 2019. Page 22.
- [86] LIU, D.; YANG, G.-H. Dynamic event-triggered control for linear time-invariant systems with  $\mathcal{L}_2$ -gain performance. **International Journal of Robust and Nonlinear Control**, Wiley Online Library, v. 29, n. 2, p. 507–518, 2019. Pages 22, 26, and 28.
- [87] LUO, S.; DENG, F.; CHEN, W.-H. Dynamic event-triggered control for linear stochastic systems with sporadic measurements and communication delays. **Automatica**, Elsevier, v. 107, p. 86–94, 2019. Pages 22, 26, and 55.
- [88] QI, Y.; XU, X.; LU, S.; YU, Y. A waiting time based discrete event-triggered control for networked switched systems with actuator saturation. **Nonlinear Analysis: Hybrid Systems**, Elsevier, v. 37, p. 100904, 2020. Pages 22 and 28.
- [89] POSTOYAN, R.; ANTA, A.; HEEMELS, W. P. M. H.; TABUADA, P.; NEŠIĆ, D. Periodic event-triggered control for nonlinear systems. In: 52nd IEEE CONFERENCE ON DECISION AND CONTROL. Florence, 2013. p. 7397–7402. Page 22.
- [90] LI, H.; YAN, W.; SHI, Y.; WANG, Y. Periodic event-triggering in distributed receding horizon control of nonlinear systems. **Systems & Control Letters**, Elsevier, v. 86, p. 16–23, 2015. Page 22.

- [91] WANG, W.; POSTOYAN, R.; NEŠIĆ, D.; HEEMELS, W. P. M. H. Stabilization of nonlinear systems using state-feedback periodic event-triggered controllers. In: IEEE 55th CONFERENCE ON DECISION AND CONTROL. Las Vegas, 2016. p. 6808–6813. Page 22.
- [92] BORGERS, D. P.; POSTOYAN, R.; ANTA, A.; TABUADA, P.; NEŠIĆ, D.; HEEMELS, W. P. M. H. Periodic event-triggered control of nonlinear systems using overapproximation techniques. **Automatica**, Elsevier, v. 94, p. 81–87, 2018. Page 22.
- [93] WANG, W.; POSTOYAN, R.; NEŠIĆ, D.; HEEMELS, W. P. M. H. Periodic event-triggered output feedback control of nonlinear systems. In: 57th IEEE CONFERENCE ON DECISION AND CONTROL. Miami Beach, 2018. p. 957–962. Page 22.
- [94] YANG, J.; SUN, J.; ZHENG, W. X.; LI, S. Periodic event-triggered robust output feedback control for nonlinear uncertain systems with time-varying disturbance. **Automatica**, Elsevier, v. 94, p. 324–333, 2018. Page 22.
- [95] WANG, Wei; POSTOYAN, Romain; NEŠIĆ, Dragan; HEEMELS, WPMH. Periodic event-triggered control for nonlinear networked control systems. **IEEE Transactions on Automatic Control**, IEEE, v. 65, n. 2, p. 620–635, 2019. Page 22.
- [96] ARANDA-ESCOLÁSTICO, E.; ABDELRAHIM, M.; GUINALDO, M.; DORMIDO, S.; HEEMELS, W. P. M. H. Design of periodic event-triggered control for polynomial systems: A delay system approach. **IFAC-PapersOnLine**, Elsevier, v. 50, n. 1, p. 7887–7892, 2017. Page 22.
- [97] PENG, C.; HAN, Q.-L.; YUE, D. To transmit or not to transmit: A discrete event-triggered communication scheme for networked Takagi–Sugeno fuzzy systems. **IEEE Transactions on Fuzzy Systems**, IEEE, v. 21, n. 1, p. 164–170, 2013. Pages 22 and 28.
- [98] JIA, X.-C.; CHI, X.-B.; HAN, Q.-L.; ZHENG, N.-N. Event-triggered fuzzy  $H_\infty$  control for a class of nonlinear networked control systems using the deviation bounds of asynchronous normalized membership functions. **Information Sciences**, Elsevier, v. 259, p. 100–117, 2014. Pages 22, 28, and 31.
- [99] ZHANG, D.; HAN, Q.-L.; JIA, X. Network-based output tracking control for T–S fuzzy systems using an event-triggered communication scheme. **Fuzzy Sets and Systems**, Elsevier, v. 273, p. 26–48, 2015. Pages 22, 28, and 30.
- [100] PAN, Y.; YANG, G.-H. Event-triggered fuzzy control for nonlinear networked control systems. **Fuzzy Sets and Systems**, Elsevier, v. 329, p. 91–107, 2017. Pages 22, 28, and 53.
- [101] MA, S.; PENG, C.; ZHANG, J.; XIE, X. Imperfect premise matching controller design for TS fuzzy systems under network environments. **Applied Soft Computing**, Elsevier, v. 52, p. 805–811, 2017. Pages 22 and 53.
- [102] PENG, C.; MA, S.; XIE, X. Observer-based non-PDC control for networked T–S fuzzy systems with an event-triggered communication. **IEEE Transactions on Cybernetics**, IEEE, v. 47, n. 8, p. 2279–2287, 2017. Pages 22, 28, and 53.
- [103] LU, A.-Y.; ZHAI, D.; DONG, J.; ZHANG, Q.-L. Network-based fuzzy  $H_\infty$  controller design for TS fuzzy systems via a new event-triggered communication scheme. **Neurocomputing**, Elsevier, v. 273, p. 403–413, 2018. Pages 22, 28, 30, and 31.

- [104] YAN, S.; SHEN, M.; NGUANG, S. K.; ZHANG, G.; ZHANG, L. A distributed delay method for event-triggered control of T–S fuzzy networked systems with transmission delay. **IEEE Transactions on Fuzzy Systems**, IEEE, v. 27, n. 10, p. 1963–1973, 2019. Pages [22](#) and [30](#).
- [105] LIU, D.; YANG, G.; ER, M. J. Event-triggered control for T–S fuzzy systems under asynchronous network communications. **IEEE Transactions on Fuzzy Systems**, v. 28, n. 2, p. 390–399, 2020. Pages [22](#), [28](#), and [53](#).
- [106] TANAKA, K.; WANG, H. O. **Fuzzy Control Systems Design and Analysis: a Linear Matrix Inequality Approach**. New York, NY, USA: John Wiley & Sons, 2001. Pages [22](#), [29](#), [35](#), and [61](#).
- [107] ROTONDO, D.; PUIG, V.; NEJJARI, F.; WITCZAK, M. Automated generation and comparison of Takagi–Sugeno and polytopic quasi-LPV models. **Fuzzy Sets and Systems**, Elsevier, v. 277, p. 44–64, 2015. Pages [22](#), [29](#), and [35](#).
- [108] EQTAMI, A.; DIMOS, V.; KYRIAKOPOULOS, K. J. Event-triggered control for discrete-time systems. In: 2010 IEEE AMERICAN CONTROL CONFERENCE. Baltimore, 2010. p. 4719–4724. Page [22](#).
- [109] HEEMELS, W. P. M. H.; DONKERS, M. C. F. Model-based periodic event-triggered control for linear systems. **Automatica**, Elsevier, v. 49, n. 3, p. 698–711, 2013. Page [22](#).
- [110] HU, S.; YUE, D.; PENG, C.; XIE, X.; YIN, X. Event-triggered controller design of nonlinear discrete-time networked control systems in TS fuzzy model. **Applied Soft Computing**, Elsevier, v. 30, p. 400–411, 2015. Page [22](#).
- [111] HU, S.; YUE, D.; YIN, X.; XIE, X.; MA, Y. Adaptive event-triggered control for nonlinear discrete-time systems. **International Journal of Robust and Nonlinear Control**, Wiley Online Library, v. 26, n. 18, p. 4104–4125, 2016. Pages [22](#) and [24](#).
- [112] GROFF, L. B.; MOREIRA, L. G.; GOMES DA SILVA JR, J. M.; SBARBARO, D. Observer-based event-triggered control: A discrete-time approach. In: 2016 IEEE AMERICAN CONTROL CONFERENCE. Boston, 2016. p. 4245–4250. Page [22](#).
- [113] GROFF, L. B.; MOREIRA, L. G.; GOMES DA SILVA JR, J. M. Event-triggered control co-design for discrete-time systems subject to actuator saturation. In: 2016 IEEE CONFERENCE ON COMPUTER AIDED CONTROL SYSTEM DESIGN. Buenos Aires, 2016. p. 1452–1457. Page [22](#).
- [114] ZHANG, Z.; LIANG, H.; WU, C.; AHN, C. K. Adaptive event-triggered output feedback fuzzy control for nonlinear networked systems with packet dropouts and actuator failure. **IEEE Transactions on fuzzy systems**, IEEE, v. 27, n. 9, p. 1793–1806, 2019. Pages [22](#), [23](#), and [28](#).
- [115] DING, S.; XIE, X.; LIU, Y. Event-triggered static/dynamic feedback control for discrete-time linear systems. **Information Sciences**, Elsevier, v. 524, p. 33–45, 2020. Page [22](#).
- [116] MERLIN, G. B.; MOREIRA, L. G.; GOMES DA SILVA JR, J. M. Periodic event-triggered control for linear systems in the presence of cone-bounded nonlinear inputs: A discrete-time approach. **Journal of Control, Automation and Electrical Systems**, Springer, v. 32, n. 1, p. 42–56, 2021. Page [22](#).

- [117] GU, Z.; TIAN, E.; LIU, J. Adaptive event-triggered control of a class of nonlinear networked systems. **Journal of the Franklin Institute**, Elsevier, v. 354, n. 9, p. 3854–3871, 2017. Pages 23, 28, and 30.
- [118] PENG, C.; Y., Mingjin; ZHANG, J.; FEI, M.; HU, S. Network-based  $H_\infty$  control for T–S fuzzy systems with an adaptive event-triggered communication scheme. **Fuzzy Sets and Systems**, Elsevier, v. 329, p. 61–76, 2017. Pages 23 and 28.
- [119] GE, X.; HAN, Q.-L. Distributed formation control of networked multi-agent systems using a dynamic event-triggered communication mechanism. **IEEE Transactions on Industrial Electronics**, IEEE, v. 64, n. 10, p. 8118–8127, 2017. Pages 23 and 28.
- [120] NING, Z.; YU, J.; PAN, Y.; LI, H. Adaptive event-triggered fault detection for fuzzy stochastic systems with missing measurements. **IEEE Transactions on Fuzzy Systems**, IEEE, v. 26, n. 4, p. 2201–2212, 2017. Pages 23 and 28.
- [121] GU, Z.; YUE, D.; TIAN, E. On designing of an adaptive event-triggered communication scheme for nonlinear networked interconnected control systems. **Information Sciences**, Elsevier, v. 422, p. 257–270, 2018. Pages 23, 28, 30, and 53.
- [122] LI, H.; ZHANG, Z.; YAN, H.; XIE, X. Adaptive event-triggered fuzzy control for uncertain active suspension systems. **IEEE Transactions on Cybernetics**, IEEE, v. 49, n. 12, p. 4388–4397, 2018. Pages 23 and 28.
- [123] GU, Z.; SHI, P.; YUE, D.; DING, Z. Decentralized adaptive event-triggered  $\mathcal{H}_\infty$  filtering for a class of networked nonlinear interconnected systems. **IEEE Transactions on Cybernetics**, IEEE, v. 49, n. 5, p. 1570–1579, 2019. Pages 23, 28, and 30.
- [124] LI, T.; LI, Z.; ZHANG, L.; FEI, S. Improved approaches on adaptive event-triggered output feedback control of networked control systems. **Journal of the Franklin Institute**, Elsevier, v. 355, n. 5, p. 2515–2535, 2018. Pages 23 and 28.
- [125] WU, Z.; XIONG, J.; XIE, M. Dynamic event-triggered  $\mathcal{L}_\infty$  control for networked control systems under deception attacks: a switching method. **Information Sciences**, Elsevier, v. 561, p. 168–180, 2021. Page 23.
- [126] POSTOYAN, R.; ANTA, A.; NEŠIĆ, D.; TABUADA, P. A unifying Lyapunov-based framework for the event-triggered control of nonlinear systems. In: 50th IEEE CONFERENCE ON DECISION AND CONTROL AND EUROPEAN CONTROL CONFERENCE. Orlando, 2011. p. 2559–2564. Pages 24 and 25.
- [127] WANG, Y.; ZHENG, W. X.; ZHANG, H. Dynamic event-based control of nonlinear stochastic systems. **IEEE Transactions on Automatic Control**, IEEE, v. 62, n. 12, p. 6544–6551, 2017. Page 25.
- [128] ZUO, Z.; GUAN, S.; WANG, Y.; LI, H. Dynamic event-triggered and self-triggered control for saturated systems with anti-windup compensation. **Journal of the Franklin Institute**, Elsevier, v. 354, n. 17, p. 7624–7642, 2017. Page 25.
- [129] YI, X.; LIU, K.; DIMAROGONAS, D. V.; JOHANSSON, K. H. Dynamic event-triggered and self-triggered control for multi-agent systems. **IEEE Transactions on Automatic Control**, IEEE, 2018. Page 25.

- [130] NEŠIĆ, D.; TEEL, A. R.; CARNEVALE, D. Explicit computation of the sampling period in emulation of controllers for nonlinear sampled-data systems. **IEEE transactions on Automatic Control**, IEEE, v. 54, n. 3, p. 619–624, 2009. Pages 25 and 27.
- [131] WU, Y.; ZHANG, H.; WANG, Z.; HUANG, C. Distributed event-triggered consensus of general linear multiagent systems under directed graphs. **IEEE Transactions on Cybernetics**, IEEE, 2020. Doi: 10.1109/TCYB.2020.2981210. Page 25.
- [132] WANG, X.; FEI, Z.; WANG, T.; YANG, L. Dynamic event-triggered actuator fault estimation and accommodation for dynamical systems. **Information Sciences**, Elsevier, v. 525, p. 119–133, 2020. Page 25.
- [133] HUONG, D. C.; HUYNH, V. T.; TRINH, H. Dynamic event-triggered state observers for a class of nonlinear systems with time delays and disturbances. **IEEE Transactions on Circuits and Systems II: Express Briefs**, IEEE, v. 67, n. 12, p. 3457 – 3461, 2020. Page 25.
- [134] ZHANG, Z. H.; LIU, D.; DENG, C.; FAN, Q. Y. A dynamic event-triggered resilient control approach to cyber-physical systems under asynchronous DoS attacks. **Information Sciences**, Elsevier, v. 519, p. 260–272, 2020. Page 25.
- [135] LI, Z.; MA, D.; ZHAO, J. Dynamic event-triggered  $\mathcal{L}_\infty$  control for switched affine systems with sampled-data switching. **Nonlinear Analysis: Hybrid Systems**, Elsevier, v. 39, p. 100978, 2021. Page 25.
- [136] BORGERES, D. P.; DOLK, V. S.; HEEMELS, W. P. M. H. Dynamic event-triggered control with time regularization for linear systems. In: 55th IEEE CONFERENCE ON DECISION AND CONTROL. Las Vegas, 2016. p. 1352–1357. Pages 25 and 26.
- [137] DOLK, V.; HEEMELS, M. P. M. H. Event-triggered control systems under packet losses. **Automatica**, Elsevier, v. 80, p. 143–155, 2017. Pages 25, 26, and 76.
- [138] DOLK, V. S.; TESI, P.; DE PERSIS, C.; HEEMELS, W. P. M. H. Event-triggered control systems under denial-of-service attacks. **IEEE Transactions on Control of Network Systems**, IEEE, v. 4, n. 1, p. 93–105, 2017. Pages 25 and 26.
- [139] DOLK, V. S.; PLOEG, J.; HEEMELS, W. P. M. H. Event-triggered control for string-stable vehicle platooning. **IEEE Transactions on Intelligent Transportation Systems**, IEEE, v. 18, n. 12, p. 3486–3500, 2017. Pages 25 and 26.
- [140] DOLK, V. S.; ABDELRAHIM, M.; HEEMELS, W. P. M. H. Event-triggered consensus seeking under non-uniform time-varying delays. **IFAC-PapersOnLine**, Elsevier, v. 50, n. 1, p. 10096–10101, 2017. Pages 25 and 26.
- [141] ABDELRAHIM, M.; DOLK, V. S.; HEEMELS, W. P. M. H. Event-triggered quantized control for input-to-state stabilization of linear systems with distributed output sensors. **IEEE Transactions on Automatic Control**, IEEE, v. 64, n. 12, p. 4952–4967, 2019. Pages 25 and 26.
- [142] MENG, X.; CHEN, T. Event detection and control co-design of sampled-data systems. **International Journal of Control**, Taylor & Francis, v. 87, n. 4, p. 777–786, 2014. Page 27.

- [143] BAN, J.; SEO, M.; GOH, T.; JEONG, H.; KIM, S. W. Improved co-design of event-triggered dynamic output feedback controllers for linear systems. **Automatica**, Elsevier, v. 111, p. 108600, 2020. Pages 27 and 75.
- [144] ZHANG, F.; MAZO JR., M.; VAN DE WOUW, N. Absolute stabilization of Lur'e systems under event-triggered feedback. **IFAC-PapersOnLine**, Elsevier, v. 50, n. 1, p. 15301–15306, 2017. Pages 27 and 49.
- [145] ABDELRAHIM, M.; POSTOYAN, R.; DAAFOUZ, J.; NEŠIĆ, D. Co-design of output feedback laws and event-triggering conditions for linear systems. In: 53rd IEEE CONFERENCE ON DECISION AND CONTROL. Las Vegas, 2014. p. 3560–3565. Pages 27 and 75.
- [146] PARK, P.; KO, J. W.; JEONG, C. Reciprocally convex approach to stability of systems with time-varying delays. **Automatica**, Elsevier, v. 47, n. 1, p. 235–238, 2011. Pages 28, 30, 52, and 53.
- [147] SEURET, A.; GOUAISBAUT, F. Wirtinger-based integral inequality: Application to time-delay systems. **Automatica**, Elsevier, v. 49, n. 9, p. 2860–2866, 2013. Pages 28 and 53.
- [148] SHEN, H.; LI, F.; YAN, H.; KARIMI, H. R.; LAM, H. K. Finite-time event-triggered  $\mathcal{H}_\infty$  control for T–S fuzzy markov jump systems. **IEEE Transactions on Fuzzy Systems**, IEEE, v. 26, n. 5, p. 3122–3135, 2018. Page 28.
- [149] ZHONG, Z.; LIN, C.-M.; SHAO, Z.; XU, M. Decentralized event-triggered control for large-scale networked fuzzy systems. **IEEE Transactions on Fuzzy Systems**, IEEE, v. 26, n. 1, p. 29–45, 2016. Page 28.
- [150] PAN, Y.; YANG, G.-H. A novel event-based fuzzy control approach for continuous-time fuzzy systems. **Neurocomputing**, Elsevier, v. 338, p. 55–62, 2019. Page 28.
- [151] PAN, Y.; YANG, G.-H. Event-based output tracking control for fuzzy networked control systems with network-induced delays. **Applied Mathematics and Computation**, Elsevier, v. 346, p. 513–530, 2019. Page 28.
- [152] BOYD, S.; El Ghaoui, L.; FERON, E.; BALAKRISHNAN, V. **Linear Matrix Inequalities in System and Control Theory**. Philadelphia, PA, USA: SIAM, 1994. v. 15. (Studies in Applied Mathematics, v. 15). ISBN 0-89871-334-X. Page 28.
- [153] LÖFBERG, J. YALMIP: A toolbox for modeling and optimization in MATLAB. In: IEEE INTERNATIONAL SYMPOSIUM ON COMPUTER AIDED CONTROL SYSTEMS DESIGN. Taipei, 2004. p. 284–289. Pages 28 and 45.
- [154] RUGH, W. J.; SHAMMA, J. S. Research on gain scheduling. **Automatica**, Elsevier, v. 36, n. 10, p. 1401–1425, 2000. Page 29.
- [155] SALA, A.; ARIÑO, C.; ROBLES, R. Gain-scheduled control via convex nonlinear parameter varying models. **IFAC-PapersOnLine**, Elsevier, v. 52, n. 28, p. 70–75, 2019. Page 29.

- [156] LÓPEZ-ESTRADA, F.-R.; ROTONDO, D.; VALENCIA-PALOMO, G. A review of convex approaches for control, observation and safety of Linear Parameter Varying and Takagi-Sugeno systems. **Processes**, Multidisciplinary Digital Publishing Institute, v. 7, n. 11, p. 814, 2019. Page 29.
- [157] PEIXOTO, M. L. C.; BRAGA, M. F.; PALHARES, R. M. Gain-scheduled control for discrete-time non-linear parameter-varying systems with time-varying delays. **IET Control Theory & Applications**, IET, v. 14, n. 19, p. 3217–3229, 2020. Page 29.
- [158] PEIXOTO, M. L. C.; COUTINHO, P. H. S.; PALHARES, R. M. Improved robust gain-scheduling static output-feedback control for discrete-time LPV systems. **European Journal of Control**, Elsevier, v. 58, p. 11–16, 2021. DOI: <<https://doi.org/10.1016/j.ejcon.2020.12.006>>. Page 29.
- [159] TANIGUCHI, T.; TANAKA, K.; OHTAKE, H.; WANG, H. O. Model construction, rule reduction, and robust compensation for generalized form of Takagi-Sugeno fuzzy systems. **IEEE Transactions on Fuzzy Systems**, IEEE, v. 9, n. 4, p. 525–538, 2001. Pages 29 and 35.
- [160] ROTONDO, D.; NEJJARI, F.; PUIG, V. Quasi-LPV modeling, identification and control of a twin rotor mimo system. **Control Engineering Practice**, Elsevier, v. 21, n. 6, p. 829–846, 2013. Page 29.
- [161] ARCEO, J. C.; SÁNCHEZ, M.; ESTRADA-MANZO, V.; BERNAL, M. Convex stability analysis of nonlinear singular systems via linear matrix inequalities. **IEEE Transactions on Automatic Control**, IEEE, v. 64, n. 4, p. 1740–1745, 2018. Page 29.
- [162] SANCHEZ, M.; BERNAL, M. LMI-based robust control of uncertain nonlinear systems via polytopes of polynomials. **International Journal of Applied Mathematics and Computer Science**, v. 29, n. 2, p. 275–283, 2019. Pages 29, 35, and 40.
- [163] ROBLES, R.; SALA, A.; BERNAL, M. Performance-oriented quasi-LPV modeling of nonlinear systems. **International Journal of Robust and Nonlinear Control**, Wiley Online Library, v. 29, n. 5, p. 1230–1248, 2019. Page 29.
- [164] COUTINHO, P. H. S.; ARAÚJO, R. F.; NGUYEN, A.-T.; PALHARES, R. M. A multiple-parameterization approach for local stabilization of constrained Takagi-Sugeno fuzzy systems with nonlinear consequents. **Information Sciences**, Elsevier, v. 506, p. 295–307, 2020. DOI: <<https://doi.org/10.1016/j.ins.2019.08.008>>. Page 29.
- [165] SEURET, A.; GOUAISBAUT, F. Stability of linear systems with time-varying delays using Bessel–Legendre inequalities. **IEEE Transactions on Automatic Control**, IEEE, v. 63, n. 1, p. 225–232, 2017. Pages 30 and 52.
- [166] WANG, G.; CHADLI, M.; CHEN, H.; ZHOU, Z. Event-triggered control for active vehicle suspension systems with network-induced delays. **Journal of the Franklin Institute**, Elsevier, v. 356, n. 1, p. 147–172, 2019. Page 30.
- [167] SEURET, A.; GOUAISBAUT, F. Delay-dependent reciprocally convex combination lemma for the stability analysis of systems with a fast-varying delay. In: **Delays and Interconnections: Methodology, Algorithms and Applications**. Gewerbestrasse: Springer, 2019. p. 187–197. Pages 30 and 52.

- [168] SEURET, A.; GOUAISBAUT, F. Hierarchy of LMI conditions for the stability analysis of time-delay systems. **Systems & Control Letters**, Elsevier, v. 81, p. 1–7, 2015. Page 30.
- [169] COUTINHO, P. H. S.; CHAGAS, T. P.; TORRES, L. A. B.; PALHARES, R. M. Robust eigenvalue assignment via sampled state-feedback for linear polytopic discrete-time periodic systems. In: 14° SIMPÓSIO BRASILEIRO DE AUTOMAÇÃO INTELIGENTE. Ouro Preto, 2019. p. 1–6. DOI: <https://doi.org/10.17648/sbai-2019-111239>. Page 31.
- [170] COUTINHO, P. H. S.; LAUBER, J.; BERNAL, M.; PALHARES, R. M. Efficient LMI conditions for enhanced stabilization of discrete-time Takagi-Sugeno models via delayed nonquadratic Lyapunov functions. **IEEE Transactions on Fuzzy Systems**, IEEE, v. 27, n. 9, p. 1833–1843, 2019. DOI: <https://doi.org/10.1109/TFUZZ.2019.2892341>. Page 31.
- [171] GOLABI, A.; MESKIN, N.; TÓTH, R.; MOHAMMADPOUR, J.; DONKERS, T. Event-triggered control for discrete-time linear parameter-varying systems. In: **Proceedings of the 2016 American Control Conference**. Boston, MA, USA: [s.n.], 2016. p. 3680–3685. Page 31.
- [172] CAMPOS, V. C. S.; FREZZATTO, L.; OLIVEIRA, T. G.; ESTRADA-MANZO, V.; BRAGA, M. F.  $\mathcal{H}_\infty$  control of event-triggered quasi-LPV systems based on an exact discretization approach – a linear matrix inequality approach. **Journal of the Franklin Institute**, Elsevier, 2021. Page 31.
- [173] COUTINHO, P. H. S.; PEIXOTO, M. L. C.; BERNAL, M.; NGUYEN, A.-T.; PALHARES, R. M. Local sampled-data gain-scheduling control of quasi-LPV systems. **IFAC-PapersOnLine**, Elsevier, v. 54, n. 4, p. 86–91, 2021. DOI: <https://doi.org/10.1016/j.ifacol.2021.10.015>. Page 31.
- [174] BRUZELIUS, F.; PETTERSSON, S.; BREITHOLTZ, C. Region of attraction estimates for LPV-gain scheduled control systems. In: IEEE. **2003 European Control Conference (ECC)**. [S.l.], 2003. p. 892–897. Page 31.
- [175] COUTINHO, P. H. S.; PALHARES, R. M. Co-design of dynamic event-triggered gain-scheduling control for a class of nonlinear systems. **IEEE Transactions on Automatic Control**, IEEE, p. 1–8, 2021. DOI: <https://doi.org/10.1109/TAC.2021.3108498>. Page 33.
- [176] COUTINHO, P. H. S.; PALHARES, R. M. Dynamic periodic event-triggered gain-scheduling control co-design for quasi-LPV systems. **Nonlinear Analysis: Hybrid Systems**, Elsevier, v. 41, p. 1–18, 2021. DOI: <https://doi.org/10.1016/j.nahs.2021.101044>. Pages 33, 55, 56, and 75.
- [177] OMRAN, H.; HETEL, L.; PETRECZKY, M.; RICHARD, J. P.; LAMNABHI-LAGARRIGUE, F. Stability analysis of some classes of input-affine nonlinear systems with aperiodic sampled-data control. **Automatica**, Elsevier, v. 70, p. 266–274, 2016. Pages 7, 44, 45, and 46.
- [178] COUTINHO, D. F.; GOMES DA SILVA JR, J. M. Computing estimates of the region of attraction for rational control systems with saturating actuators. **IET Control Theory & Applications**, IET, v. 4, n. 3, p. 315–325, 2010. Page 47.

- [179] TARBOURIECH, S.; SEURET, A.; MOREIRA, L. G.; GOMES DA SILVA JR, J. M. Observer-based event-triggered control for linear systems subject to cone-bounded nonlinearities. **IFAC-PapersOnLine**, Elsevier, v. 50, n. 1, p. 7893–7898, 2017. Pages 49 and 76.
- [180] ZHANG, X.-M.; HAN, Q.-L.; SEURET, A.; GOUAISBAUT, F. An improved reciprocally convex inequality and an augmented Lyapunov–Krasovskii functional for stability of linear systems with time-varying delay. **Automatica**, Elsevier, v. 84, p. 221–226, 2017. Page 52.
- [181] COUTINHO, D. F.; SOUZA, C. E de; GOMES DA SILVA JR, J. M.; CALDEIRA, André F; PRIEUR, Christophe. Regional stabilization of input-delayed uncertain nonlinear polynomial systems. **IEEE Transactions on Automatic Control**, IEEE, v. 65, n. 5, p. 2300–2307, 2019. Page 57.
- [182] LIU, K.; FRIDMAN, E. Delay-dependent methods and the first delay interval. **Systems & Control Letters**, Elsevier, v. 64, p. 57–63, 2014. Page 57.
- [183] ÇİMEN, T. Systematic and effective design of nonlinear feedback controllers via the state-dependent Riccati equation (SDRE) method. **Annual Reviews in control**, Elsevier, v. 34, n. 1, p. 32–51, 2010. Page 61.
- [184] DEB, K. **Optimization for Engineering Design: Algorithms and Examples**. New Delhi: PHI Learning Pvt. Ltd., 2012. Page 69.
- [185] MOREIRA, L. G.; GOMES DA SILVA JR, J. M.; TARBOURIECH, S.; SEURET, A. Observer-based event-triggered control for systems with slope-restricted nonlinearities. **International Journal of Robust and Nonlinear Control**, Wiley Online Library, v. 30, n. 17, p. 7409–7428, 2020. Page 75.
- [186] GUERRA, T. M.; MÁRQUEZ, R.; KRUSZEWSKI, A.; BERNAL, M.  $H_\infty$  LMI-based observer design for nonlinear systems via Takagi–Sugeno models with unmeasured premise variables. **IEEE Transactions on Fuzzy Systems**, IEEE, v. 26, n. 3, p. 1498–1509, 2017. Page 76.
- [187] PÉREZ-ESTRADA, A.-J.; OSORIO-GORDILLO, G.-L.; DAROUACH, M.; ALMA, M.; OLIVARES-PEREGRINO, V.-H. Generalized dynamic observers for quasi-LPV systems with unmeasurable scheduling functions. **International Journal of Robust and Nonlinear Control**, Wiley Online Library, v. 28, n. 17, p. 5262–5278, 2018. Page 76.
- [188] QUINTANA, D.; ESTRADA-MANZO, V.; BERNAL, M. An exact handling of the gradient for overcoming persistent problems in nonlinear observer design via convex optimization techniques. **Fuzzy Sets and Systems**, Elsevier, 2020. Page 76.
- [189] MAZO JR., M.; TABUADA, P. Decentralized event-triggered control over wireless sensor/actuator networks. **IEEE Transactions on Automatic Control**, IEEE, v. 56, n. 10, p. 2456–2461, 2011. Page 76.